1-1-2012

Biofuels production from hydrotreating of vegetable oil using supported noble metals, and transition metal carbide and nitride

Huali Wang
Wayne State University,

BIOFUELS PRODUCTION FROM HYDROTREATING OF VEGETABLE OIL USING SUPPORTED NOBLE METALS, AND TRANSITION METAL CARBIDE AND NITRIDE

by

HUALI WANG

DISSERTATION

Submitted to the Graduate School

of Wayne State University,

Detroit, Michigan

in partial fulfillment of the requirements

for the degree of

DOCTOR OF PHILOSOPHY

2012

MAJOR: CHEMICAL ENGINEERING

Approved by:

_____

Advisor Date

_____

Co-Advisor Date

_____

_____

DEDICATION

This work is dedicated first and foremost to my advisors. Your constant encouragement and guidance made this journey possible. Also, to my family, friends, instructors, and colleagues who supported, encouraged, and mentored me throughout this process … thank you all from the bottom of my heart.

ACKNOWLEDGMENTS

I would like offer sincere gratitude to my supervisors Dr. K. Y. Simon Ng and Dr. Steven O. Salley for their invaluable guidance and time spent in helping me complete the magnitude of work that is contained within this dissertation. I am grateful of their input and knowledge that was of great importance to the direction of this work. I am thankful for their patience and support throughout this entire process. I also would like to express my deep gratitude to the members of my advisory committee, Dr. Charles Manke and Dr. Ratna Naik, for their contributions and guidance. The postdoc research associates in our lab, Dr. Shuli Yan, Dr Manhoe Kim, Dr Haiying Tang, and Dr Kapila Wadumesthrige, whose friendship, unflagging support, advice, mentoring, and encouragement made all the difference in the world.

Finally I would like to thank all my family, friends and colleagues for their prayers, support, and love.

TABLE OF CONTENTS

LIST OF TABLES

LIST OF FIGURES

CHAPTER 1. INTRODUCTION

In recent years, many researchers are concentrating on developing biofuels from alternative and renewable sources to replace commercial petroleum products. The suitable properties of plant oils and animal fats (renewable and low sulfur, nitrogen and heavy metal content), which are made up of triglycerides with long chained fatty acid groups 16 to 24 carbon atoms in length, makes them ideal sources for the production of synthetic fuels and useful chemicals [1]. At present, the most successful class of biofuels is biodiesel, which is produced from plant oils or animals fats by a liquid-phase catalyzed transesterification process at low temperature or a solid catalyzed catalytic cracking process at high temperature. However, the process requires a large investments for the production units in order to ensure high efficiency[2]. Also biodiesel product is not stable compared with the petroleum fuel because of its low oxidation stability and poor cold flow properties.

Recently, an alternative method of converting plant oils and animal fats into biofuel products has been studied by using a catalytic hydrotreating process similar to what is found in the oil and gas industry[3, 4]. Two important chemical steps occur during the conversion of biomass-derived oils into biofuel products: oxygen removal (hydrodeoxygenation (HDO), hydrodecarbonylation, and hydrodecarboxylation) and hydrocracking[5]. Both of these chemical processes are included in a larger group of processes generally referred to as hydroprocessing. During the process, a dual function catalyst composed of a metallic part and amorphous mixed oxides of acidic nature or proton exchanged crystalline zeolites is required, where metallic sites are required for hydrogenation and dehydrogenation reactions and the acid sites are necessary for isomerization and cracking activities. Therefore, it is very important to design the acidic sites and metal components as well as tailor the balance between the metal and acid for the product selectivity, catalyst activity and stability[6-8].

At present, two types of catalysts have been reported as effective hydrotreating catalysts in converting vegetable oils to biofuels, especially green diesel: supported noble metal catalysts (Pd and Pt)[9-12] and sulfided bimetallic catalysts (usually Mo- or W-based sulfides promoted with Ni or Co)[13-17] . The subject has been covered in several publications[18-21]. However, there are disadvantages of using these catalysts. On one hand, the rarity and high price of noble metal catalysts has made the process economically unfeasible. Furthermore, since noble metal catalysts are very sensitive to catalyst poisons[22], impurities (such as sufur, heavy metals and oxygenated compounds) in feedstock can cause significant deactivation of the catalysts[23]. Therefore, it is necessary to remove impurities from the biomass feedstock before the reaction. On the other hand, conventional γ-Al_2O_3 supported sulfided bimetallic catalysts (usually Mo- or W-based sulfides promoted with Ni or Co) as presently used for desulphurization of fossil diesel streams need to be operated under high energy consumption conditions, such as high temperature, high pressure, and large amount of hydrogen consumption[24]. The process is costly and the yield of product can be low because of formation of coke, which causes its deactivation and delta P build-up in the reactor[25]. The products obtained in the mentioned processes over the bimetallic aluminum oxide supported catalysts are mainly n-paraffins (n-C15 up to n-C18) which solidify at low temperatures, so, they are unsuitable for high quality diesel fuels, kerosene and gasoline compounds[26]. More importantly, the transition metals in these hydrotreating catalysts need to be maintained in the sulfided form in order to maintain the activity at process conditions. Therefore, a sulfurization co-feed needs to be added to the biomass feedstock.

In recent years, the nitrides and carbides of early transition metals have been identified as a new class of promising hydrotreating catalysts which possess excellent catalytic properties and are competitive with the conventional bimetallic sulfided catalysts. After carburization or nitridation,

the early transition metals can exhibit high activity similar to the noble metals because the introduction of carbon or nitrogen into the lattice of the early transition metals results in an increase of the lattice parameter a_0 and leads to an increase in the d-electron density[27]. As a substitute for sulfide catalysts, mono- and bimetallic carbides and nitrides based on transition metals have been successfully applied to the upgrading process of petroleum oil and bio-oil including hydrodesulfurization (DNS), hydrodenitrogenation (HDN), and hydrodeoxygenation (HDO)[28-31]. During catalytic hydrotreating, the triglycerides and free fatty acids in vegetable oils and animal fats are deoxygenated first and then converted into hydrocarbon fuels. It has been reported that transition metal nitrides exhibited excellent activity and selectivity for hydrodeoxygenation of benzofuran[32]. Moreover, Han et al.[33] reported –ª °-#transition metal carbide catalyst, Mo_2C, showed high activity and selectivity for one-step conversion of vegetable oils into branched diesel-like hydrocarbons.#Nitrides of molybdenum, tungsten and vanadium supported on γ-Al_2O_3 were also used for hydrodeoxygenation of oleic acid and canola oil[34]. The oxygen removal exceeded 90% over the supported molybdenum catalyst for a long reaction duration (450 hours) and the yield of middle distillate hydrocarbons (diesel fuel) ranged between 38 and 48 wt%. Although most of the transition metal carbides and nitrides catalysts described above have interesting hydrotreating properties, bimetallic nitride and carbide catalysts were found to be much more active and stable than the mono-metallic ones[28]. However, there are only few reports on the use of bimetallic catalysts for vegetable oils hydroprocessing.

1.1. Significance of this study

The study has three-fold significance:

First, the biofuel feedstocks in this study are renewable biomass (plant oils or animal fats). One of the most frequently cited benefits of biomass derived fuels is their ability to help to offset the

point where there's less crude oil in the ground than we've extracted -- i.e., so-called "peak oil". In 2009, the National Petroleum Council released a landmark report commissioned by the U.S. Department of Energy (DOE) coming up strategies to resolve declining crude oil reserves. One of those recommendations was to expand and diversify energy production from sources other than petroleum oils, especially bio-based renewable sources. The renewable biomass resources have also drawn strong support from the agricultural community which would benefit from increased farm income.

Second, development of biofuel alleviates the environmental problems caused by burning fossil fuels. Take aviation fuel for example, the ground level emissions from commercial, military and general aviation have been considered as a major cause of the decreasing local air quality[35]. Aircraft produces up to 4% of the annual global CO_2 emissions from fossil fuels near the Earth's surface as well as at higher altitudes (25,000 to 50,000 feet). Replacement of fossil jet fuels with biomass derived ones helps to maintain the carbon balance on the earth and reduce the greenhouse emissions. It was reported by renewable fuels company, Sustainable Oils, that results from a life cycle analysis (LCA) of biojet fuel produced from camelina seeds invented by the company showed the fuel reduces carbon emissions by as high as 84% compared to conventional petroleum jet fuel[36].

And finally, this research develops the catalysts of the carbides of early transition metals which can exhibit high activity similar to the noble metals. This study fills the gaps in the literature identified above by investigating the hydrotreating activities and selectivity of bimetallic (NiMo) carbides and nitrides catalysts. And the application of the technology eliminates the need to add a sulfur compound to a biomass-derived feedstock.

1.2. Objectives of the study

With abundant renewable energy sources, vegetable oils can be converted to gasoline to diesel fuel range hydrocarbons by catalytic hydrotreating. The overall research objective for this project is to develop bifunctional carbide and nitride catalysts for hydrocracking of triglycerides under milder conditions to produce drop-in biofuels. In order to achieve the overall objective, three secondary specific objectives listed below have been identified to direct the research ultimately towards the overall objective. The specific objectives are:

- Synthesize, characterize and test three different types of catalysts, supported noble metal, supported metallic nitride and carbide catalysts to determine which one has the highest activity for hydrotreating of soybean oil. The three catalysts to be tested are: Ru, NiMo carbide and nitride supported on ZSM-5. Also catalytic cracking activity of ZSM-5 will be tested.
- After determining the most active catalyst(s), investigate the process parameters effect on catalyst activity and product selectivity. Optimize the most active catalyst for its activity for hydroprocessing of vegetable oils with respect to important catalyst parameters, such as metal loading, and important operating parameters, such as temperature, hydrogen partial pressure, and residence time (LHSV).
- Synthesize, characterize and test catalysts with five different types of supports. The supports are: ZSM-5, zeolite-β, USY zeolite, γ-Al_2O_3 and Al-SBA-15

CHAPTER 2. LITERATURE REVIEW

This section reviews various areas of interest that are important to the production of biofuels from biomass-derived oils, including different production methods, feedstocks, hydrotreating catalysts and reaction mechanism.

2.1 biofuel production

In order to overcome the reliance on crude oil resources, there exist several commercial and research programs around the world aimed at creating alternative fuels based on alternative feedstocks.

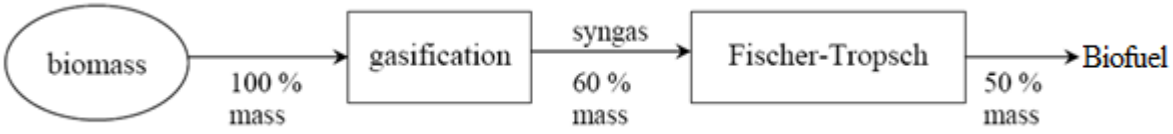

Figure 1. Biofuel from biomass gasification and Fischer-Tropsch synthesis of biomass[37]

Syntroleum[39] and Sasol[40] have independently produced biofuels based on gas-to-liquid (GTL) Fischer-Tropsch (FT) processes of cellulose plants. FT synthetic crude oil is sulfur free, nitrogen free and residues with little heteroatom contamination, making its purification and separation less complicated than that of crude oil[41]. To obtain biofuel, the biomass must undergo a chemical conversion before the FT process. Although there are varieties of conversion processes, it is normally assumed that the biomass is converted exclusively through gasification and then Fischer-Tropsch synthesis, which is one of the best options for the production of biofuel, especially biojet fuel that is currently commercially available. Figure 1 is a general flow diagram of this conversion process.

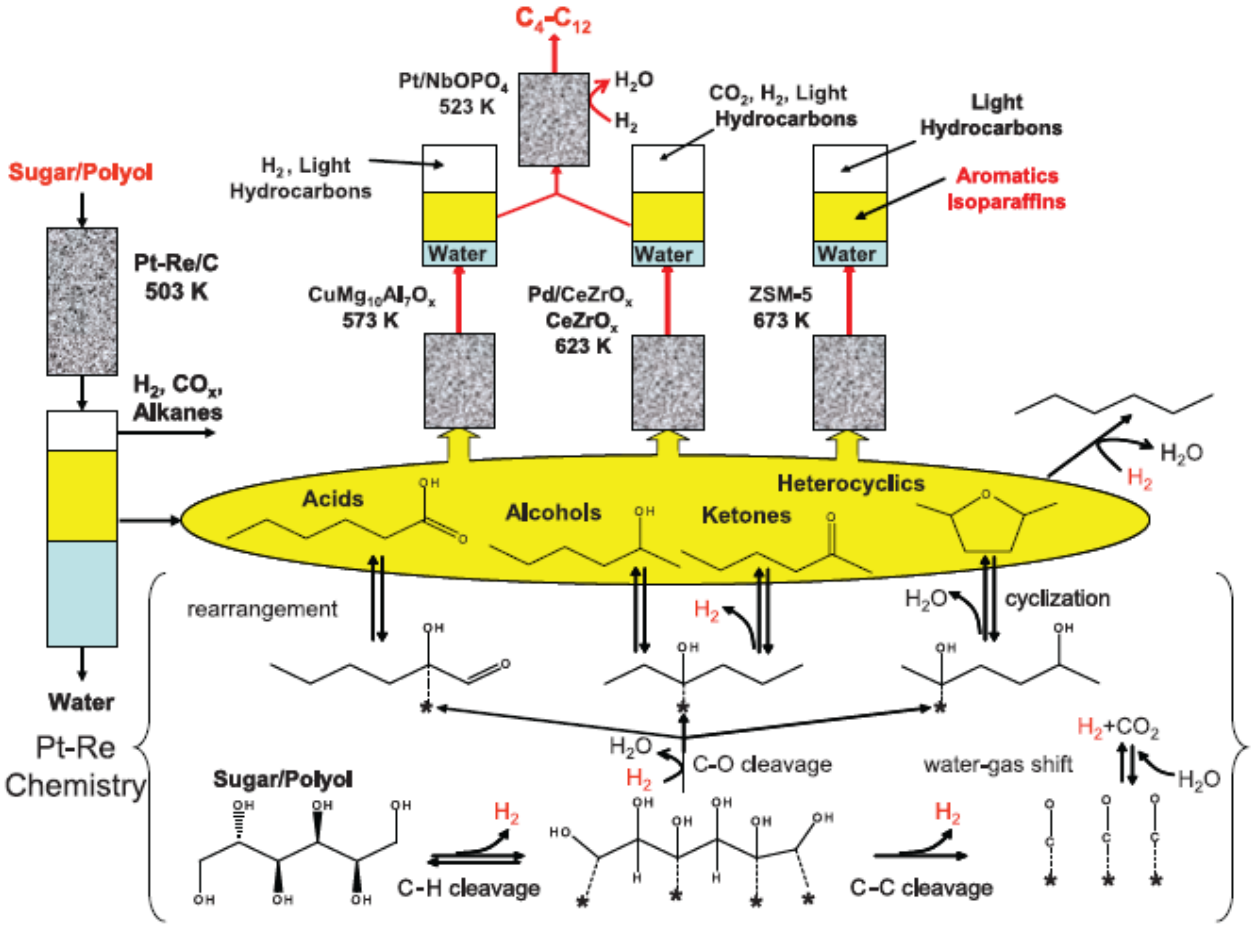

Figure 2. Schematic representation of reactor sequence and proposed chemistries used to generate monofunctional organic compounds from catalytic processing of sorbitol or glucose, providing a platform for the production of liquid transportation fuels[38]

Most recently, Kunkes[38] report a catalytic approach for the conversion of carbohydrates (sugars and polyols) to specific species of hydrocarbons which can be used as liquid transportation fuels. The approach can be modified for the production of shorter chain, branched hydrocarbons and aromatic compounds in gasoline, or longer-chain, less highly branched hydrocarbons in diesel and jet fuels. It begins from converting sugars and polyols over a Pt-Re catalyst to form primarily

ketones, carboxylic acids, hydrophobic alcohols, and heterocyclic compounds as shown in Figure 2. Promising yields of mono-functional hydrocarbons were achieved by this method. However, the process is still not economical for commercialization mainly because of the large numbers of processing steps.

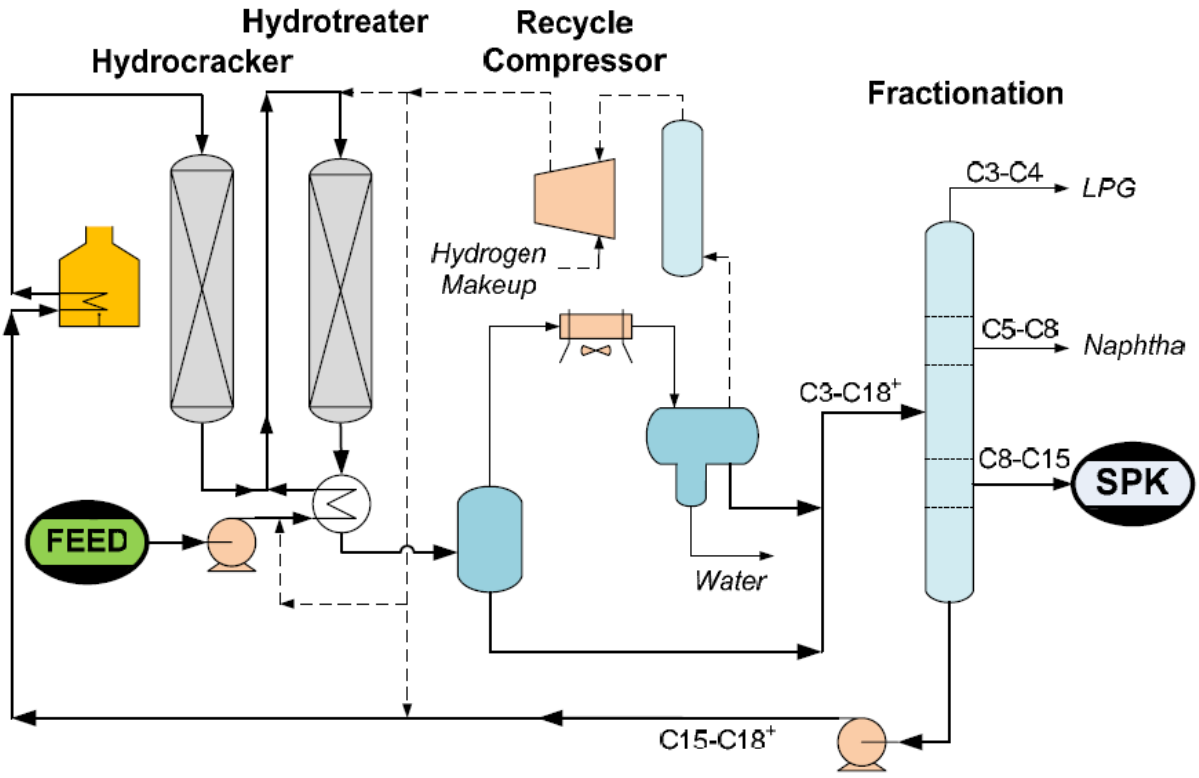

Figure 3. Bio-Synfining™ process[37]

Nowadays, many researchers are concentrating on developing alternative biofuels from plant oils and animal fats to replace commercial petroleum products in the future. Several patents[42-45] were published within the field discussing the process for production of biofuels from these resources in recent years. Bio-Synfining™ is a low capital cost process developed by Syntroleum[46] for producing high quality synthetic paraffinic kerosene (SPK) from bio-renewable feeds such as fats, greases, and algae oils. As shown in the schematic flow diagram of Figure 3, the Bio-

Synfining™ configuration for SPK is a simple single-train hydroprocessing unit which processes the biomass with heat, hydrogen and proprietary catalysts. Pre-treated bio-feed is combined with the hydrocracker effluent which acts as solvent/diluent for the exothermic hydrotreater reactions. After separation from hydrogen and light hydrocarbons, the reaction products are transferred to fractionation. UOP LLC, a Honeywell company, also developed a process to produce green jet and diesel fuels from natural, renewable, fats and oils, based on UOP's over 90 years of experience in technology for the refining industries. However, since certification and commercialization must happen for these fuels to be used on a widespread basis, it may still be several years before this kind of alternative fuels can be applied on the commercial market.

2.2 Renewable sources for biofuels

Biomass-derived oils can be obtained from many sources, such as animal fats, plants and microbial plants. Each source has advantages and disadvantages in terms of availability and cost. Those that are already grown widely and used for some form of bioenergy or biofuel production are called 1st generation feedstocks. Most of them present food versus fuel conflicts. At present, 2nd generation non-food biomass sources are being explored for biofuel production.

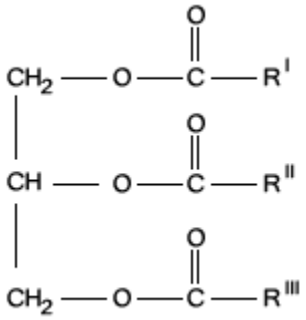

Figure 4. Chemical structure of triglyceride

Table 1. Chemical structure of common fatty acids

Fattycacidc	Systematiccname	Structure	Formulae
Lauric	Dodecanoic	12:0	$C_{12}H_{24}O_2$
Myristic	Tetradecanoic	14:0	$C_{14}H_{28}O_2$
Palmitic	Hexadecanoic	16:0	$C_{16}H_{32}O_2$
Stearic	Octadecanoic	18:0	$C_{18}H_{36}O_2$
Arachidic	Eicosanoic	20:0	$C_{20}H_{40}O_2$
Behenic	Docosanoic	22:0	$C_{22}H_{44}O_2$
Lignoceric	Tetracosanoic	24:0	$C_{24}H_{48}O_2$
Oleic	cis-9-Octadecenoic	18:1	$C_{18}H_{34}O_2$
Linoleic	cis-9,cis-12-Octadecadienoic	18:2	$C_{18}H_{32}O_2$
Linolenic	cis-9,cis-12,cis-15-Octadecatrienoic	18:3	$C_{18}H_{30}O_2$
Erucic	cis-13-Docosenoic	22:1	$C_{22}H_{42}O_2$

Table 2. Fatty acid composition of vegetable oils

Vegetable oil	Fatty acid composition, wt.%									
	14:0	16:0	18:0	20:0	22:0	24:0	18:1	22:1	18:2	18:3
Corn (Maize Oil)	0	11	2	0	0	0	28	0	58	1
Cottonseed	0	28	1	0	0	0	13	0	58	0
Crambe	0	2	1	2	1	1	19	59	9	7
Linseed	0	5	2	0	0	0	20	0	18	55
Peanut	0	11	2	1	2	1	48	0	32	1
Rapeseed	0	3	1	0	0	0	64	0	22	8
Safflower	0	9	2	0	0	0	12	0	78	0
H.O. Safflower	Trace	5	2	Trace	0	0	79	0	13	0
Sesame	0	13	4	0	0	0	53	0	30	0
Soy bean	0	12	3	0	0	0	23	0	55	6
Sunflower	0	6	3	0	0	0	17	0	74	0

First-generation feedstocks are primarily cereal and oilseed food crops, such as corn (*Zea mays L.*) starch, sugarcane (*Saccharum officinarum L.*), soybean (*Glycine max L.*) oil, rapeseed (*Brassica napus L.*), etc. Vegetable oils are especially ideal candidates for the production of biodiesel and

biojet, because they are made up primarily of 90 to 98% triglycerides, which contain a glycerol group that has three fatty acid chains attached to it (Figure 4). Fatty acids in the triglyceride molecule vary in their carbon chain length and in the number of double bonds. Table 1[47] shows the structures of common fatty acids. The fatty acids which are commonly found in vegetable oils are stearic, palmitic, oleic, linoleic and linolenic[48]. Tables 2 summarize the fatty acid composition of some vegetable oils[49]. The remainder (2~10%) of vegetable oils is made up of mono- and diglycerides, as well as free fatty acids (generally 1 to 5%), phospholipids, phosphatides, carotenes, tocopherols, sulfur compounds and traces of water.

Due to the large selection of normal plant oils that can be used to produce jet fuel products, the choice of feedstock may depend significantly on the grain growing patterns of the local region to reduce tariffs and transportation costs. For example, in the United States, because of the climate and soil conditions, soybean oil is produced in a higher quantity than many other plant oils[48]. This makes soybean oil the most logical choice of feedstock in this region. Shown below in Figure 5 is the soybean production from 2000 to 2009[50].

In order to meet growing biofuel demand without compromising valuable food, land and water resources, the development and use of second and even third generation feedstock like algal oils is necessary. There are several leading candidate energy crops for biofuel production, such as jatropha, halophytes, camelina and algae. For example, Jatropha is a drought tolerant, pest resistant, perennial shrub in the Euphorbiaceae family, native to Mexico and Central America, and also being naturalized in many tropical and subtropical areas, including India, Africa, and North America. There is up to 27-40% oil content in its seeds[51]. The seeds' oil contents and physical–chemical properties of two genus of the Jatropha family, the *Jatropha gossypiifolia (JG)* and *Jatropha curcas L. (JC),* are presented in Table 3[52]. The oil can be combusted directly as fuel without being refined,

and byproducts make suitable organic fertilizers and insecticides. Currently, the oil from Jatropha curcas seeds is used to make biodiesel in the Philippines and in Brazil, where it naturally grows. Moreover, jatropha oil is being proposed as an easily grown biofuel crop in many projects all over India and other developing countries [52] and yield-limiting asynchronous seed maturation[53] .

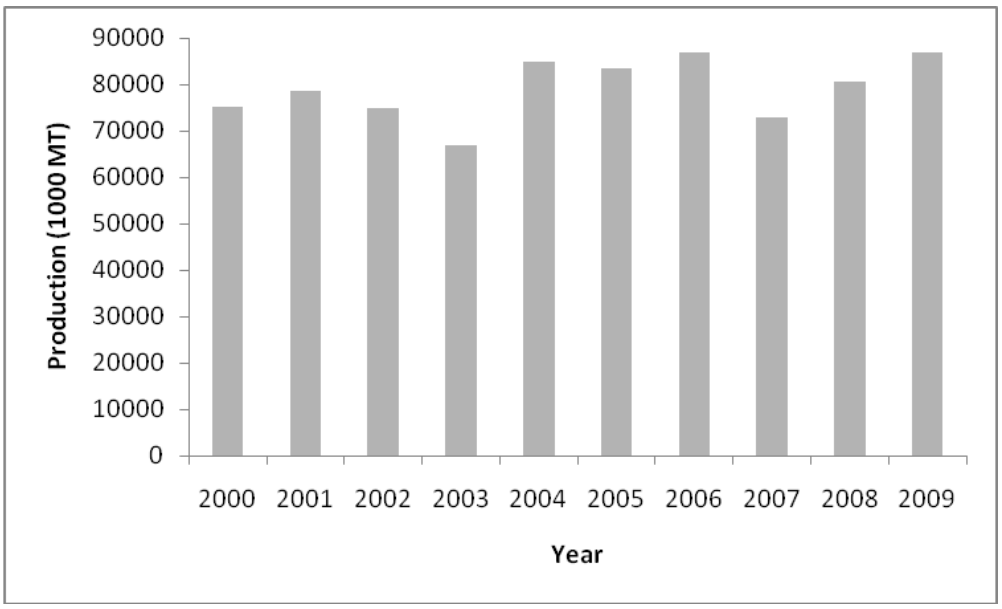

Figure 5. United States Soybean Production

Algae are another example of promising biomass feedstock. Algae are small biological factories that transform carbon dioxide and sunlight into energy through photosynthesis and grow their weight several times a day. The yield of algae can be up to 20 and 200 times more oil/acre than palm and soy, respectively. Algae are exceedingly high in oil content, with average lipid contents up to 90% of dry weight under ideal conditions [54].

Table 3. J. curcas L. (JC) and J. gossypiifolia (JG) seeds' oil contents and physical–chemical properties of the oils

Property	Jatropha gossypiifolia (JG)	Jatropha curcas L. (JC)
Density at 15 ^{o}C (g/cm^{3})	0.8874	0.8826
Kinematic viscosity at 40 ^{o}C (cSt)	3.889	4.016
Water content (w/w %)	0.020	0.003
Conradson carbon	0.3666	0.0223
Pour point (^{o}C)	-6	-5
Flash point (^{o}C)	133	117
Cupper strip corrosion	1a	1a
Ash content (w/w %)	Not detected	Not detected
Calorific value (MJ/kg)	40.32	41.72

Algae oils are long-chain polyunsaturated fatty acids and differ from those of animal and vegetable sources. The oils can be converted into biodiesel or jet fuel. In 2009, Trimbur *et al.*[55] described a method for genetic modification of microalgae including *Chlorella* and similar microbes to provide organisms which have characteristics to facilitate the production of lipid suitable for conversion into renewable diesel, jet fuel, or other hydrocarbon compounds by fluid catalytic cracking (FCC) and hydrodeoxygenation (HDO) methods. The fuel from algae is called

algae fuel, also called algal fuel, oilgae[56,] algaeoleum or third-generation biofuel[57]. However, there are no commercialized algae oils at present because of the low yield and high production cost. The first commercialized microbial oils in 1985 was unsuccessful[58], but infrastructure requirements and cost competitiveness remain largely prohibitive.

2.3 Hydrotreating catalysts

Commercial catalysts for hydroprocessing are conventional Mo- or W-based sulfides promoted with Ni or Co supported on γ-Al_2O_3. Most of the patents published[42, 43, 45, 55, 59, 60] related to biofuel production from biomass hydroprocessing use conventional sulfided metallic catalysts. Many hydroprocessing catalysts have been reported using amorphous mixed oxides-$SiO_2 \cdot Al_2O_3$ as the supports because of its high acidity and low cost. However, the cracking activities of the amorphous oxide supported catalysts are much lower than those of the zeolite containing catalysts[61]. Plant oils have been reportedly converted to fuels and chemicals over different zeolites[62-64]. It was reported[64] that the de-aluminated ultra stable Y (USY) zeolite gave the highest selectivity for kerosene and diesel-range hydrocarbons, which is also most successfully applied in industrial hydrocracking. The chemical formula of zeolite Y is $0.9\pm0.2NaO:(Al_2O_3):wSiO_2:xH_2O$, where $3<w\leq6$ and $0\leq x\leq9$. Typical NaY zeolite has a Si/Al molar ratio of 5.0 or greater. Commercially made NaY has a unit cell size of 24.65-24.70 Å, a surface area of >800 m^2/g, and a crystallite size in the range of 0.5-3 microns. The de-aluminated ultra stable Y was obtained by hydrothermally treating ammonium exchanged Y zeolite at about 600 °C in the presence of steam to reduce framework Al content[65, 66].

Group VIB and VIII metals have been used in industrial hydroprocessing catalysts. Sulfided Ni/Mo and Ni/W combinations are the most commonly used base metal systems, which function well in the typical hydroprocessing reaction environment where high concentrations of H_2S, NH_3 and H_2O are generated from their organic precursors present in the feedstock. The concentration of

base metals in hydroprocessing catalysts varies from 1 to 6 wt-% for Ni and from 8 to 20 wt-% for W, which are needed to be maintained in their sulfided form in order to be active at process conditions, and therefore a small H_2S co-feed is commonly added. However, for it is necessary to decrease the use sulfur, particularly because of environmental reasons, these catalysts are not desired. Further, the products from the above mentioned processes are mainly n-paraffins which solidifies at subzero temperatures. So, they are unsuitable for production of high quality diesel, kerosene and gasoline fuels[26]. Patent FI 100248[67] describes a two-step process for producing middle distillate from vegetable oil by hydrotreating fatty acids or triglycerides in vegetable oils using commercial sulfur removal catalysts (NiMo and CoMo) to give n-paraffins and then by isomerizing above mentioned n-paraffins using metal containing molecule sieves or zeolites to obtain branched-chain paraffins. The process was conducted at the reaction temperatures of 330-450 °C.

Noble metals can also be used in hydroprocessing catalysts and exhibit much higher metal activities than the sulfided base metal catalysts in a clean reaction environment although not being used so widely as the base metals[68]. In Alafandi's invention, it was found that the hydroprocessing catalysts, when combined with a catalyst promoter chosen from the group of the noble metals, palladium or platinum, results in a high catalyst activity. Miller[69] invented a process for hyroprocessing free fatty acids derived from triglyceride-containing, biologically-derived oils to obtain biofuels over the hydroprocessing catalyst which is selected from the group consisting of cobalt-molybdenum (Co-Mo) catalyst, nickel-molybdenum (Ni-Mo) catalyst, noble metal catalyst, and combinations thereof. Hydroprocessing conditions generally include temperatures in the range 350 °C-450 °C and pressure in the range of 4.8 MPa to 15.2 MPa. However, there is no direct application of noble metals for jet fuel production from vegetable oil or animal fat hydroprocessing.

With more strict limitations on fuels, such as lower allowable limits for toxic elements such as sulfur and nitrogen, the application of metallic nitride and carbide catalysts for hydroprocessing has been attracting a lot of researchers' attention. In the review by Furimsky[27], many important topics about metallic carbide and nitride catalysts were addressed, such as catalysts structure, preparation techniques, hydrogen adsorption and catalyst activity and stability. It was emphasized in this review that the carbides and nitrides of Mo and W can absorb and activate hydrogen. The effects of particle size and surface area on the total amount of absorbed hydrogen differ from those observed for transition metal sulfides. For metal carbides and nitrides, the amount increases with increasing particle size and/or decreasing surface area as a result of the involvement of the sub-surface regions of the crystallites during hydrogen adsorption. The activity for hydrogenation, hydrodesulfurization and hydrodenitrogenation exhibits similar trends. These catalysts are stable under typical hydroprocessing conditions although a partial sulfidation of their surface during HDS cannot be avoided. The most common and most successful transition metal used in these catalysts was molybdenum. Tungsten also showed potential to be a good transition metal in metallic nitride and carbide catalysts, as did vanadium, iron and nickel when used in specific applications. In Sulimma's work[70], six γ-Al_2O_3 supported metallic nitride and carbide catalysts (molybdenum (Mo) carbide and nitride, tungsten (W) carbide and nitride, and vanadium (V) nitride and carbide) were chosen for a screening test to produce a diesel fuel cetane enhancer from canola oil. It was found that the supported molybdenum nitride catalyst demonstrated superior performance when converting canola oil into a diesel fuel cetane enhancer as compared to five other supported metallic carbide and nitride catalysts.

2.4 Hydrotreating mechanism and kinetics

In a fixed bed hydrotreating process, the reactions take place in a three-phase system: the liquid feed trickles down over the solid catalyst in the presence of a hydrogen-rich gas phase. The reaction pathway includes the hydrogenation of the C=C bonds of the vegetable oils and then followed by oxygen removal to produce alkanes through three different pathways: decarbonylation, decarboxylation and hydrodeoxygenation. Then the straight chain alkanes undergo isomerization and cracking to produce lighter hydrocarbons (C5 to C16) with some degree of branching. The major reactions in the process are given below[71]:

- Olefin Saturation

- Decarboxylation/Decarbonylation

$$RCOOH \xrightarrow{Catalyst} RH + CO_2 \quad (1)$$

$$RCOOH + H_2 \xrightarrow{Catalyst} RH + CO + H_2O \quad (2)$$

$$CO + H_2O \underset{}{\overset{Catalyst}{\rightleftharpoons}} CO_2 + H_2 \quad (3)$$

- Hydrodeoxygenation

$$RCOOH + 3H_2 \xrightarrow{Catalyst} CH3R + 2H_2O \quad (4)$$

- Hydroisomerization

$$n\text{-}RH \xrightarrow[Catalyst]{H_2} iso\text{-}RH \quad (5)$$

- Hydrocracking

$$iso\text{-}RH \xrightarrow[Catalyst]{H_2} iso\text{-}R_1H + iso\text{-}R_2H \quad (6)$$

During the hydroprocessing, the cracking and hydrogenation reactions take place simultaneously on a dual function catalyst, in which the acid sites of the catalyst are necessary for isomerization and cracking activities while the metallic sites are required for hydrogenation and dehydrogenation reactions. Though the overall reaction of the hydrotreating of triglycerides was carried out as early as 1980s[72, 73], the mechanism and kinetics of the process are still under investigation because of its complexity.

In 2009, Donnis et al.[74] studied how the three carboxylic acids of triglycerides are stepwise liberated and hydrogenated into linear alkanes of the same length or one carbon atom shorter. In order to understand the reaction routes, the researchers used both model compound (methyl laurate) tests and real feed tests with mixtures of straight-run gas oil and rapeseed oil. Schematic representation of the two different mechanisms for the removal of triglyceride oxygen by hydrotreating is shown in Figure 6. The mechanism showed by the unbroken red lines in Figure 6 indicates the hydrogenation/hydrodeoxygenation (HDO) reaction, in which it was proposed that the oxygen was removed as a form of water. By the other mechanism exemplified by the blue lines, which is usually called decarboxylation or decarbonylation, the triglyceride is converted into propane, carbon dioxide and/or carbon monoxide and into an n-alkane one C-atom shorter than the total length of the fatty acid.

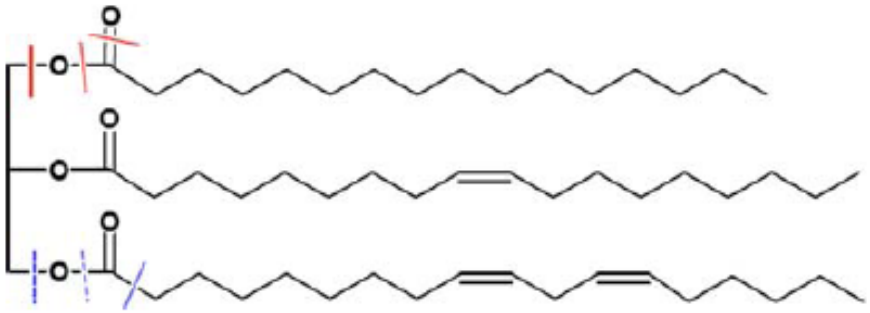

Figure 6. Schematic representation of the two different reaction pathways for the removal of triglyceride oxygen by hydrotreating[74]

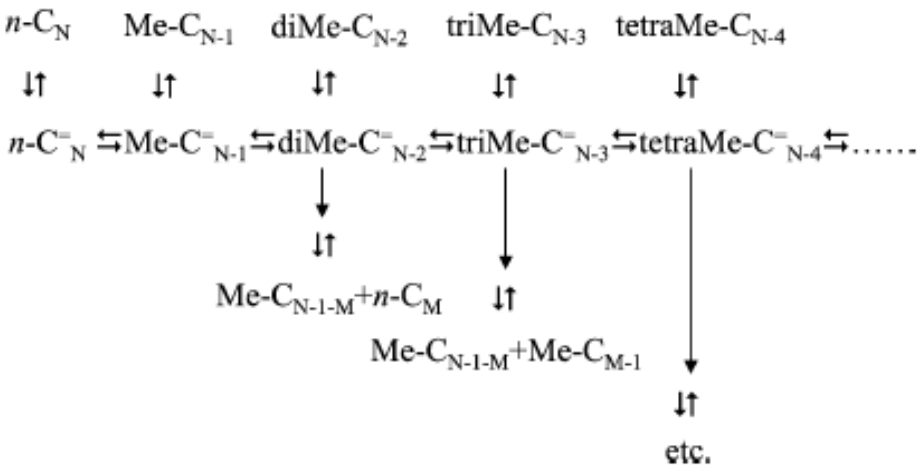

Figure 7. n-Alkane hydroconversion mechanism: n-alkane feed and hydroisomerization products (top) dehydrogenate into alkene intermediates (vertical⇆, e.g., Pt catalyzed). Alkenes hydroisomerize in a chain of acid-catalyzed hydroisomerization reactions (horizontal⇆). With increasing degree of branching it is increasingly more likely that isomers crack (vertical→, acid catalyzed) and hydrogenate into a smaller alkanes (vertical ⇆, e.g., Pt catalyzed)[75]

After the thermal breakdown and oxygen removal of the triglyceride molecule, the heavy hydrocarbon compounds are then cracked into paraffins and olefins as a result of thermal and catalytic mechanisms. During the process, an n-alkane can be hydroisomerized with some degree of

branching, which can be described as illustrated in Figure 7 if only considering methyl group branches for simplification

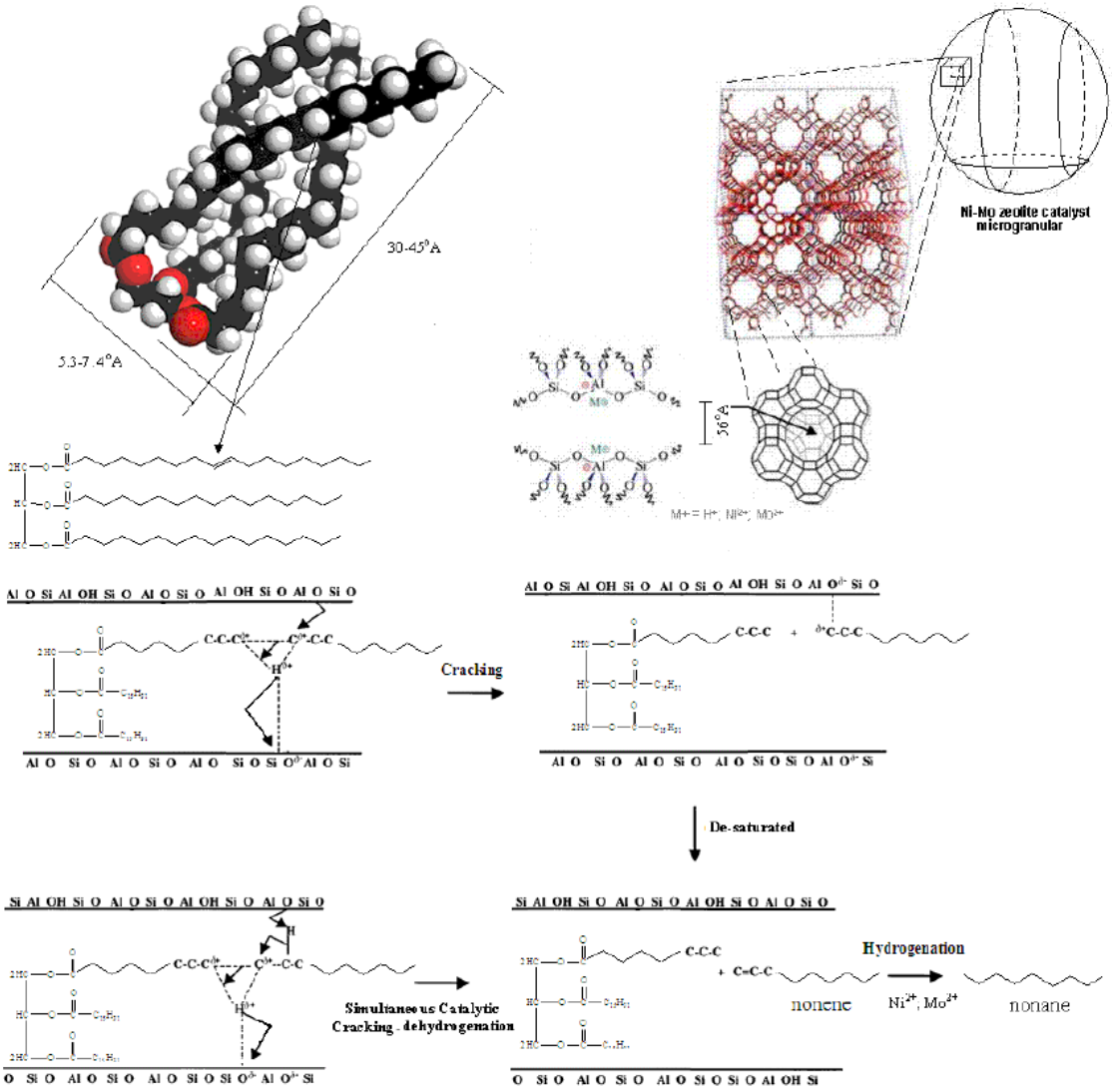

Figure 8. Expected mechanism of the simultaneous catalytic cracking and hydrogenation reaction[76]

In order to investigate the overall reaction mechanism of the triglyceride hydroprocessing, Nasikin et al[76] studied the palm oil hydrotreating process using a liquid phase batch reactor at atmospheric pressure with the presence of hydrogen gas over NiMo/zeolite catalyst. The expected

reaction mechanism above is illustrated in Figure 8. It can be seen that the triglyceride molecule was able to enter the zeolite catalyst pore first and then cracked because its longitudinal section diameter (around 5.3- 7.4°A) and chain length (around 30-45°A) was smaller than the catalyst pore (±0.56°A, diameter). And then the metallic sites of the catalyst saturated the double bond in the nonene molecules that was removed from catalyst pore to form more stable molecules (nonane).

The kinetics of triglyceride hydroprocessing is poorly understood and general rate equations are not available because of the complicated reaction mechanism. Only considering the two oxygen removal reactions during the hydroprocessing: hydrodecarboxylation (HDC) and hydrodeoxygenation (HDO), completed by water–gas-shift reaction and CO formation, Smejkal *et al.*[77] presented a methodology of thermodynamic data estimation and predicted a thermodynamic model for vegetable oil hydrogenation over commercial hydrotreating and hydrogenation catalysts (Ni-Mo/Al_2O_3 and Ni/Al_2O_3, respectively). Reaction enthalpy ΔH_r^T at temperature T can be recalculated as

$$\Delta H_r^T = \Delta H_r^\circ + \int_{298}^{T} c_{p,T}\,dT \rightarrow \Delta H_r^T = \Delta H_r^\circ + \overline{c_{p,T}}(T - 298) \qquad (7)$$

Where ΔH_r^0 is standard reaction enthalpy, $c_{p,T}$ heat capacity, and $\overline{c_{p,T}}$ average heat capacity

For entropy of the reaction system, a similar calculation is defined

$$\Delta S_r^T = \Delta S_r^\circ + \int_{298}^{T} \frac{c_{p,T}}{T}\,dT \rightarrow \Delta S_r^T = \Delta S_r^\circ + \overline{c_{p,T}} \ln\left(\frac{T}{298}\right) \qquad (8)$$

The model predictions are in a good agreement with experimental data. Additionally, the estimations suggest that the reaction is limited by hydrogen transfer.

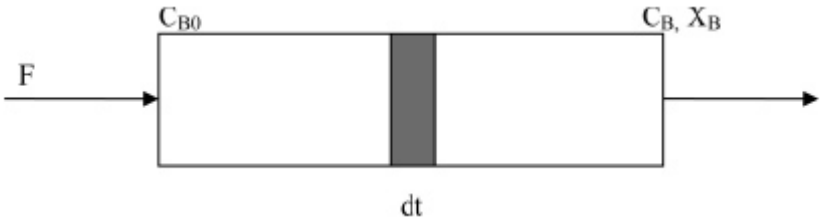

Figure 9. Schematic diagram of the reactor[78]

In 2005, Charusiri *et al.*[78] investigated the kinetic model for the catalytic cracking of used vegetable oil to become liquid fuel over sulfated zirconia. The conversion was performed in a 70 cm^3 batch micro-reactor by varying the factors of temperature (over a range of 400-430 °C), reaction time (over a range of 30-90 min), and initial hydrogen pressure (over a range of 10-30 bar) over sulfated zirconia. A 2^k factorial experimental design was used to investigate the parameters that affect the gasoline fractions. Figure 9 is the schematic diagram of the reactor.

The rate equation for the gray part of the reactor, depicted in Figure 11, was simplified as

$$-r_{\mathrm{B}} = -\frac{\mathrm{d}C_{\mathrm{b}}}{\mathrm{d}t} = k_n C_{\mathrm{B}}^n \qquad (9)$$

If a first-order reaction is considered, the following is obtained after the integration:

$$\ln(C_{\mathrm{B}}) = \ln(C_{\mathrm{B0}}) - k_1 t \qquad (10)$$

If it is a second-order reaction, then the following is obtained:

$$\frac{1}{C_{\mathrm{B}}} = \frac{1}{C_{\mathrm{B0}}} + k_2 \mathrm{t} \qquad (11)$$

Though some work in this area has been done as described above, the kinetic and mechanistic aspects need to be investigated further along with the role of the catalyst in determining the product selectivity. Additional information is needed to define the mechanisms and rate determining steps more precisely.

CHAPTER 3. PRODUCT ANALYSIS METHOD DEVELOPMENT

3.1 Analysis of Sterol Glycosides in Biodiesel and Biodiesel Precipitates*

3.1.1 Introduction

Biodiesel is attractive as an alternative fuel mainly because it is renewable, biodegradable and environmentally friendly, and also can be manufactured from common feedstocks, such as vegetable oils and animal fats. Biodiesel is produced by the transesterification of fats and oils with an alcohol using a base catalyst. The properties of biodiesel are affected by the by-products of the transesterification reaction, such as water, free and bonded glycerides, free fatty acids, catalyst, residual alcohol, and unsaponifiable matter (plant sterols, tocopherols and hydrocarbons)..

Sterols are some of the most common minor components distributed in animal fats and vegetable oils and are found in many forms, such as free sterols, acylated (sterol esters), alkylated (sterol alkyl ethers), sulfated (sterol sulfate), or linked to a glycoside moiety (sterol glycosides) which can be itself acylated (acylated sterol glycosides) [79-81]. Among the several common sterols, sterol glycosides have been found to be a major component of biodiesel precipitates [82-84] . In plant tissues and in vegetable oils, sterol glycosides occur naturally as both sterol glycosides (SG) and acylated sterol glycosides (ASG). During the transesterification process, acylated sterol glycosides can be converted into sterol glycosides due to the alkaline catalysts. Therefore, the SG concentration in biodiesel is normally higher than that in the feedstock oils. The polar SG in biodiesel may change the crystallization onset temperature and cause the formation of cloud-like

*"This work was published in Journal of the American Oil Chemists Society, 87 (2):215-221. (2009)

agglomerates of various sizes composed of discrete 10 to 15 micron particles even at room temperature and at relatively low levels (35 parts per million or higher) [85].

Gas chromatography (GC) has been broadly applied to identify and quantify minor components in biodiesel due to its relatively high sensitivity and accuracy. Gas chromatography (GC) with flame ionization detection (FID) is a test method standardized by ASTM D6584 to determine the free and total glyceride contents in biodiesel, through which the amount of free and total glyceride in the range of 0.005 to 0.05 mass % and 0.05 to 0.5 mass % can be detected, respectively. A detailed test procedure according to ASTM D 6584 with GC-FID was reported by Ruppel et al. [86]. Recently, a GC method for the quantitative evaluation of sterol glucoside (SG) concentrations in biodiesel precipitates was presented by Bondioli *et al*[82]. However, the GC method has certain disadvantages in biodiesel analysis. First of all, due to low volatilities, most of the samples must be derivitized by silylating reagents such as N-methyl-N-trimethylsilyltrifluoroacetamide (MSTFA) or N,O-bis (trimethylsilyl)trifluoroacetamide (BSTFA) before the analysis. Secondly, different internal standards are required for different feedstocks in the quantification analysis when applied to biodiesel analysis. Last, but not least, the accuracy of GC analyses is susceptible to many factors such as baseline drift, overlapping signals, and auto-oxidation of standards and samples.

As an alternative to GC, high performance liquid chromatographic (HPLC) methods have been developed for analyzing transesterification reaction mixtures [87-90] because of advantages such as no derivatization of samples, shorter analysis times, and direct applicability to most biodiesel fuels and all neutral lipid classes. The early literature related to biodiesel analysis with HPLC [88] used an isocratic solvent system (chloroform with an ethanol content of 0.6%) on a cyano-modified silica column coupled to two GPC columns with density detection to detect mono-, di- and tri- glycerides as well as methyl esters. The method can be used for monitoring conversion degree of the

transesterification reaction. A recent paper [91] proposed a binary gradient method using non-aqueous reverse phase HPLC with a UV detector to analyze the monoglycerides (MGs), fatty acid methyl esters (FAMEs), diglycerides (DGs) and triglycerides (TGs) in biodiesel mixtures. There are also several other publications[92-94] which describe the application of HPLC in the monitoring of biodiesel products and production process. Qualitative and quantitative analysis with these HPLC methods were provided without saponification and off-line pre-separation.

Though HPLC has many advantages over GC, the analysis of sterols in biodiesel by HPLC is still problematic because sterols such as cholesterol and related compounds cannot be separated very well from fatty acid methyl esters[95]. Also because of the relatively low concentrations in biodiesel and relatively low response of SG with HPLC compared to GC techniques, it is a great challenge to directly detect the SG content in biodiesel by HPLC without precipitation and extraction. In 2007, *Ringwald*[96] collected the biodiesel residue from fuel filters and analyzed it by a LC method with a silica column and an ELSD detector. The isolation of SG from the residue was done by solid phase extraction (SPE) prior to the analysis. More recently, SG content has been reported to be separated from various commercial biodiesel precipitates by HPLC coupled with different detectors [84]. After precipitation from the turbid liquids, no further purification process was performed before the normal-phase or reversed-phase HPLC. Calibration curves were reported for both ELSD and UV detectors. However, there were no further attempts to recover SG from biodiesel and determine the detection limit of SG in liquid biodiesel by these methods. In summary, all previous studies have shown that the analysis of this class of compounds in biodiesel directly by HPLC is not as successful as for biodiesel precipitates.

The main objective of this work is to apply reversed phase HPLC-ELSD for the identification and quantification of sterol glycosides in biodiesel. Compared with previous HPLC methods, there

are two major improvements with this new study. Firstly, a high carbon load C18 column, an alternative to normal C18, which has a higher sample load capacity, is used. With the higher sample load capacity, biodiesel with low SG concentration could be injected in larger amounts and without further separation. Furthermore, the high carbon load makes the column more nonpolar and, therefore, the most retentive of the reversed phases, providing good resolution of non-polar and polar compounds and allowing for higher organic solvent in the mobile phase which contributes to greater sensitivity in the LC-MS application. The second improvement of this study is to quantify the SG content in biodiesel with an HPLC-ELSD method after a simple centrifugation process. FTIR was also used to analyze the similarities and differences among SG, SBO B100, and SBO B100 precipitates before the HPLC analysis.

3.1.2 Materials

Soy oil based biodiesel (B100) was obtained from Wacker Oil Co. (Manchester, MI). The biodiesel precipitates was contributed by REG (Renewable Energy Group Inc., Ames, IA). The sterol glycosides standard (98+%) was acquired from Matreya (Pleasant Gap, PA). HPLC-grade methanol and methylene chloride were purchased from Fisher Scientific (Pittsburgh, NJ). The sterol glycoside standard and all of the biodiesel precipitates were dissolved in MeOH/CH_2Cl_2 (1:2, v/v). The precipitates were purified with various solvents by REG (Renewable Energy Group Inc., Ames, IA) and verified to be clean by FTIR in the ester and soap region before being sent to our lab. In order to obtain a higher concentration of SG in the oil, 3g of the B100 was centrifuged in a 5-mL centrifuge tube at 5000g and ambient temperature for 15 min using an Eppendorf Centrifuge 5804 R with a fixed-angle Rotor A-4-44 (Eppendorf North America, Inc., Westbury, NY). After centrifugation, the clear oil sample became turbid because the SG precipitated out. All of the solutions were filtered through the Whatman filter with 125mm diameter and the stock solutions

were stored in a refrigerator at 4°C. Before use, standard working solutions were prepared by diluting appropriate amounts of the stock solution in MeOH/ CH_2Cl_2 (1:2, v/v).

3.1.3HPLC conditions

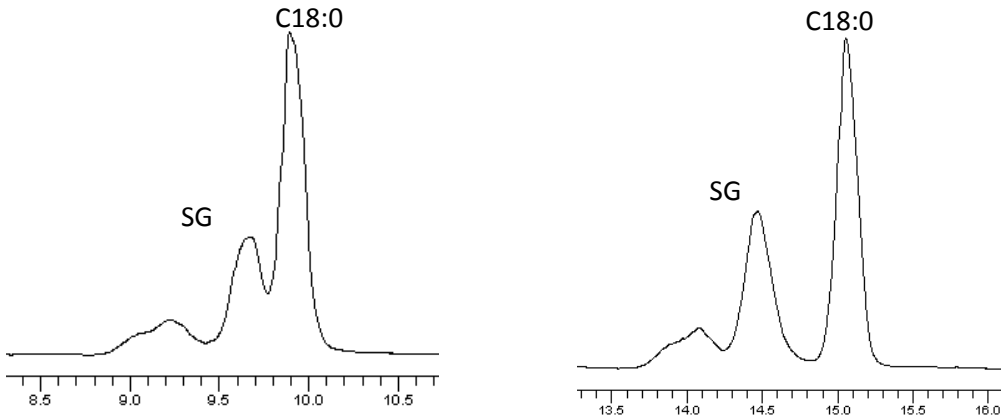

(a) (b)

Figure 10. HPLC separation of methyl stearate and SG under two gradient conditions: (a) First gradient condition; (b) Second gradient condition

The HPLC analysis was conducted using a PerkinElmer Series 200 with an Altech 3300 Evaporative Light Scattering Detector (ELSD) and a high carbon load reversed phase column—Altech C18-HL (250×4.6mm i.d., 5µm) with guard column (7.5×4.6mm i.d., 5µm) as the stationary phase. Mobile phase solvents were methylene chloride (Phase A) and methanol (Phase B). The samples were analyzed with a gradient of CH_2Cl_2/MeOH at a flow rate of 1mL/min. The column temperature was set to 25 °C and the injection volume was 20µL. Two gradient conditions were evaluated for the analysis. After 15min equilibrium at 0% (A):100% (B), the first gradient condition

was: 0% (A):100% (B) maintained for 10 min and then 0% (A):100% (B) to 50% (A):50% (B) in 10 min; in the following 4 min, 50% (A):50% (B) to 75% (A): 25% (B), and back to 100% (B) within 1 min, then the run was finished. With However, with this method, the separation of methyl stearate (C18:0) and SG was not satisfactory as shown in Fig 10 (a). Thus, the HPLC condition was optimized to the gradient condition illustrated in Table 4. With this HPLC method, good separation of methyl stearate (C18:0) and SG was obtained (Figure 10 (b)).

Table 4. Gradient Condition of the HPLC method

Step	Time (min)	Flow rate (mL/min)	A%	B%
Equilibrium	15	1	0	100
1	5	0.5	15	85
2	17	1	25	75
3	5	1	50	50
4	3	1	70	30
5	5	1	70	30

3.1.4 Results and discussion

FTIR spectra

Figure 11 shows FTIR spectra obtained from the sterol glycosides (SG) standard, SBO B100, and SBO B100 precipitates. The typical C=O stretching band of the methyl ester usually appears at 1750±50 cm^{-1}. Both SBO B100 and PBO B100 (palm oil based biodiesel) show a strong peak in this range. An -O-H stretching band around 3400 cm^{-1} in the spectrum of the SBO B100 precipitates indicates the presence of hydroperoxyl and hydroxyl groups. The spectrum of the sterol

glycosides standard in Figure 11 shows the similar -O-H stretching band and fingerprint area as that of the SBO B100 precipitates. In the spectra of both SG standard and SBO B100 precipitates, the strongest peak in the area of 1300~1000 cm^{-1} is due to the C-O moiety. Also finger print areas and the strong absorptions of the two spectra caused by CH_3 and CH_2 vibrations are similar. Therefore, from the IR spectra, it can be concluded that the major component of the precipitates from REG is SG, which is consistent with the HPLC results discussed later.

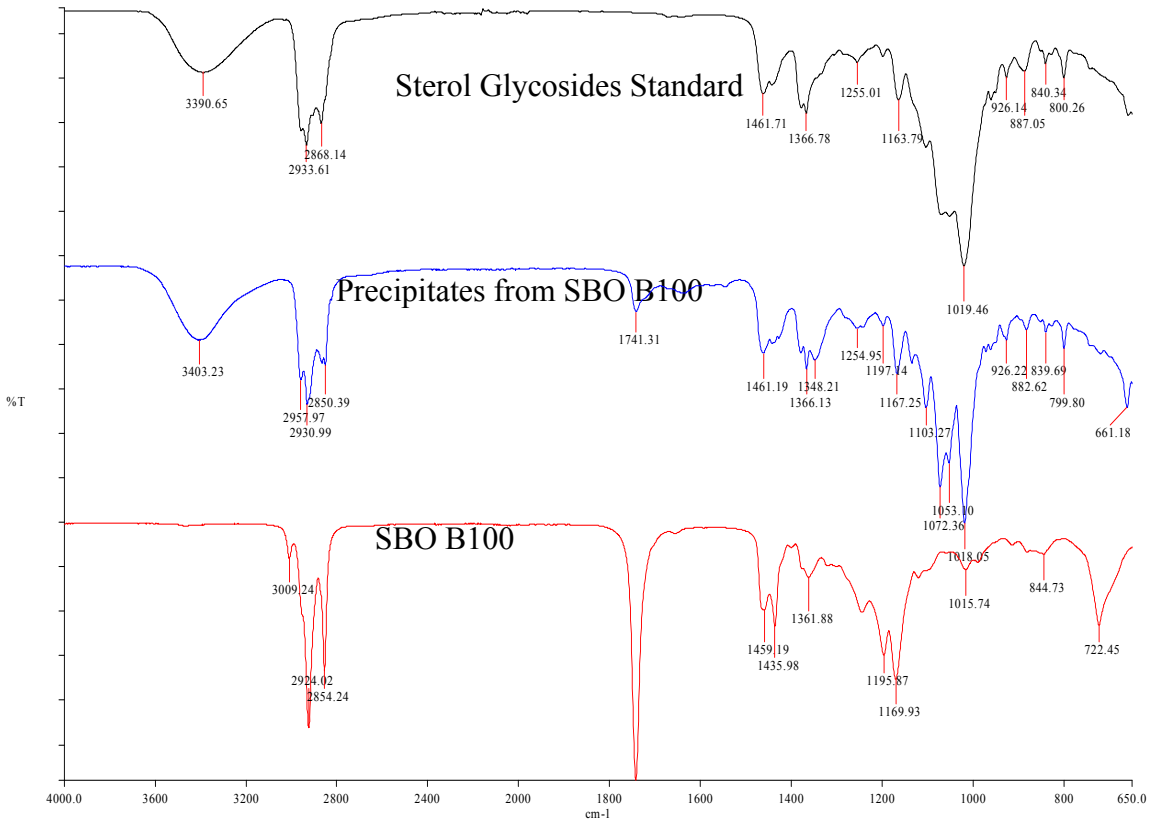

Figure 11. FTIR spectra of sterol glycosides (SG) standard, SBO B100 and SBO B100 precipitate

HPLC calibration and analysis

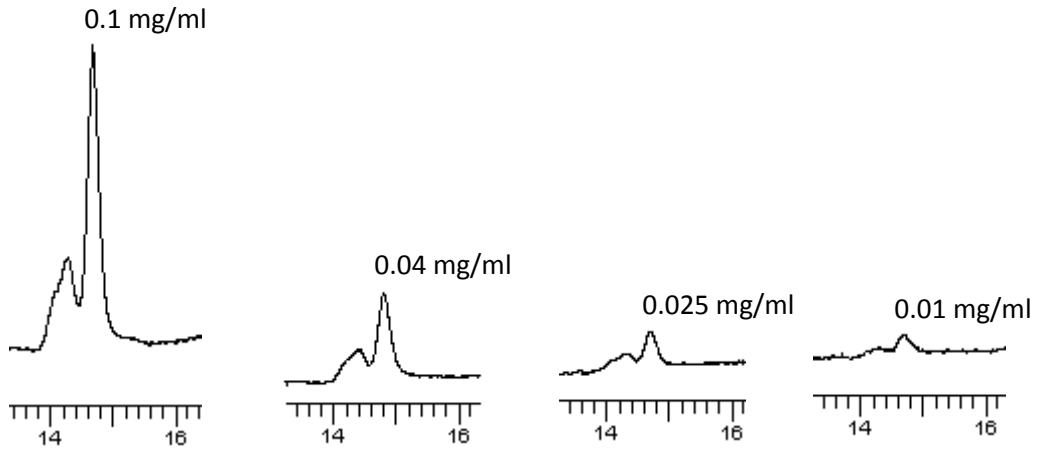

Figure 12. HPLC chromatogram of sterol glycosides standards with concentrations of 0.1, 0.04, 0.025 and 0.01 mg/ml

The retention time of SG was 14.6 min with the second gradient method. The lowest concentration of detection for SG standard was about 0.005 mg/mL. Therefore, standard solutions of sterol glycosides with concentrations ranging from 0.005 to 0.1 mg/mL were prepared for calibration. Figure 12 depicts the chromatograms of sterol glycoside standards with four concentrations including 0.1, 0.04, 0.025 and 0.01 mg/mL. With careful examination of the chromatograms, there are three peaks (of which 2 co-eluted as a peak with a shoulder and a third one was clearly separated) of SG can be observed in Figure 12. The peaks can be attributed to three steryl glycosides, namely campesteryl 3-ß-d-glucopyranoside, stigmasteryl 3-ß-d-glucopyranoside and sitosteryl 3-ß-d-glucopyranoside[97]. It can be seen that with decreasing concentration, the first two peaks decreased and almost disappeared at the low concentration of 0.01 mg/mL. In order to calculate the amount of SG in very low concentrations for which there was no detectable first peak, the calibration was based on the area of the third peak. Figure 13 shows the calibration curve of the SG based on HPLC. Because of the nonlinear concentration response of the ELSD detector[98], the

parameters of the calibration curves were obtained by fitting the experimental data points to a cubic polynomial, resulting in the fit equation: $y = 2E+09x^3 - 1E+08x^2 + 2E+07x$, where y is the peak area (mV·min) and x represents the analyte concentration (mg/mL).

Table 5. Accuracy validation of the HPLC analytic method for SG in biodiesel. The recoveries range from 75% to 99%

Sample	SG Concentration (mg/mL in	SG Concentration (w% in	Recovery
1	0.003	0.05	75
2	0.006	0.1	78
3	0.01	0.2	82
4	0.02	0.4	88
5	0.03	0.55	93
6	0.04	1.01	99

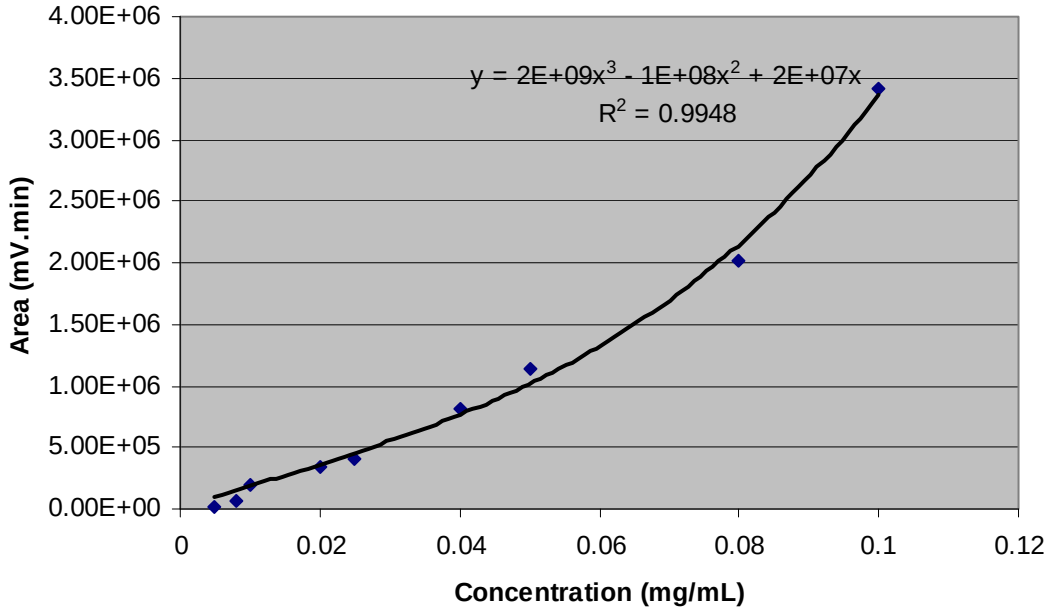

Figure 13. The calibration curve of the SG

For accuracy validation, the SG solution (0.10 mg/ml) was mixed with B100 (5.95 mg/mL) at different ratios to obtain solutions of known concentration as listed in Table 5. The recoveries are shown in the table, range from 75% to 99%. With the decreasing SG concentration, the recovery decreases. Figure14 depicts the chromatogram of the sample with 1.01% SG in B100.

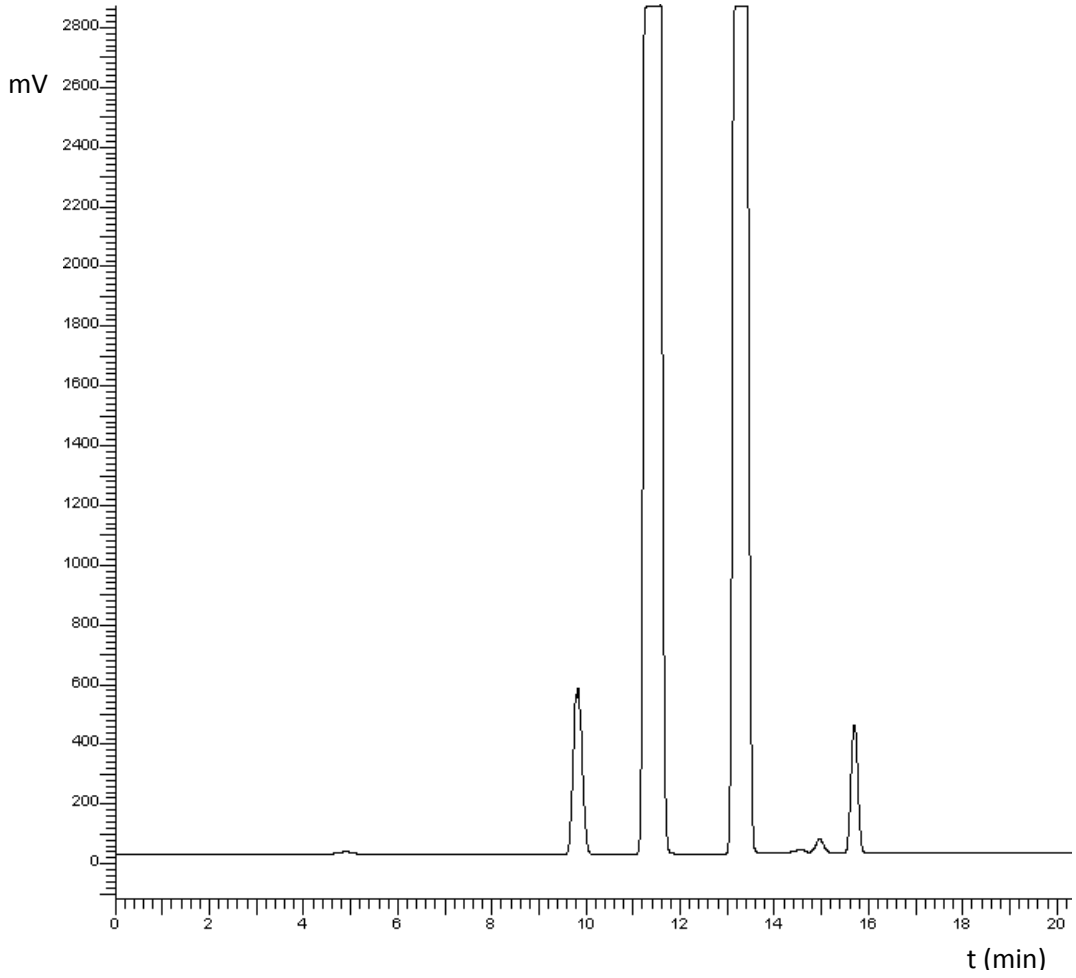

Figure 14. HPLC chromatograms of the sample with 1.01% SG in B100

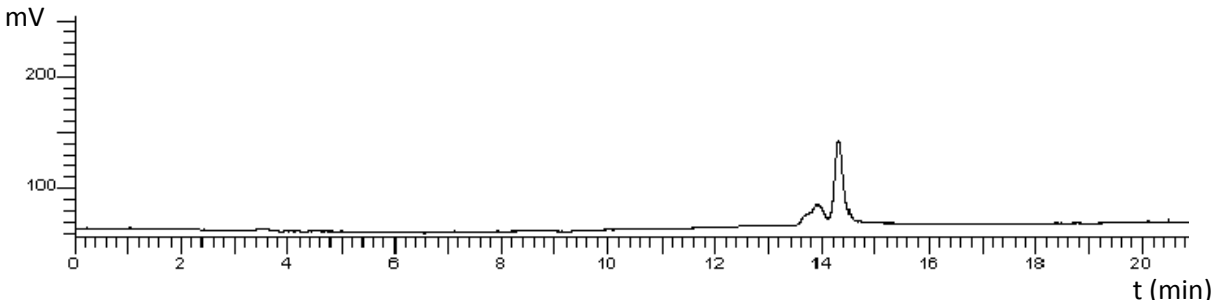

Figure 15. HPLC chromatogram of the biodiesel precipitates

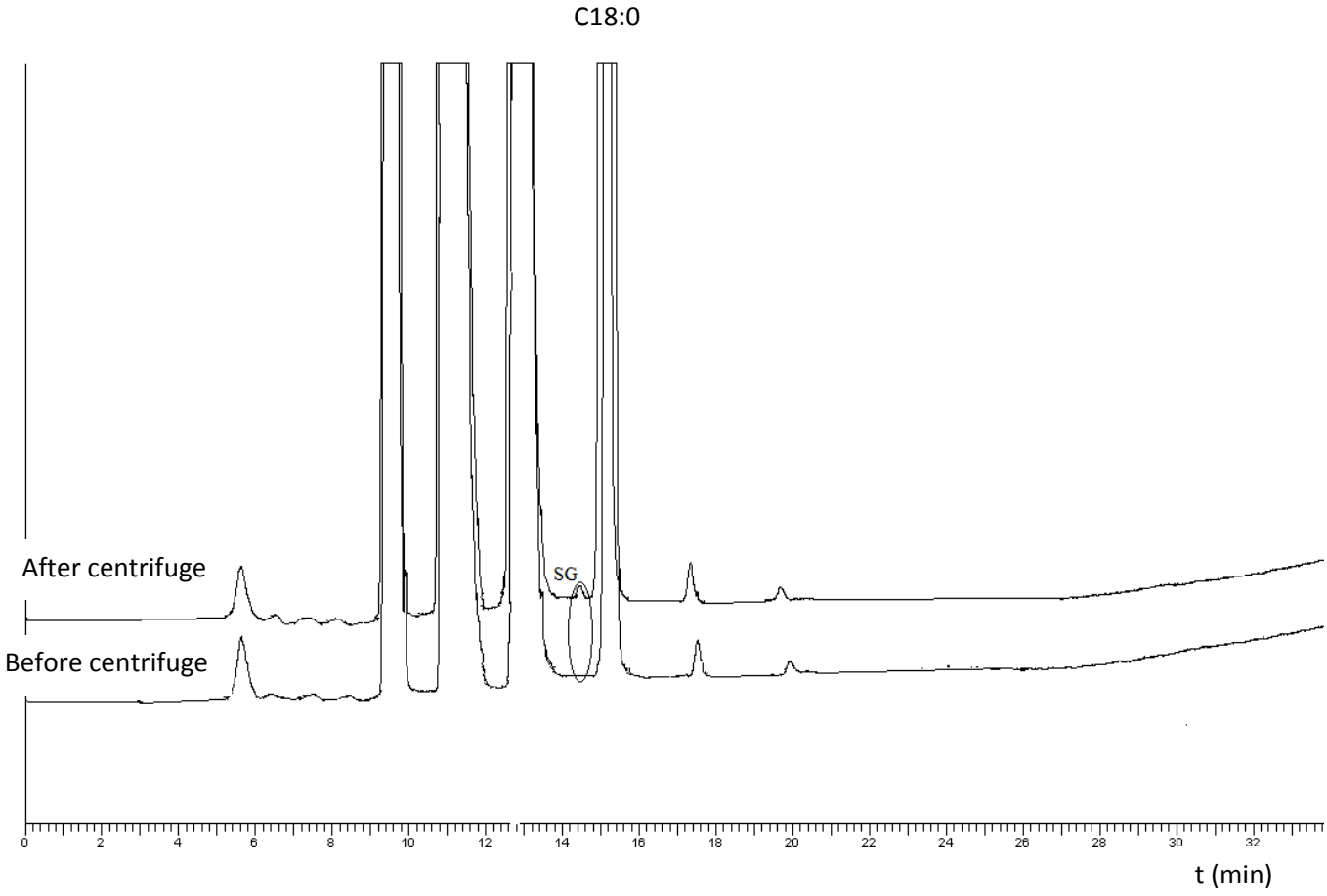

Figure 16. HPLC chromatogram of B100 before and after centrifuge

In the subsequent analysis, sterol glycosides in B100 and the precipitates were determined. Figure 15 shows the chromatogram of the biodiesel precipitates. Using this method the levels of SG in this precipitate sample were estimated to be 91.1% (w/w), SD=0.01. Figure 16 shows the chromatogram of B100 before and after centrifugation. However, no SG peak was detected in the Wacker B100 sample before centrifugation because of the low SG concentration. In order to obtain a higher concentration of SG in B100, the sample was concentrated by centrifugation and white SG particles precipitated out. Then the bottom part (around five volume percentage) of the concentrated sample was taken and stirred to form a turbid phase. It can be seen from Figure 16 that a small but obvious SG peak appears right before C18:0 in the turbid B100 sample which has concentrated SG composition. In the turbid sample, sterol glycosides were identified with an average weight concentration of 592 ppm. Because the turbid phase is roughly five volume percent of the original sample, it can be estimated that the SG concentration in the original Wacker B100 sample was about 30 ppm. Distilled soy oil based B100 was also analyzed with and without addition of SG to verify the SG position in the biodiesel chromatogram.

3.1.5 Conclusion

In this paper we have presented a study on the direct determination of the level of sterol glycosides in biodiesel by reversed phase HPLC with an Evaporative Light Scattering Detector (ELSD). The method allows the detection of concentration levels of sterol glycosides down to around 0.01 mg/mL in the solvent. Analysis of B100 with concentrated sterol glycosides showed that sterol glycosides could be separated from methyl ester peaks and quantified without separation when the amount is above the level of the detection limit. The HPLC method offers the advantage that it is a rapid method that can analyze sterol glycosides in biodiesel just after a simple centrifugation process. From the weight or volume percentage of the concentrated part, the SG

concentration in the original sample can be calculated from the one in the concentrated sample. The limitation of this method is that it is only applicable for SG concentrations in biodiesel which are higher than or equal to 30 ppm, not below this value. The centrifugation step can be studied more rigorously in order to meet the analysis requirement of lower amount of SG in samples of biodiesel.

3.2. Total Acid Number Determination of Biodiesel and Biodiesel Blends*

3.2.1 Introduction

Biodiesel, defined as mono-alkyl (methyl or ethyl) esters produced from plant oils and animal fats[99] by transesterification reactions, plays a very important role as an alternative to conventional petroleum diesel. Transesterification, also called alcoholysis [48], has been widely used to reduce the viscosity of triglycerides and produce biodiesel. However, the relatively simple production process does not ensure high quality biodiesel. Small amounts of reactants and by-products during the transesterification reaction, including water, free glycerin, bonded glycerin, free fatty acids (FFAs), catalyst, residual alcohol, unsaponifiable matter (plant sterols, tocopherols and hydrocarbons), and soaps[100] may contaminate the final product. These minor components may cause severe operational problems, such as engine deposits, filter clogging, or fuel deterioration. Therefore, many American Society for Testing and Materials (ASTM) standards are in place to restrict the amount of most minor components that can affect biodiesel quality. One of the most important ASTM standards for biodiesel quality is ASTM D664, which is the reference method for the total acid number (TAN) [101]. The TAN, mainly an indication of degree of oxidation and hydrolysis, is expressed as the mass of

* This work is published in Journal of the American Oil Chemists Society, 85 (11):1083-1086. (2008)

potassium hydroxide (KOH) in milligrams that is required to neutralize the acids in one gram of sample[101]. And it is a facile method for monitoring fuel quality [102]. The maximum TAN value of biodiesel specified in ASTM D6751 [1] is 0.50 mg KOH/g. The free fatty acids are the major causes of the high TANs in biodiesel. Biodiesel with a low TAN is considered "safe" for storage and transportation, whereas those with TANs above the ASTM specification may not only result in the severe operational problems mentioned above, but also can cause corrosion during storage.

ASTM D664 is a widely used method for the TAN assessment not only because of its good repeatability, but also the advantages of being valid for deeply colored samples, and measuring both the strong acid number and the total acid number. For example, ASTM D 664 was employed to determine the TANs of deeply colored heavy oils and bitumens by Fuhr *et al* [103]. However, there are still many problems related to this method, such as toxic aqueous calibration fluids (Toluene/2-Propanol), mediocre reproducibility, non-specified accuracy, and ester hydrolysis in the aqueous solution. In Fuhr *et al*'s work[103], the reproducibility of ASTM D664 was improved from 21.3% to 3% without changing the basic procedures. Modifications to the toxic aqueous calibration fluids used in this method[104] were reported in 2004, which adopted the commercialized calibration fluids without compromising the repeatability and reproducibility of ASTM D664. Researchers in Canada[105] recommend ASTM D974 for TAN determination of biodiesel instead of ASTM D664, because it displayed better reproducibility in their three labs' results. The accuracy of ASTM D974 was evaluated in the study, but that of ASTM 664 was not tested for comparison. However, it was reported that the potentiometric method was more reliable compared with the color titrations[106]. There were also other studies [107-111] related to the acidity or basicity measurement of oil. However, the detection limit of ASTM D664 remains debatable. In our work, the accuracy of ASTM D664 in biodiesel and biodiesel blends was evaluated.

Biodiesel is commonly sold in blends with ultra-low sulfur diesel (ULSD), of which B20 is one blend used for commercial applications. ASTM D664 is commonly used for the TAN determination of B20 though there is no specific standard for biodiesel blends. The current standard for pure biodiesel is set at 0.50 mg KOH/g. A limit of 0.3 mg KOH/g is proposed for B20 by the biodiesel industry. However, engine manufacturers and fuel delivery companies believe that this limit may not be sufficient to protect biodiesel storage and application systems. Since the lower the TAN, the higher quality of the oil, it would be desirable if the acid number could be accurately measured down to 0.15 mg KOH/g in B20 with this method. However, ASTM D664 gives no information on accuracy for petrodiesel, which was believed to be caused by the uncertainty of the acid species that can be identified as contributing to the acid number of petrodiesel [105]. The lower determination limit of ASTM D664 was presumably 0.3 mg KOH/g in biodiesel. In order to investigate the limit, the accuracy of ASTM D664 at various acid levels was evaluated by varying the amount of free fatty acids in biodiesel and B20.

3.2.2 Materials

Soybean oil based biodiesel (B100) was obtained from Wacker Oil Co. (Wacker Oil Co., MI). Certification #2 ultra low sulfur diesel (ULSD) was obtained from Haltermann Products (Channelview, Texas). B20 was prepared by mixing B100 and ULSD at a volume ratio of 1:4. Palmitic acid (99%) was obtained from Nu-Chek Prep (Elysian, MN). The chemicals used to prepare the TAN titration solvent, 2-propanol (ACS), and toluene (ACS) were purchased from Mallinckrodt Baker (Phillipsburg, NJ). The titrant solution used, 0.1N KOH in isopropanol, was supplied by LabChem (Pittsburgh, PA).

3.2.3 Method

The titration solvent was prepared as detailed in ASTM 664 [101]. Blends of B100 and ULSD were prepared to obtain weight percentages ranging from 0 to 90% biodiesel. Palmitic acid was added to solutions of B20 and B100 in order to obtain a range of known acid levels ranging from 0.30 to 0.53. TAN was determined for each mixture using the Titrado 809 instrument from Brinkmann (Westbury, NY). Experimental procedures were according to ASTM D664. Each sample was titrated in triplicate. After each titration, the electrode was rinsed with toluene first and then carefully dried with a toluene wetted tissue. The electrode was then immersed in distilled water for at least ten minutes. Before each titration, the electrode was taken out of water and gently dried with a tissue.

3.2.4 Results and Discussion

According to the repeatability definition in ASTM D664, only one out of twenty cases for the difference between two successive results by the method should exceed the following values with the same apparatus under constant operating conditions and on identical test samples [101]:

$$\text{Fresh Oils} = 0.044(X + 1) \tag{12}$$

$$\text{Used Oils Buffer end point} = 0.117X \tag{13}$$

Where X= the average of the two test results

Here, the repeatability values were calculated with the following formula[106]:

$$\text{Repeatability} = \frac{2.77 \times SD}{\text{Experimental Mean}} \times 100\% \tag{14}$$

Where *SD* is the standard deviation

The errors in this paper were calculated with the following formula:

$$\text{Error} = \frac{\text{Experimental Mean-Calculated TAN}}{\text{Calculated TAN}} \times 100\% \qquad (15)$$

Where the calculated TAN was based on the sum of the original TAN and the amount of the free fatty acid added to the oil.

Table 6. Experimental means and calculated TANs of B100 & ULSD Mixtures with ASTM D664 (Unit: mg KOH/g)

V% B100	Exp. Results	Mean	Cal.	SD	Repeatability	Err.
100.00	0.262, 0.242, 0.236	0.247	---	0.013	15.28%	---
88.48	0.197, 0.212, 0.208	0.206	0.222	0.008	10.46%	-7.21%
78.12	0.182, 0.183, 0.190	0.185	0.199	0.004	6.53%	-7.01%
67.87	0.167, 0.150, 0.167	0.161	0.177	0.010	16.85%	-8.67%
58.73	0.130, 0.151, 0.134	0.138	0.155	0.011	22.33%	-10.90%
48.69	0.118, 0.111, 0.113	0.114	0.132	0.004	8.76%	-13.76%
38.75	0.095, 0.089, 0.108	0.097	0.109	0.010	27.64%	-10.66%
29.89	0.079, 0.078, 0.076	0.078	0.087	0.002	5.45%	-11.12%
19.17	0.057, 0.057, 0.062	0.059	0.064	0.003	13.63%	-8.25%
10.50	0.050, 0.047, 0.062	0.051	0.042	0.005	24.89%	22.51%
0.00	0.016, 0.018, 0.018	0.017	---	0.001	18.45%	---

The first experiment was done by mixing B100 and ultra-low sulfur diesel (ULSD) to adjust the TAN values of the biodiesel blends. The results are shown in Table 6. According to the literature[104],

the acceptable repeatability was set as 12% of the mean value. But in this experiment, almost half of the repeatability results are out of this range. The accuracies are very poor. The largest error is up to 23%. After further investigation, it was found that this poor reproducibility was caused by the dehydration of the electrode.

Table 7. Experimental means and calculated TANs of the B20 samples with ASTM D664 (Unit: mg KOH/g)

Samples	Composition (W%)		Exp. Results	Mean	Cal. TAN	SD	Repeatability	Err.
	B20-1	B20-2						
B20-1	100	0	0.083, 0.083, 0.084	0.083	---	0.0006	1.92%	---
B20-2	0	100	0.383, 0.383, 0.385	0.383	---	0.0015	1.10%	---
Mixture 1	90.06	9.94	0.120, 0.124, 0.124	0.123	0.118	0.0023	5.21%	4.13%
Mixture 2	79.98	20.02	0.154, 0.153, 0.158	0.155	0.153	0.0026	4.73%	1.25%
Mixture 3	70.30	29.70	0.187, 0.185, 0.186	0.186	0.187	0.001	1.49%	-0.52%
Mixture 4	59.58	40.42	0.220, 0.224, 0.224	0.223	0.224	0.0023	2.87%	-0.80%
Mixture 5	50.00	50.00	0.230, 0.229, 0.229	0.229	0.232	0.0006	0.70%	-1.36%
Mixture 6	39.78	60.22	0.263, 0.262, 0.263	0.263	0.263	0.0006	0.61%	0.00%
Mixture 7	30.00	70.00	0.305, 0.300, 0.298	0.301	0.292	0.0036	3.32%	2.98%
Mixture 8	16.85	83.15	0.336, 0.331, 0.330	0.332	0.332	0.0032	2.68%	0.00%

ASTM D664 suggests that after each test, the electrode should be cleaned with organic solvent first, soaked in water at least five minutes, and then rinsed with organic solvent immediately before use. Usually intensive cleaning of the electrode with organic solvent is needed for the high viscous

oil samples. However, large amount of the organic solvent makes the electrode dehydrated and decreases the sensitivity of the electrode, which causes poor accuracy of the TAN determinations. Based our findings, five minutes are too short for the recovery of the electrode during the biodiesel sample tests with ASTM D664. Cleaning with organic solvent before use also increases the likelihood of dehydrating the electrode.

So, in order to minimize measurement errors attributed to the electrode dehydration during the application, the electrode should be soaked in water at least ten minutes and then dried gently with a tissue before use. The electrode after measuring biodiesel samples needs to be cleaned more thoroughly than after measuring ULSD samples (i.e. repeated rinse with organic solvent, followed by a long soaking time in water).

With these modifications, we carried out the TAN determination for the B20 and B100 samples. The results are shown in Tables 7 and 8. B20-1 and B100-1 in Tables 7 and 8 are the original samples without adding palmitic acid. B20-2 and B100-2 are the samples with calculated amount of pamitic acid added into the original ones to obtain the target TANs. Mixtures 1-8 and mixtures 1-5 in Tables 7 and 8 were obtained by mixing B20-1 and B20-2 or B100-1 and B100-2 at different ratios to produce different TAN samples. From Table 7, it can be seen that the lowest repeatability is 0.70% compared with 5.45% in Table 1 whereas the highest is 5.21% compared with 24.89% in Table 6. The overall repeatability in Table 3 is a little higher than those in Table 7. Possible cause of the variability may be hydrolysis of methyl esters in B100 in the aqueous TAN solvents. From Table 7, one can see that the experimental errors of all eight B20 mixture samples range from 0.00% to 4.13%. The absolute experimental errors of all five B100 mixture samples in Table 8 range from 0.00% to 1.14%. The results illustrated in Tables 7 and 8 show good accuracies for

ASTM D664 when applied to both B20 and B100 samples. For B20, ASTM D664 can measure TAN values even at a level as low as 0.123 with small error (4.13%).

Table 8. Experimental means and calculated TANs of the B100 samples with ASTM D664 (Unit: mg KOH/g)

Samples	Composition (W%)		Exp. Results	Mean	Cal.	SD	Repeatability	Err.
	B100-1	B100-2						
B100-1	100	0	0.205, 0.201, 0.203	0.203	---	0.002	2.73%	---
B100-2	0	100	0.526, 0.533, 0.524	0.528	---	0.0047	2.48%	---
Mixture 1	20.12	79.88	0.462, 0.451, 0.459	0.457	0.463	0.0057	3.44%	-1.14%
Mixture 2	42.29	57.71	0.382, 0.390, 0.408	0.393	0.391	0.0133	9.38%	0.71%
Mixture 3	50.18	49.82	0.377, 0.375, 0.365	0.372	0.365	0.0064	4.78%	2.03%
Mixture 4	70.68	29.32	0.299, 0.296, 0.298	0.298	0.298	0.0015	1.42%	0.00%
Mixture 5	85.93	14.07	0.252, 0.253, 0.249	0.251	0.249	0.0021	2.29%	1.05%

For B100, TAN around 0.3 was measured with the best accuracy. This observation is important because it demonstrates that TAN standards can be set for biodiesel mixtures that reflect the B100 TAN standard.

Application of ASTM D664 to B20 to measure the TAN value even down to 0.123 mg KOH/g was tested with good accuracy, which demonstrates that a lower TAN specification for B20 is

possible. Since the electrode is a critical factor affecting the accuracy and reproducibility of ASTM D664, it is recommended to put different guidelines on the electrode use, storage and maintenance procedures with different fuel samples.

CHAPTER 4. JET FUEL HYDROCARBONS PRODUCTION FROM CATALYTIC CRACKING AND HYDROCRACKING OF SOYBEAN OIL*

4.1 Introduction

In recent years, many researchers have investigated the production of biofuels from biomass to replace commercial petroleum products. These sources, which include plant oils and animal fats, have many desirable properties such as low levels of sulfur, nitrogen and heavy metals. Generally composed of triglycerides with fatty acid chains of 16 to 24 carbon atoms in length, they are ideal for the production of synthetic fuels and biochemicals[1].

At present, one of the most successful classes of biofuels from oils and fats is biodiesel, which is produced by a homogeneous liquid-phase catalyzed transesterification process at low temperature or a heterogeneous catalyzed process at slightly higher temperatures. However, biodiesel cannot meet the requirements of an aviation turbine fuel due to its poor cold flow properties. For example, canola methyl ester ("CME") and soy methyl ester ("SME") biodiesel have typical cloud points of 1.0 °C and 3.0 °C, respectively; and pour points of -9.0 °C and -3.0 °C, respectively [112]. But, according to aviation fuel specifications [113, 114], aviation turbine fuel should be completely resistant to the formation of solid particles at temperatures as low as −47 °C.

Jet fuel is an aviation fuel designed for use in aircraft powered by gas-turbine engines. Typical jet fuel is called narrow-cut or kerosene-type (C_8-C_{16}) jet composed of paraffins (70-85%), aromatics (<25%), olefins (<5%), and other contaminates such as sulfur, nitrogen and oxygenates. Recently, an alternative method of converting plant oils and animal fats into jet fuel products, using

* This work was accepted for being published in Current Catalysis, xxx (2012) xxx–xxx.

a hydrotreating process similar to what is found in the oil and gas refining industry, has been reported. This process avoids bed plugging due to tar and coke formation using the method of catalytic cracking over zeolite catalysts. A patent by Seames [43] has shown that by hydrotreating plant oils to produce jet fuel, a product with a cloud point of less than -30 °C can be obtained. The research by Bezergianni [115] has shown that vegetable oil hydrocracking of a vacuum gas oil and vegetable oil mixture at a ratio of 70/30 (v/v) over a standard commercial sulfide hydrocracking catalyst can yield up to 16% kerosene jet and 50% diesel fuel hydrocarbons at 1000 - 2000 psi and 350 - 390 ^{o}C. Catalytic hydrocracking of fresh and used cooking oil were also carried out over commercial sulfide hydrocracking catalysts at 350 - 390 ^{o}C [116] yielding roughly 17% kerosene jet at 390 ^{o}C and 2000 psi with a very high H_2/oil ratio (1069 Nm^3/m^3).

Several patents have focused on the production of jet fuel from biomass hydroprocessing using supported sulfided bimetals as catalysts. Ginosar [42] invented a process for the production of jet fuels, for example, JP-8, from plant seed oils using a combined hydrocracking and reforming process by using sulfided NiMo catalyst supported on alumina as the hydrocracking catalyst. The same type of catalyst was also used in Abhari's work [45]. Using these processes, claims of achieving good quality jet fuels with 89% energy efficiency and 72% mass efficiency have been made. Also several catalytic systems and reaction units, such as hydrotreating, hydrocracking and hydroisomerization, have been utilized at a high pressure (2000 psi or above) during the process.

Compared to hydrotreating, catalytic cracking is one of the most efficient methods to produce hydrocarbon fuels by cracking of vegetable oil in the presence of suitable catalyst. Although catalytic cracking is regarded as a cheaper route by requiring no hydrogen and using atmospheric pressure, poor yields and quality of hydrocarbons and high yields of coke (8–25%) and/or

condensation of oil molecules are the major issues of the process[117]. It has been reported that kerosene jet fuels can be obtained from catalytic cracking of palm oils over various types of zeolite catalysts such as ZSM-5, zeolite β, ultrastable Y (USY) zeolite, rare earth-Y (REY) zeolite, MCM-41 and SBA-15 mesoporous materials at a temperature range of 300-500 °C [64, 118-121]. Various products, including light gases, organic liquid products, water, coke and tar were produced from this process. Organic liquid products were composed of gasoline, kerosene jet, and diesel boiling range hydrocarbons whereas the gaseous fraction contained both paraffinic and olefinic hydrocarbons. The yield of kerosene jet hydrocarbons depends on the choice of the shape selective zeolite catalysts which control the product distribution in the process [122]. It has been reported that ZSM-5 had the highest activity for producing biofuels from palm oil[64].

In order to find a feasible process to produce a drop-in jet fuel from plant oils and animal fats by developing new hydrocracking catalyst and comparing the catalytic cracking method to hydrocracking process, jet fuel hydrocarbons production from both hydrocracking over a developed bifunctional Ru/ZSM-5 catalyst and catalytic cracking of soybean oil over commercialized ZSM-5 and were investigated. Fresh catalysts were loaded for each experimental condition. ZSM-5 zeolites were purchased from *Zeolyst International* (Kansas City, KS). And ruthenium supported on ZSM-5 was prepared by an impregnation method and tested for activity in a high-pressure flow reactor system using soybean oil and hydrogen gas as the reactants.

4.2 Experimental Section

4.2.1 Catalyst Preparation

A known quantity of Ruthenium–Ruthenium (III) chloride hydrate (*Sigma-Aldrich,* St. Louis, MO) was dissolved in a volume of water equal to the total pore volume of the catalyst support. This solution was then immediately poured over the prepared catalyst support evenly and agitated slightly to ensure that the entire pore volume of the catalyst was impregnated. Following this, the impregnated catalyst support was placed in a 50 °C oven for 12 hours, and then dried in a programmable high-temperature oven for 12 hours at 120 °C. As a final preparation step, the catalyst was calcined at 400 °C for 6 hours.

Commercial ZSM-5 zeolites were purchased from *Zeolyst International* (Kansas City, KS). These powder zeolites were calcined at 580 °C for four hours in the flow reactor prior to use in the catalytic cracking studies.

4.2.2 Catalyst Characterization

An X-ray Diffraction (XRD) analysis was carried out on the Ru/ZSM-5 catalyst using a Rigaku RU2000 rotating anode powder diffractometer (*Rigaku Americas Corporation,* TX) at a scan rate of 4˚/min. A Brunauer-Emmett-Teller (BET) analysis was carried out to determine the physical characteristics of the catalysts (surface area and pore size) using a Micromeritics model ASAP 2010 surface area analyzer (*Micromeritics Instrument Corporation*, GA), with nitrogen (99.99% purity) as the analysis gas. The catalyst samples were heated to 150 °C at a rate of 10 °C/min and then held for 2 hours under a nitrogen atmosphere, and the adsorption/desorption isotherms were acquired at 77.35 K using a 5 s equilibrium time interval. The catalyst samples were degassed at 150 °C for 6 h

prior to analysis to remove any adsorbed molecules from the pores and surfaces. Metal loading was determined by using a Hitachi S-2400 Scanning Electron Microscope (SEM)-energy dispersive spectrometer (EDS) (*Hitachi High Technologies America, Inc.*, CA) with a maximum operating voltage of 25kV.

4.2.3 Experimental Procedure

The reactor system consisted of a BTRS – Jr® tubular reactor (*Autoclave Engineers*, PA), a gas and liquid delivery system, liquid collection system, and online gas characterization. The reactor is a fixed bed reactor with the dimension of 1.31 cm i.d. × 61 cm. Brooks Smart 5850E Mass Flow Controllers (*Brooks Instrument*, PA) were used for the delivery of argon and hydrogen. Soybean oil was delivered to the reactor by a Series III pump (*Chrom Tech, Inc.*, MN) from a reservoir bottle.

Cracking experiments were carried out according to the established procedures[62, 64, 123-125] over the ZSM-5 zeolite catalyst at different temperatures and space velocities. Approximately 2 g of the fresh catalyst (5 mL) was loaded in the reactor for each run. The catalyst was calcined at 580 ^{o}C for 4 hours and then brought to the desired reaction temperature under argon gas flowing at a rate of 8 mL/min. After the temperature was stabilized, the flow of argon gas was stopped, and the oil was fed at the desired liquid hourly space velocity (LHSV, h^{-1}) without H_2 flowing into the system. The gas and liquid products were separated by a gas liquid separator at room temperature. The gaseous products were collected in a gas sampling bag. Depending on the oil flow rate, the duration of each run varied from 2 - 4 hours with a total of 20 mL oil fed. After the feed pump was shut off, the OLP and water content were collected first by switching on the gas liquid separator. The reactor was then flushed with argon at a low flow rate (16 - 20 mL/min) for two hours to remove the remaining products from the reactor. The catalyst was washed with hexane to collect the viscous tar

products and residual oil content that remained in the system. The hexane was then evaporated by drying the mixture under vacuum for 12 hours. The washed catalyst was dried in an oven for an hour prior to coke analysis. The organic liquid product was separated from the aqueous phase using a syringe.

For the hydrocracking experiments, approximately 2 g of the 1.11% Ru/ZSM-5 catalyst was loaded in the reactor. The catalyst was reduced in a hydrogen flow (30 mL/min) at 450 ^{o}C for two hours. The reactor pressure was then increased up to 650 psi. The reactions were carried out at 360 ^{o}C and 450 ^{o}C. Quartz beads with a size of 160 - 630 μm were used to dilute the catalyst bed at a 1:1 (v/v) ratio in order to minimize the mass and heat transfer effects of the catalyst beds. One set of experiments was also carried out at 450 ^{o}C without dilution of the catalyst bed. After the temperature and pressure were stabilized, soybean oil was fed at a flow rate of 0.125 mL/min. The molar ratio of H_2 to soybean oil was held at the ratio of 10:1. Steady flow was reached usually after 2-4 days on stream, based on the amount of liquid product collected and jet fuel selectivity.

4.2.4 Analysis of Products

A) Gaseous Products

The gaseous products were analyzed with an online gas chromatograph (GC) (*Perkin Elmer*, Model Clarus 500, MA) with a built-in Arnel Model 2106 Analyzer. The GC was equipped with both flame ionization (FID) and thermal conductivity detectors (TCD). Helium and nitrogen were used as carrier gases. The FID was used to detect the hydrocarbon components (C_1 - C_5) present in the gaseous product, and the TCD was used to determine other gaseous products such as CO_2, H_2, and CO.

B) Organic Liquid Product

The organic liquid product (OLP) was collected by vacuum filtration to separate the liquid oil products from solids and analyzed using a GC with a capillary glass column (100% dimethyl polysiloxane 60m×0.32×1.0µm, *Restek*, PA) and a flame ionization detector. The gas chromatography system was calibrated by injecting standard HC mixtures of gas or liquid n-alkanes to cover the hydrocarbon range of the samples. In the OLP, the C_8 - C_{16} fraction was defined as jet fuel and C_{12} - C_{20} as diesel.

C) Residue oil and aromatic contents

The residual soybean oil was determined by reversed-phase high-performance liquid chromatography (HPLC) (PerkinElmer Series 200, *PerkinElmer, Inc.,* MA) with Evaporative Light Scattering Detector (ELSD) (Altech 3300, NJ). The HPLC analysis was conducted according to the literature method [126] by using a high carbon load reversed phase column (Altech C18-HL, 250×4.6 mm i.d., 5 µm, *Altech Corporation*, NJ,) with guard column (7.5×4.6 mm i.d., 5 µm) as the stationary phase. Triglycerides were calibrated with a gradient of CH_2Cl_2 (A)/Acetonitrile (ACN) (B) at a flow rate of 1 mL/min. Standard working solutions were prepared by diluting appropriate amounts of the soybean oil solution in MeOH/ACN (1:1, v/v). The column temperature was set to 25 ^{o}C and the injection volume was 20 µL. The gradient condition was: 0% (A):100% (B) maintained for 15 min and then to 15% (A):85% (B) for 5 min; then changed to 70% (A):30% (B) and held for 2 min; finally, returned to the initial condition for another 3 min.

The total aromatics in the OLP was determined, using the method developed by Zoccolillo et al. [127], by HPLC with diode array detector (PerkinElmer Series 200 HPLC-DAD, *PerkinElmer, Inc.,*

MA). The OLP samples, diluted in acetonitrile (1 mg/mL), were analyzed under the following conditions: $CH_3CN:H_2O$ = 60:40%, flow rate 1 mL/min; λ_1= 205 nm, λ_2= 254 nm.

4.2.5 Results and discussion

The XRD pattern of Ru/ZSM-5 bifunctional catalyst shows no ruthenium oxide crystalline structures on the surface, suggesting that the ruthenium oxide is in an amorphous state. BET analysis shows that the catalyst has a surface area of 325.32 m^2/g and a pore size of 0.0905 cm^3/g. Ruthenium metal loading was determined to be 1.11 wt% on the catalyst by SEM-EDS technique.

A) Catalytic cracking over ZSM-5

(i) Conversion of soybean oil

For catalytic cracking studies, both reaction temperature and space velocity were found to have an inconsistent effect on the conversion of soybean oil. As seen from Figure 17, within the temperature range of 340 - 400 ^oC, the maximum conversion of soybean oil was attained at 360 ^oC at both 1 and 1.5 h^{-1} space velocities, and then decreased with an increase in reaction temperature. This decrease in conversion may be due to coke formation at higher reaction temperatures (Table 9). Within the temperature range from 360 - 400 ^oC, the conversion of soybean oil decreased with increasing space velocity. Leng et al. [120] proposed that oil first undergoes thermal and catalytic cracking on the external surface of catalysts to produce heavy hydrocarbons and oxygenates, which are then further cracked into light alkenes and alkanes, water, carbon dioxide and carbon monoxide within the internal pore structure of zeolite catalysts at a temperature range of 360 to 420°C. At different reaction temperatures, different reactions may be dominant, which could explain the irregular temperature effect on the conversion. At 420 ^oC and a higher space velocity of 1.5 and 2 h^-

[1], the reaction within the internal pore structure appears to be more dominant, which can be observed from the increased gas phase product formation (Table 9). This may explain the increasing conversion of soybean oil with increasing temperature after 420 ^{o}C. When the space velocity was increased from 1 h^{-1} to 1.5 h^{-1}, a 3-7% decrease in conversion was observed in the temperature range from 340 to 400 °C.

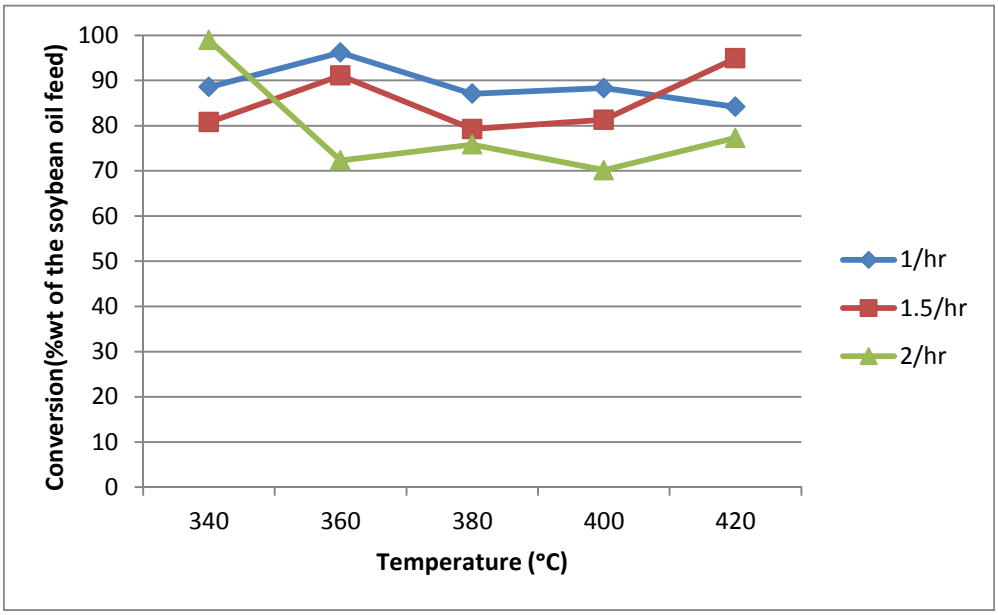

Figure 17. Effect of reaction temperature and LHSV (h^{-1}) on soybean oil conversion over ZSM-5

Table 9. Effects of reaction temperature and LHSV on product distribution of soybean oil cracking over a commercial ZSM-5 catalyst

Temperature (^oC)	Space Velocity (h^{-1})	Gas (%wt)	OLP (%wt)	Tar (%wt)	Residual oil (%wt)	Coke (%wt)
340	1	9.6	17.0	55.0	11.5	4.9
	1.5	5.6	14.3	58.5	19.2	2.5
	2	4.5	49.0	9.5	1.1	36.0
360	1	11.3	37.8	26.4	3.8	3.9
	1.5	15.0	34.2	40.6	8.9	1.4
	2	10.4	21.3	39.5	27.7	1.1
380	1	14.2	14.7	47.7	13.0	7.1
	1.5	9.3	21.3	44.9	20.8	3.7
	2	6.3	27.8	31.3	24.2	10.4
400	1	13.2	25.0	37.1	11.7	10.4
	1.5	8.4	27.6	38.4	18.7	6.9
	2	11.9	19.7	37.6	29.9	1.0
420	1	16.8	31.0	23.5	15.8	6.5
	1.5	13.0	35.3	43.2	5.1	3.4
	2	15.7	34.5	25.0	22.7	2.1

(ii) Organic liquid product and kerosene jet yield

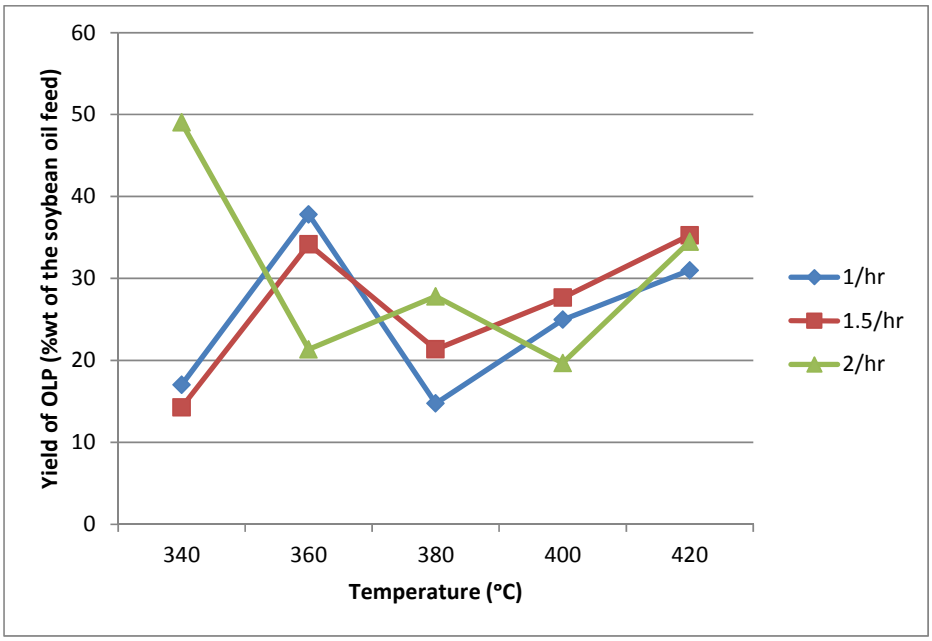

Figure 18. Effect of reaction temperature and LHSV (h^{-1}) on the yield of OLP over ZSM-5

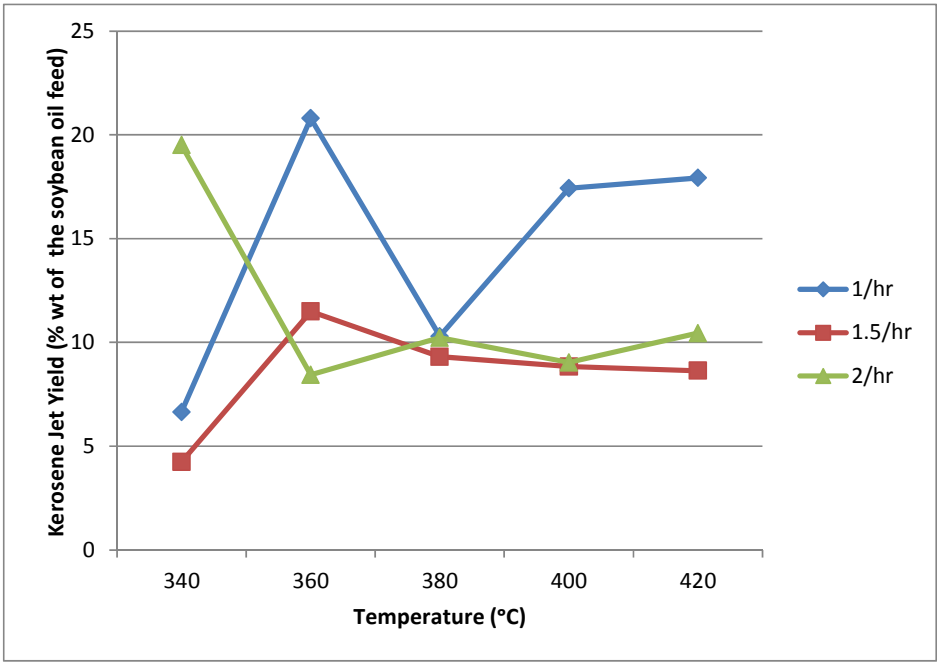

Figure 19. Effect of reaction temperature and LHSV (h^{-1}) on the yield of kerosene jet fuel over ZSM-5

Since OLP was one of the desired products, the effects of reaction temperature and space velocity on OLP yields were of greatest interest (Figure 18). No general trend could be observed in the OLP yields as a function of space velocity. This is similar to the findings of Katikaneni et al. [63] for space velocities from 1.8 to 3.6 h^{-1} over various zeolites such as HZSM-5, H-mordenite, and ZSM-5 at temperatures from 375 to 500 ^{o}C.

As shown in Figure 19, the kerosene jet (C_8 - C_{16}) selectivity was between 4 and 21 wt% over ZSM-5 zeolite. The selectivity for the kerosene jet was found to change in a similar trend with the yields of OLP at all of the space velocity levels. The higher yield of OLP indicates more cracking of the soybean oil resulting in an increase of kerosene jet. At 360 ^{o}C, the yield of kerosene jet fuel was as high as 21% at a space velocity of 1 h^{-1}. The conversion of the soybean oil was also the highest under this condition. Compared with the 16% yield at a temperature of ~450 ^{o}C [64], ZSM-5 shows a better selectivity to jet fuel at a lower temperature.

(iii) Aromatic content

During the catalytic cracking process, a considerable amount of aromatics, such as benzene, toluene, ethylbenzene, trimethylbenzene and xylenes were produced by aromatization, alkylation and isomerization of heavier olefins and paraffins. Coke is produced by direct condensation of oil and polymerization of aromatics [128]. Figure 20 shows the effect of reaction temperature and LHSV (h^{-1}) on the yield of total aromatics over ZSM-5 zeolite. It can be observed that lower selectivity for aromatic hydrocarbons was obtained with the ZSM-5 catalyst when the space velocity was higher, which was also observed by catalytic cracking of palm oil and canola oil over other zeolite catalysts [63, 120]. This might due to the fact that the higher the space velocity, the shorter the contact time between the oil and the surface of the catalyst, and the smaller amount of the intermediate products converted to aromatics.

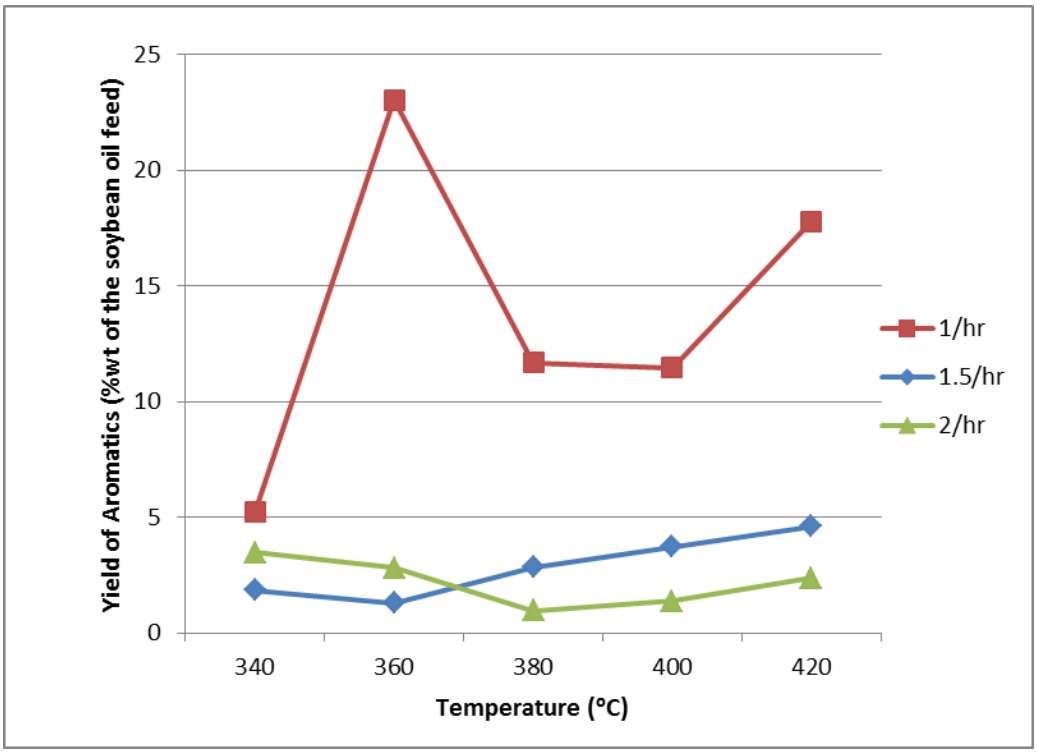

Figure 20. Effect of reaction temperature and LHSV (h^{-1}) on the yield of total aromatics over ZSM-5

At $1h^{-1}$, total aromatic yield varies significantly with an increasing temperature. The highest yield of 24% was observed at 360 ^{o}C. As Chang and Silvestri [129] reported, the main reaction was dehydration when the temperature was below 300 ^{o}C. Between 340 °C to 375 °C, aromatic hydrocarbon formation was predominant, while above 400 °C, light olefins and methane became significant as a result of secondary cracking reactions. That is the most probable reason why the highest yield of aromatics was obtained at 360 ^{o}C. Temperature effects on the selectivity towards the formation of aromatic hydrocarbons was not so obvious when the space velocity was above 2 h^{-1} due to limited amount of the intermediate products were converted to aromatics at higher space velocities.

B) Hydrocracking with Ru/ZSM-5

Four sets of hydrocracking runs over Ru/ZSM-5 were carried out under different conditions, three of which were performed with a diluted catalyst bed. The first run was performed at 360 ^{o}C for six days. After six days, the temperature was raised to 450 ^{o}C and the reaction continued for 5 more days. The third run was conducted at 450 ^{o}C with a batch of fresh catalysts. After the runs with the diluted catalysts, one run at 450 ^{o}C was conducted with a non-diluted catalyst bed. The conversion and product yield resulting from hydrocracking of soybean oil is given in Table 10. Figure 21 shows the jet fuel selectivity based on the distribution of hydrocarbons in the liquid product on each day.

Compared with the thermal cracking reactions, the conversion of soybean oil was almost complete under all of the hydrocracking reaction conditions. Furthermore, a stable continuous flow reaction was obtained with this bifunctional Ru/ZSM-5 zeolite catalyst. This is most probably because the hydrocracking process hydrogenates the unsaturated bonds in the triglycerides and reaction intermediate molecules, which reduces polymerization and minimizes the tar accumulation on the catalyst bed. The yield of jet fuel range hydrocarbons was 14 - 16% at 450 ^{o}C. Bezergianni et al. [115] observed a similar yield of jet fuel products, but at a much higher pressure (1000 - 2000 psi) by hydrocracking of vacuum gas oil-vegetable oil mixtures over commercial hydroprocessing catalysts. In addition, approximately 20-29% diesel yield was also obtained during our process.

Table 10. The conversion and product yield resulting from hydrocracking of soybean oil over Ru/ZSM-5 catalyst

	360 °C (diluted catalyst)	360 °C to 450 °C (diluted catalyst)	450 °C (diluted catalyst)	450 °C (non-diluted catalyst)
Conversion (%wt)	98.1	100.0	100.0	100.0
OLP Yield (%wt)	86.5	55.1	69.0	66.9
Jet Fuel Yield (%wt)	1.4	14.0	14.0	16.2
Diesel Yield (%wt)	1.1	20.7	27.0	28.6
Water Yield (%wt)	0.1	2.7	0.3	1.7

Figure 22 shows a typical GC chromatogram of the organic liquid product compared with those of commercial JP-8 and ultra-low sulfur diesel (ULSD). It can be seen that most of the OLP was in the range of jet fuel and diesel fuel. In spite of a high conversion of soybean oil at a low temperature of 360 °C, little jet fuel range hydrocarbons were obtained due to the low yield of cracking products.

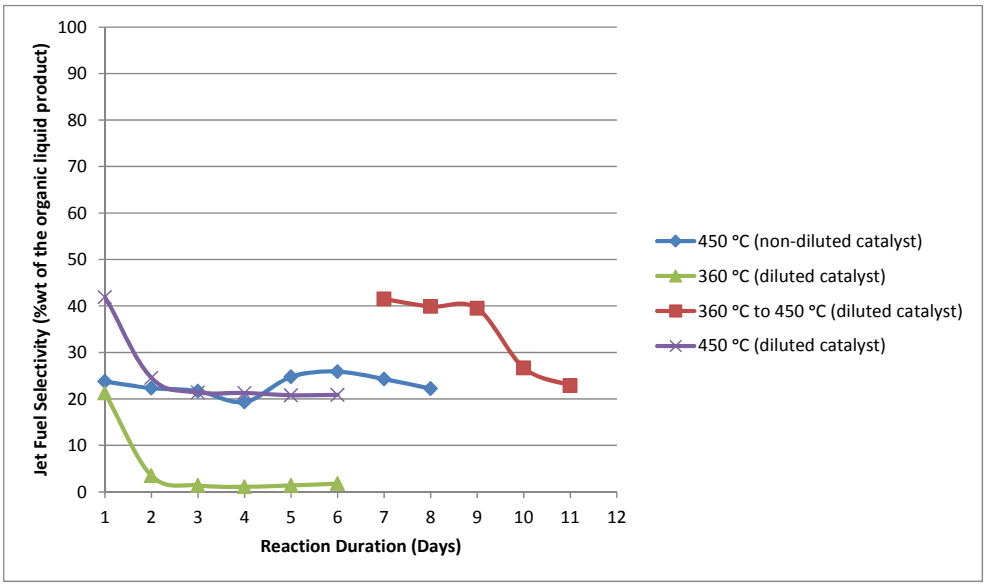

Figure 21. Jet fuel selectivity in liquid product of hydrocracking over bifunctional Ru/ZSM-5 catalyst

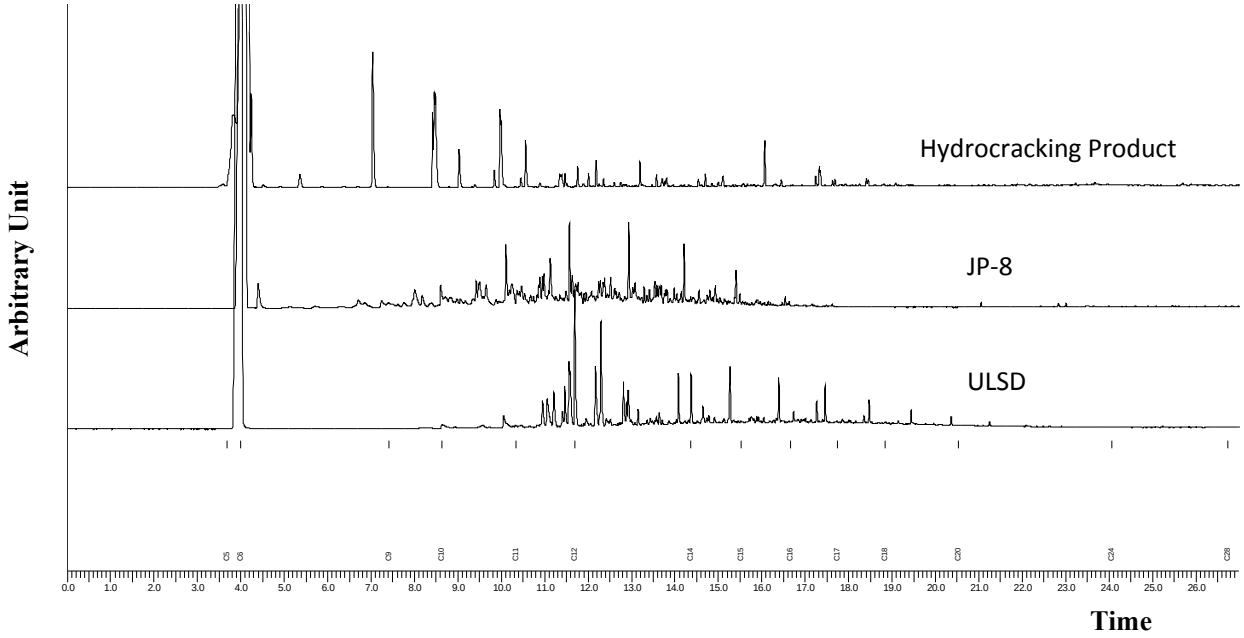

Figure 22. GC Chromatogram of the hydrocracking product, JP-8 and ULSD

According to the study by Bezergianni et al.[116], the system usually reached steady state after 5-6 days on stream. From the jet fuel selectivity in Figure 21, it appears that the reaction reached steady state after two days at both 360 ^{o}C and 450 ^{o}C with the diluted catalysts. However, the non-steady

state period was as long as 5 days with a non-diluted catalyst bed at 450 ^{o}C, possibly due to the heat and mass transfer effects. The selectivity toward jet fuel increased back to ~20% as the temperature was increased to 450 ^{o}C after 6 days of reaction at 360 ^{o}C with diluted catalysts. This suggests that the catalyst has experienced no significant deactivation.

4.3 Conclusion

ZSM-5 showed relatively high jet fuel yields from catalytic cracking of soybean oil. Both reaction temperature and space velocity were found to have inconsistent effects on the conversion of soybean oil and jet fuel yield. At lower space velocities, such as 1 and 1.5 h^{-1}, the conversion of soybean oil decreased at the higher reaction temperature due to coke formation. The selectivity toward aromatics can be varied by adjusting the oil space velocity. However, the experiment was suffering from severely plugging due to large amount of coke and tar production. On the other hand, jet fuel HC products were obtained through a one-step hydrocracking reaction over a non-sulfided precious metal catalyst (Ru/ZSM-5 catalyst). A comparable yield of jet fuel (16%) was obtained under a much lower pressure (650 psi) compared to about 17% kerosene jet yield over the commercialized hydrocracking catalyst at 2000 psi reported by Bezergianni et al. [116]. A 20 - 29% diesel yield was also obtained by varying reaction conditions during the process. Compared to the catalytic cracking process, less tar and coke were formed during the hydrocracking process and stable continuous flow reaction was obtained by using the bifunctional Ru/ZSM-5 catalyst.

CHAPTER 5. HYDROCARBON FUELS PRODUCTION FROM HYDROCRACKING OF SOYBEAN OIL USING TRANSITION METAL CARBIDES AND NITRIDES SUPPORTED ON ZSM-5*

5.1 Introduction

Increasing amount of greenhouse gases, especially carbon dioxide from burning of fossil fuels, along with non-renewability of the fossil resources, drove the study on the development of biofuels from alternative and renewable sources to displace commercial petroleum products. It is well known that triglyceride based vegetable oils, animal fats, and recycled grease have the potential to be suitable sources of fuel or hydrocarbons under the right processing conditions. At present, the most successful class of oil-derived biofuels is biodiesel, which is produced from plant oils or animals fats by a liquid-phase catalyzed transesterification process at low temperature or a solid catalyzed transesterification at high temperature. Though biodiesel has significant advantages and benefits, there are several major disadvantages compared to petroleum fuels, such as poor cold flow properties, low oxidation stability, and about 10% lower energy content, among others.

In order to address the above mentioned issues, interest in producing green fuels comparable to conventional fuels by catalytic hydrotreating of triglycerides has increased significantly in the last few years. Fuels produced from the hydrotreating have properties similar to petroleum diesel, and show better properties than the biodiesel produced via transesterification. Moreover, the engine fuel economy is improved[3]. As an alternative biofuels technology which can employ the existing

* This work was accepted for being published in *Industrial & Engineering Chemistry Research,* xxx (2012) xxx–xxx.

infrastructure of petroleum refineries[4, 13], hydrotreating has already been developed to incorporate renewables as part of refining operations[130].

Hydrocracking is considered as a more severe hydrotreating process. It converts heavier feedstocks into more valuable, low boiling products. During the hydrocracking process, the cracking and hydrogenation reactions take place simultaneously on a dual function catalyst, in which the acid sites of the catalyst are necessary for isomerization and cracking activities while the metallic sites are required for hydrogenation and dehydrogenation reactions[76].

Two types of catalysts have been reported as effective hydrotreating catalysts in converting vegetable oils to diesel range hydrocarbons: supported noble metal catalysts (Pd and Pt)[9-12] and sulfided bimetallic catalysts (usually Mo- or W-based sulfides promoted with Ni or Co)[13-17] . The catalytic reactions take place in the presence of a hydrogen-rich gas phase. The reaction pathway involves hydrogenation of the C=C bonds of the vegetable oils followed by alkane production by different reactions: decarbonylation, decarboxylation and hydrodeoxygenation. The straight chain alkanes can further undergo isomerization and cracking to produce lighter fuel range hydrocarbons (C5 to C16) with some degree of branching[71]. However, there are disadvantages of using these catalysts. On one hand, the limited availability and high price of noble metal catalysts has made the process economically not viable. Furthermore, since noble metal catalysts are very sensitive to catalyst poisons[22], contaminates (such as oxygenated compounds) in the feedstock can cause significant deactivation of the catalysts[23]. Therefore, it is necessary to remove impurities from the biomass feedstock. On the other hand, the products obtained in the mentioned processes over the bimetallic aluminum oxide supported catalysts are essentially n-paraffins (n-C15 up to n-C18) solidifying at subzero temperatures and therefore they are not suitable for producing high quality

diesel fuels, kerosene and gasoline compounds[26]. More importantly, the base metals in these hydrotreating catalysts need to be maintained in their sulfided form in order to be active at process conditions, and therefore a sulfurization co-feed needs to be added to the feedstock.

In recent years, the nitrides and carbides of early transition metals have been identified as a new class of promising hydrotreating catalysts which possess excellent catalytic properties and are competitive with the conventional bimetallic sulfided catalysts. After carburization or nitridation, the early transition metals can exhibit high activity similar to the noble metals because the introduction of carbon or nitrogen into the lattice of the early transition metals results in an increase of the lattice parameter a_0 and leads to an increase in the d-electron density[27]. As a substitute for sulfide catalysts, mono- and bimetallic carbides and nitrides based on transition metals have been successfully applied to the upgrading process of petroleum oil and bio-oil including hydrodesulfurization (DNS), hydrodenitrogenation (HDN), and hydrodeoxygenation (HDO)[28-31]. During catalytic hydrotreating, the triglycerides and free fatty acids in vegetable oils and animal fats are deoxygenated first and then converted into hydrocarbon fuels. Therefore, by considering using the nitrides and carbides of transition metals for hydrotreating of vegetable oils, the HDO activity of the catalysts is a very important factor. It has been reported that transition metal nitrides exhibited excellent activity and selectivity for hydrodeoxygenation of benzofuran[32]. Moreover, Han et al.[33] reported –ª °-#transition metal carbide catalyst, Mo_2C, showed high activity and selectivity for one-step conversion of vegetable oils into branched diesel-like hydrocarbons.#Nitrides of molybdenum, tungsten and vanadium supported on γ-Al_2O_3 were also used for hydrodeoxygenation of oleic acid and canola oil[34]. The oxygen removal exceeded 90% over the supported molybdenum catalyst for a long reaction duration (450 hours) and the yield of middle distillate hydrocarbons (diesel fuel) ranged between 38 and 48 wt%. Although most of the transition metal carbides and nitrides

catalysts described above have interesting HDO properties, bimetallic nitride and carbide catalysts were found to be much more active and stable than the mono-metallic ones[28]. However, there are few reports on the use of bimetallic catalysts for vegetable oils hydrocracking. The objective of this work is to evaluate the hydrocracking activities and selectivity of bimetallic (NiMo) carbides and nitrides catalysts supported on ZSM-5. ZSM-5 is an industrially important catalyst support, and has been widely used in the petroleum refinery process due to its strong acidy and specific pore structures. The effects of Ni:Mo ratio and process parameters (i.e., temperature and oil flow rate) on the conversion and the yield of the total biofuel products were investigated under a relatively low pressure condition.

5.2 Experimental

5.2.1 Catalyst Preparation

The oxide precursors were prepared through incipient wetness impregnation of ZSM-5 (*Zeolyst International*, Kansas City, KS) using aqueous solutions with the appropriate salts. 10 g of $Ni(NO_3)_2$ and 7.3 g of $(NH_4)_6Mo_7O_{24}{\cdot}4H_2O$ (*Sigma-Aldrich*, St. Louis, MO) were dissolved in a volume of water equal to the total pore volume of the catalyst support. This solution was then immediately poured over 40 g of catalyst support and agitated slightly to ensure that the entire pore volume of the catalyst was impregnated. Following this, the impregnated catalyst was placed in a 50 °C oven for 12 hours, and then dried in a programmable high-temperature oven for 12 hours at 120 ^{o}C, followed by calcination at 400 °C for 6 hours. The final step in the procedure is the carburization or nitriding of the metal oxide precursor using the temperature-programmed reduction (TPR)[131-133]. Firstly, 10 grams of the metal oxide precursor is loaded into a quartz reactor and placed in a temperature-controlled oven. Then the carburization is carried out using a flow of 250

cm^3 min^{-1} of 20 vol % CH_4/H_2 over the metal oxides at a heating rate of 10 K min^{-1} to 250 ^oC and then at a 1.98 K min^{-1} to a final temperature of 730 °C, which previous studies have shown to be suitable for carbide formation[134]. In the final stage, the temperature was maintained at 730 ^oC for half an hour to complete the reaction. The ammonia nitridation of oxides is carried out in a flow of 100 cm^3 min^{-1} of ammonia. In the first stage, the temperature was increased at 10 K min^{-1} to 250 ^oC. In the second stage, the temperature was raised to 700 ^oC and held for half an hour. Finally, the sample was cooled down to room temperature in argon and then passivated in flowing mixed gases (1% O_2/Ar) for 2 hours[28].

5.2.2 Catalyst Characterization

An X-ray Diffraction (XRD) analysis was carried out using a Rigaku RU2000 rotating anode powder diffractometer (Rigaku Americas Corporation, TX) at a scan rate of 4° /min. A Brunauer-Emmett-Teller (BET) analysis was carried out to determine the surface area and pore size of the catalysts using a Micromeritics model ASAP 2010 surface area analyzer (Micromeritics Instrument Corporation, GA), with nitrogen (99.99% purity) as the analysis gas. The catalyst samples were heated to 150 °C at a rate of 10 °C/min and then held for 2 hours under a nitrogen atmosphere, and the adsorption/desorption isotherms were acquired at 77.35 K using a 5 second equilibrium time interval. The catalyst samples were degassed at 150 °C for 6 hours prior to analysis to remove any adsorbed molecules from the pores and surfaces.

5.2.3 Experimental Procedure

The reactor system consisted of a BTRS – Jr® tubular reactor (Autoclave Engineers, PA), a gas and liquid delivery system, liquid collection system, and online gas characterization. The reactor is

a fixed bed reactor with the dimension of 1.31 cm i.d. × 61 cm. Approximately 2 g of the catalyst was loaded in the reactor. The catalyst was reduced in a hydrogen flow (30 mL/min) at 450 ^{o}C for two hours. The reactor pressure was then increased up to 650 psi. The reactions were carried out at 360, 400 or 450 ^{o}C. Quartz beads with a size about 200 μm were used to dilute the catalyst bed at a 1:1 (v/v) ratio in order to improve the mass and heat transfer of the catalyst beds. After the temperature and pressure were stabilized, soybean oil was fed. The liquid and gaseous products were separated in the gas-liquid-separator after the reaction. The reactor was considered to be in a steady state when the liquid product yield and the selectivity for gasoline to diesel range hydrocarbons maintain relatively constant on a daily basis, usually after 4–5 days on stream. Gaseous products were analyzed by an online gas chromatograph (Perkin Elmer, Calculus 500) equipped with a built-in Arnel Model 2106 Analyzer and a thermal conductivity detector (TCD). Helium and nitrogen were used as carrier gases. Liquid samples were collected at intervals of 24 h. The organic liquid product (OLP) was separated from the aqueous phase using a syringe. Hydrocarbon fuels in the OLP, such as gasoline (C_5-C_{12}), jet fuel (C_8 - C_{16}) and diesel (C_{12} - C_{22}), were analyzed quantitatively by a GC with a capillary glass column (100% dimethyl polysiloxane 60m×0.32×1.0μm, *Restek*, PA) and a flame ionization detector. Conversion (%), OLP yield (%), and product selectivity in OLP (%) were computed as the following:

$$\text{Conversion (\%wt)} = \frac{F-R}{F} \times 100 \qquad (16)$$

$$\text{OLP yield (\%wt)} = \frac{P_{OLP}}{F} \times 100 \qquad (17)$$

$$Product\ selectivity\ in\ OLP\ (\%wt) = \frac{P_{gasoline,kerosene,or\ diesel}}{P_{OLP}} \times 100 \qquad (18)$$

Where F and R are the weight of feed soybean oil and residue oil in the product respectively, P is the product weight (OLP, gasoline, kerosene, or diesel).

5.3 Results and discussion

5.3.1 Catalysts Characterization

Figure 23 shows the X-ray diffraction (XRD) patterns of the bimetallic NiMo carbide and nitride phases supported on ZSM-5. Mo_2N, Ni_3N, NiC, and Mo_2C phases were found. Surface area, pore volume, and pore size of the catalysts are summarized in the Table 11. It can be seen that both carbide and nitride of NiMo/ZSM-5 catalysts show a reduced surface area as compared with the ZSM-5 support. This could be attributed to the combination of structural loss and pore/channel blockage[135] after loading metal oxides, nitrides and carbides on the zeolite. The distinct heats of formation of different nitrides and carbides caused the catalysts to consist of both mixed Ni-Mo phase ($NiMoO_4$) together with single Ni and Mo carbides (Mo_2C and NiC) and nitrides (Mo_2N and Ni_3N), respectively[31].

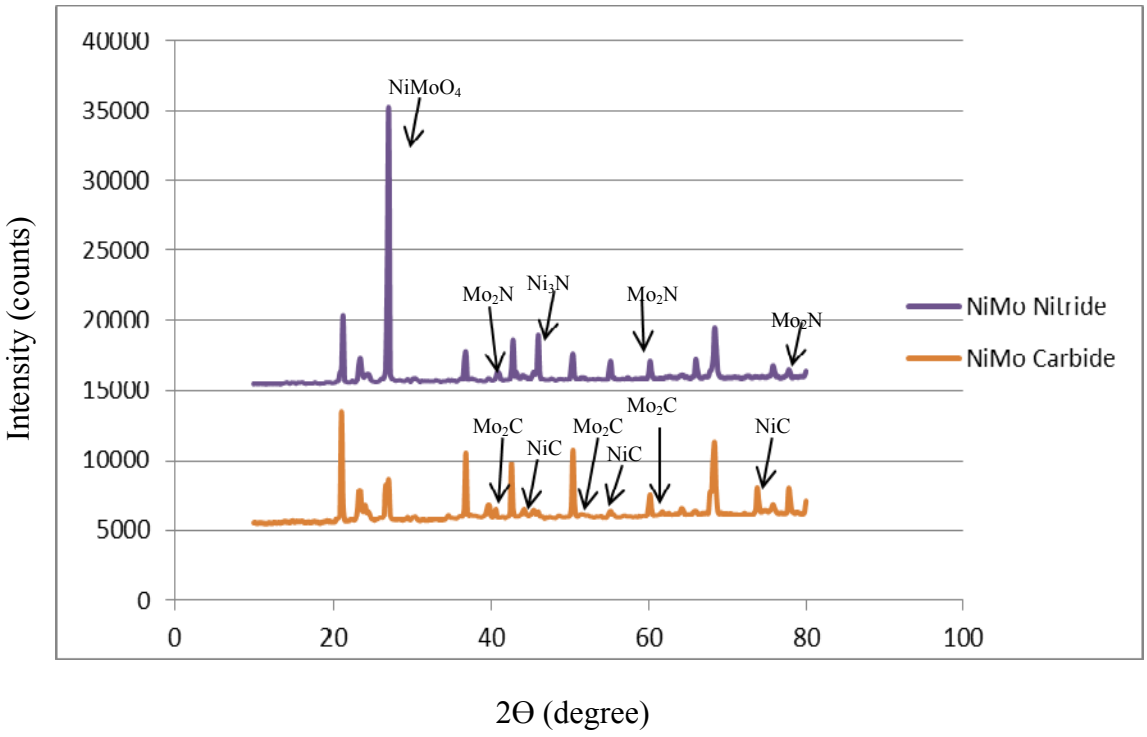

Figure 23. XRD patterns of NiMo/ZSM-5 carbide and nitride catalysts

Table 11. BET surface area, pore size and pore volume of the catalysts

Sample	Surface Area (m^2/g)	Pore Size (Å)	Pore Volume(cm^3/g)
NiMo/ZSM-5 Carbide	345.5	55.1	0.131
NiMo/ZSM-5 Nitride	298.6	55.6	0.108
ZSM-5	420.5	45.5	0.310

5.3.2 Hydrocracking of soybean oil

5.3.2.1 Temperature effects on the hydrocracking products

Hydrocracking yields an organic liquid product (OLP), together with gaseous products and water. The OLP not only contains hydrocarbon fuels, but also other side products, such as partially converted triglycerides, oxygenates, monomers, dimers, and tars, among others.

$$\text{Triglycerides} \xrightarrow{H_2} \text{Propane} + R_1CH_3 + R_2CH_3 + R_3CH_3 + 6H_2O \quad (19)$$

$$\text{Triglycerides} \xrightarrow{H_2} \text{Propane} + R_1 + R_2 + R_3 + 3CO + 3H_2O \quad (20)$$

$$\text{Triglycerides} \longrightarrow \text{Propane} + R_1 + R_2 + R_3 + 3CO_2 \quad (21)$$

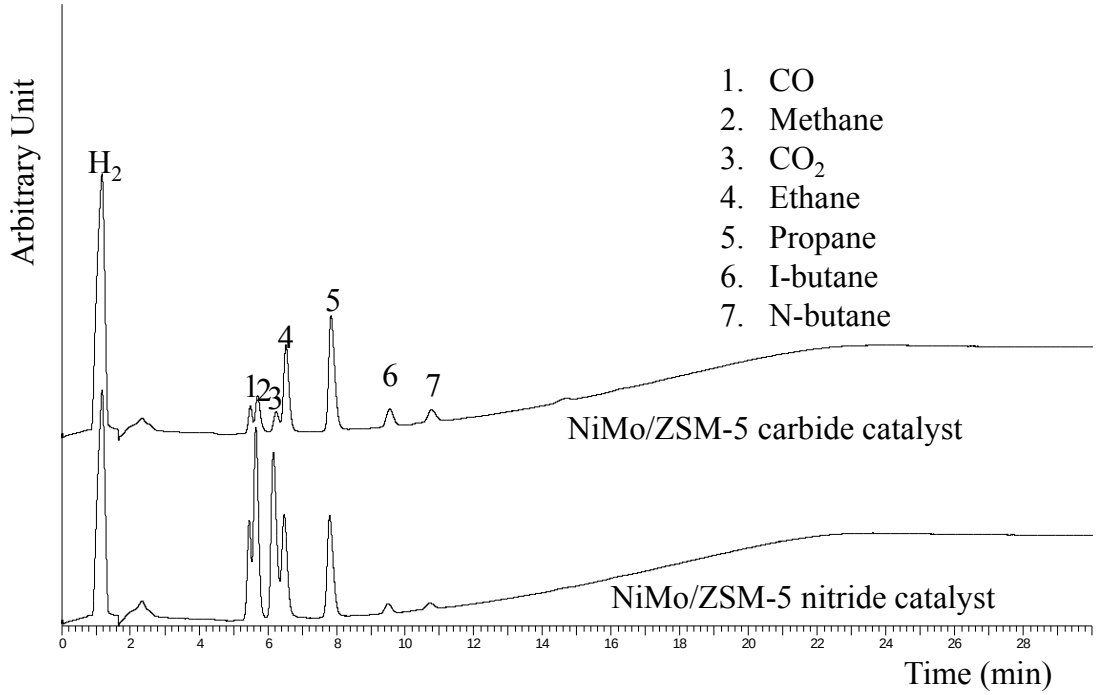

Figure 24. TCD analysis of gaseous products at 1.5 hr^{-1}, 450 ^oC

When the LSHV was 1.5 hr^{-1}, the conversion of triglycerides was found to be 100% over both of the nitride and carbide catalysts at 360 ^{o}C and 450 ^{o}C. Hydrocracking over both the nitride and carbide catalysts yielded about 4-5% water due to hydrodeoxygenation (Reaction (19)). It can be seen in Figure 2 that the oxygen in the triglyceride molecule was also removed as CO and CO_2 by decarbonylation (Reaction (20)) and decarboxylation (Reaction (21)) respectively. As shown in Figure 24, both decarbonylation and decarboxylation are more significant reactions with the nitride catalyst compared to the carbide catalyst because of larger amounts of CO and CO_2 formed. Moreover, it can be seen from the chromatogram that larger amount of methane was produced over the nitride catalyst by the methanation reaction since hydrotreating catalysts are known to be active for both reverse water gas shift (WGS) (Reaction (23)) and methanation[24]. Methane is basically one of the unwanted side products since it is a low energy compounds and its formation consumes large amount of hydrogen.

$$CO + 3H_2 \longleftrightarrow CH_4 + H_2O \quad (22)$$

$$CO_2 + H_2 \longleftrightarrow CO + H_2O \quad (23)$$

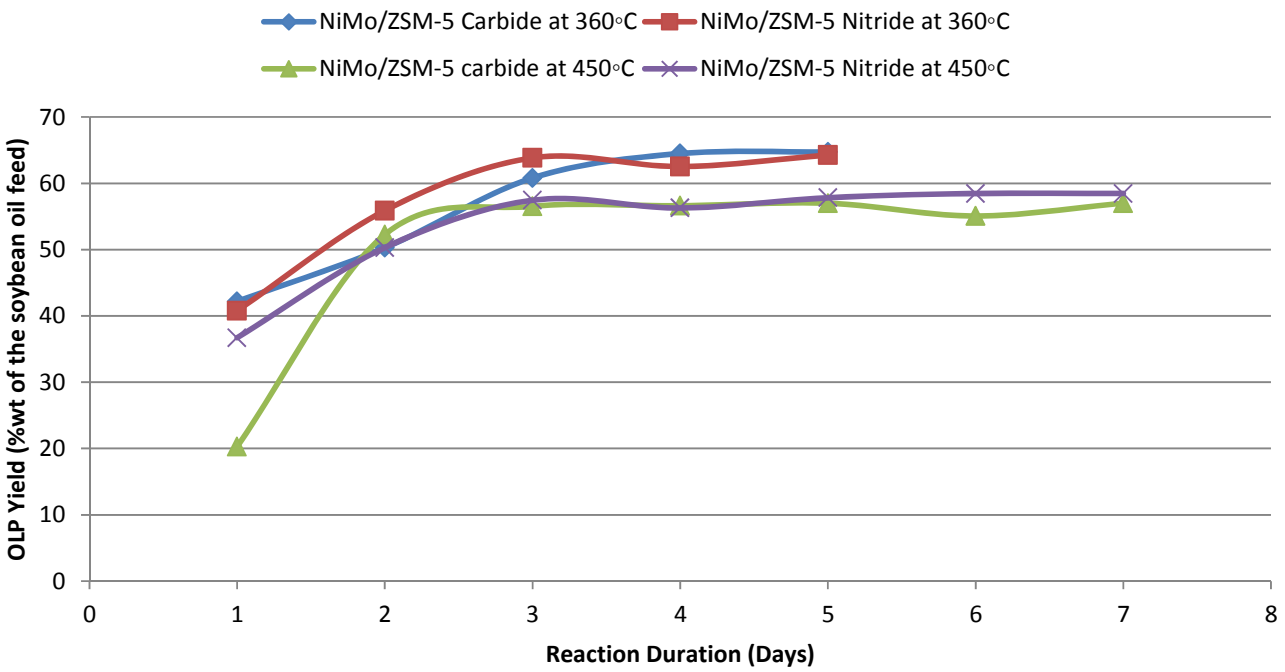

Figure 25. Organic liquid product (OLP) yield over the nitride and carbide catalysts at 360 °C and 450 °C

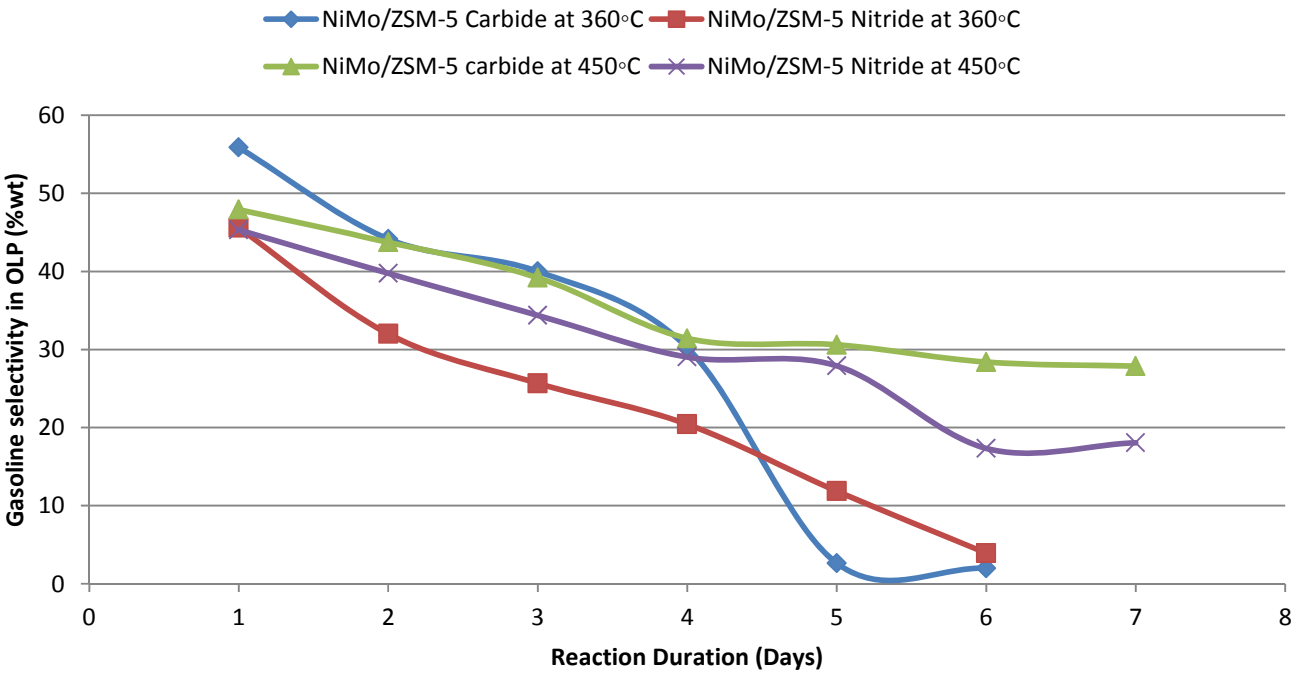

Figure 26. Gasoline selectivity in OLP over the nitride and carbide catalysts at 360°C and 450°C

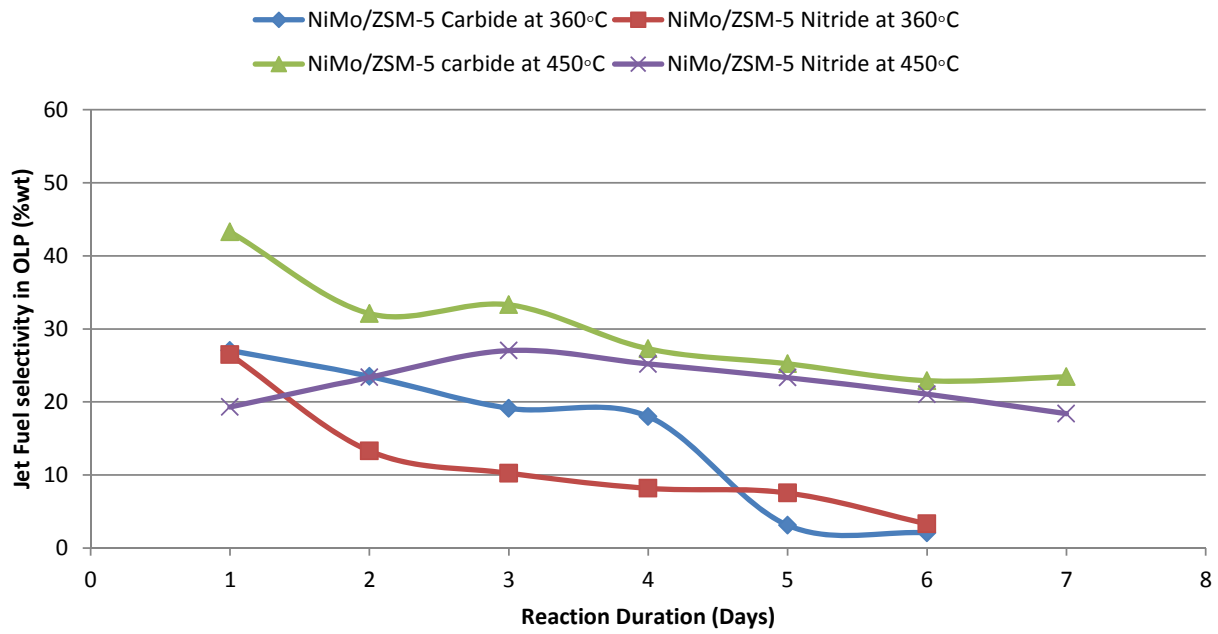

Figure 27. Jet fuel selectivity in OLP over the nitride and carbide catalysts at 360°C and 450°C

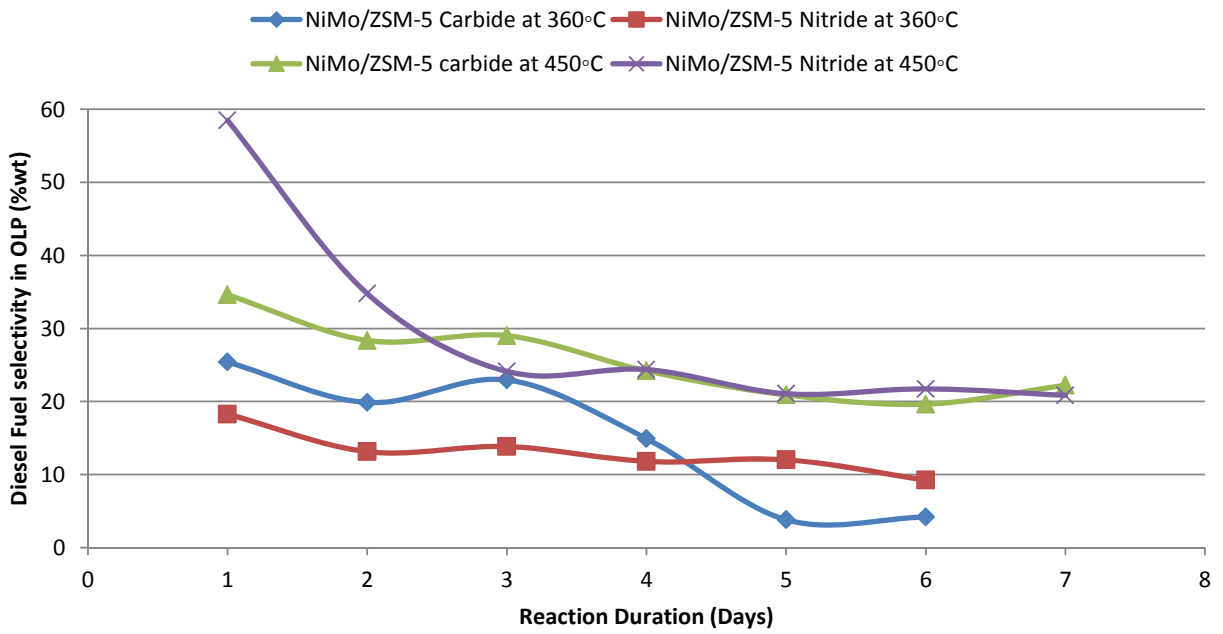

Figure 28. Diesel fuel selectivity in OLP over the nitride and carbide catalysts at 360°C and 450°C

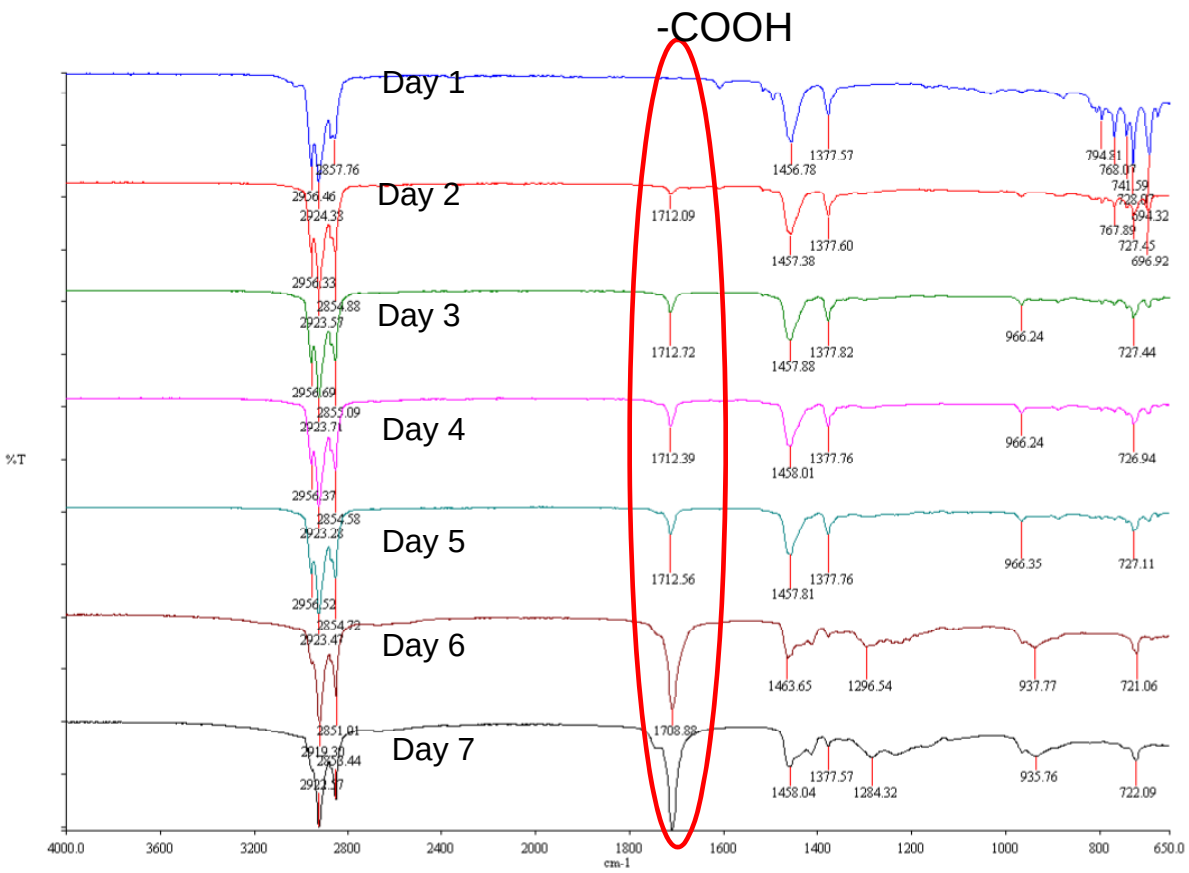

Figure 29. FTIR spectra of the OLPs over NiMo/ZSM-5 nitride catalysts at 360 ^{o}C, 1.5 hr^{-1}

Though similar amounts of OLP (Figure 25) were obtained at two temperature levels (360 ^{o}C and 450 ^{o}C), the physical and chemical properties of the OLPs were completely different. The catalyst deactivated rapidly at the low temperature (360 ^{o}C) as shown in Figure 25-28). Little amount of hydrocarbon fuels were obtained after 4 days reaction over both of the catalysts. Creamy and viscous products were produced instead of OLPs. The increasing carboxyl acid group (-COOH) in the FTIR spectra (Figure 29) indicates that larger amounts of carboxyl acids were produced along with a longer reaction time. Total acid number (TAN) of the products (Figure 30) was determined by using a Titrado 809 (Brinkmann, Westbury, NY). It can be observed that the acid number at 360 ^{o}C was increased sharply from 0 to 140 mg KOH/g within 6 days, which was caused by the large

amount of carboxyl acids compounds in the final product. Apparently, the active centers are poisoned at this temperature level by the strong adsorption of water which could be removed at a higher reaction temperatures[136]. This can be seen from Figure 30 where the acid number of the OLP at 450 ^{o}C decreased significantly compared to the products at 360 ^{o}C. The absorbed water can influence the metal/acid balance of hydrocracking catalysts and change the hydrocracking activity and product selectivity[137-139] . At 450 ^{o}C, both carbide and nitride catalysts showed comparable selectivities to jet and diesel range hydrocarbons (Figure 27-28). However, the gasoline selectivity over the nitride catalyst was about 10% lower after the reaction reached steady state (5 days later) than that over the carbide catalyst. This might be due to the fact that more carbons from the feedstock were converted to methane over the nitride catalyst, which has a higher methanation activity as mentioned above. Therefore, the following study will focus on the carbide catalyst since it is less active to methanation and more selective to higher hydrocarbons compared to the nitride catalyst.

To determine the effect of feed space velocity on the hydrocracking process over the carbide catalyst, continuous flow reactions with three LHSV levels (1, 2 and 3 hr^{-1}) at 400 ^{o}C and 650 psi were conducted. One hundred percent conversion of triglycerides was obtained for all of the conditions.

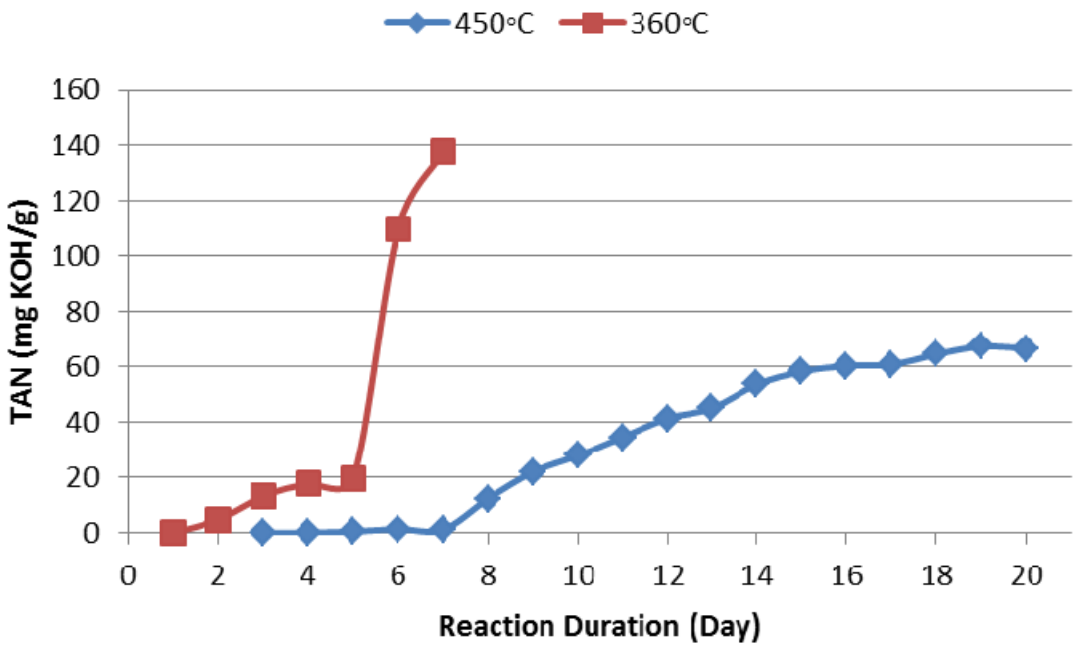

Figure 30. Total Acid Number (TAN) determination of the products over NiMo nitride catalyst at 360 ^{o}C and 450 ^{o}C

5.3.2.2 Space velocity effects on the hydrocracking process over the carbide catalyst

The OLP yields and selectivities to gasoline, kerosene/jet, and diesel hydrocarbons are given in Figure 31-34. As can be seen in Figure 31, the OLP yields do not exhibit a direct correlation with LHSV. At a lower LHSV of 1 hr^{-1}, more cracking hydrocarbon products as well as gaseous phase products were generated than at 2 hr^{-1}. Less OLP but the highest selectivity to gasoline range hydrocarbons (35%) was obtained compared with higher LHSV. When the LHSV was as high as 3 hr^{-1}, less OLP was obtained, probably due to the polymerization of the feed oil. This might be due to the shorter the contact time between the oil and the catalytic sites with higher space velocity, with a larger amount of the unsaturated intermediates polymerizing instead of being hydrogenated to saturated hydrocarbons since the reactor was severely plugged by viscous products after 5 days reaction. Thus, the highest organic liquid product yield (about 80%) was observed at 2 hr^{-1}.

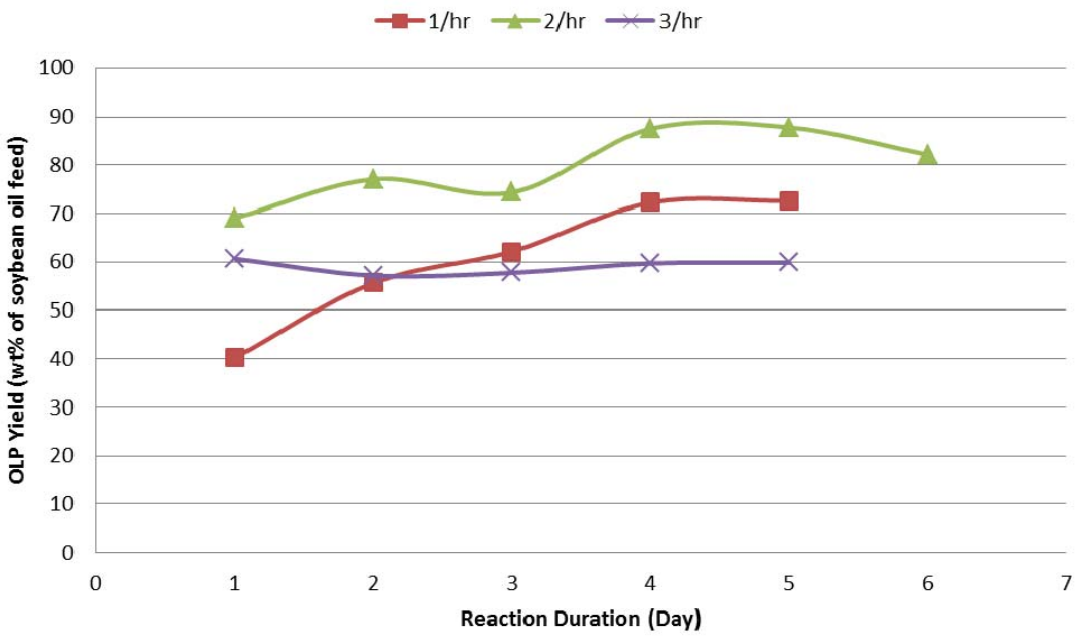

Figure 31. The effects of LHSV on OLP yields

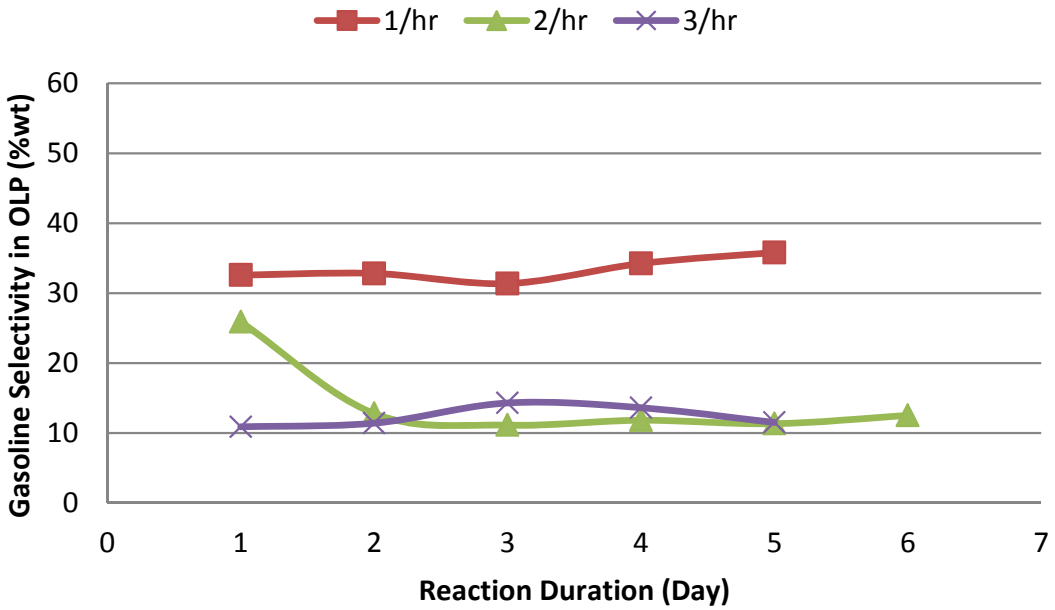

Figure 32. The effects of LHSV on gasoline selectivity in OLP

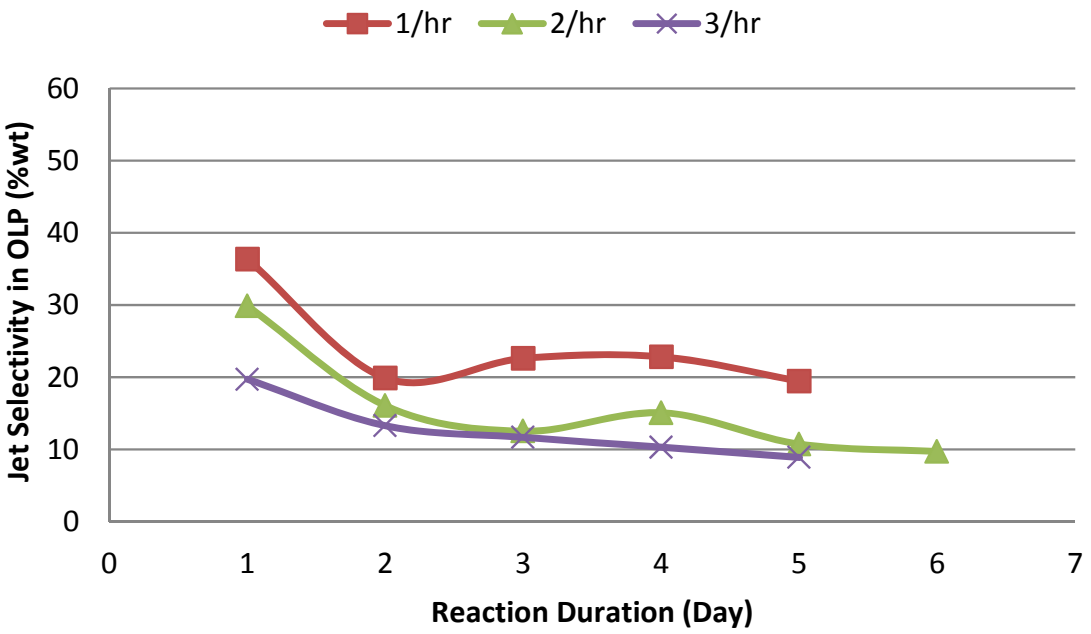

Figure 33. The effects of LHSV on jet fuel selectivity in OLP

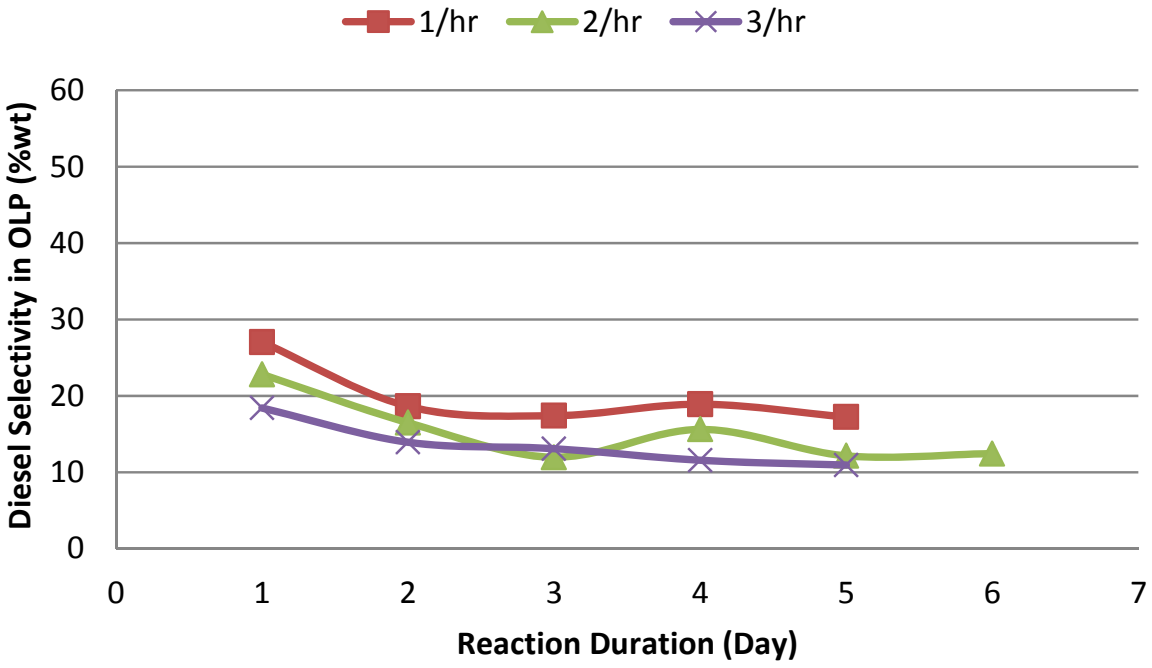

Figure 34. The effects of LHSV on diesel fuel selectivity in OLP

5.3.2.3 Effect of catalyst composition on the hydrocracking process over the carbide catalyst

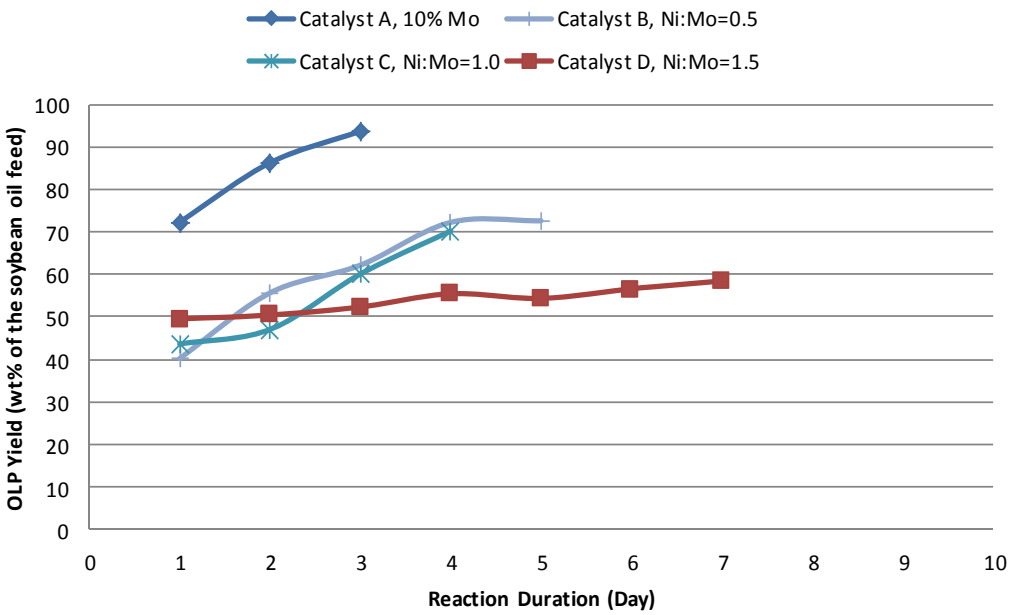

Figure 35. The effects of Ni/Mo ratio on OLP yields

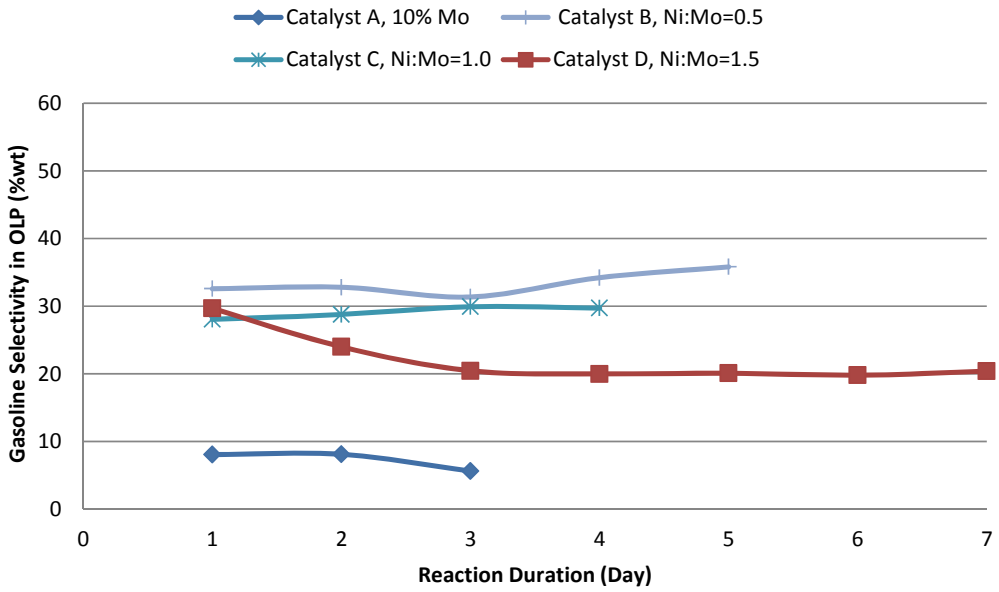

Figure 36. The effects of Ni/Mo ratio on gasoline selectivity in OLP

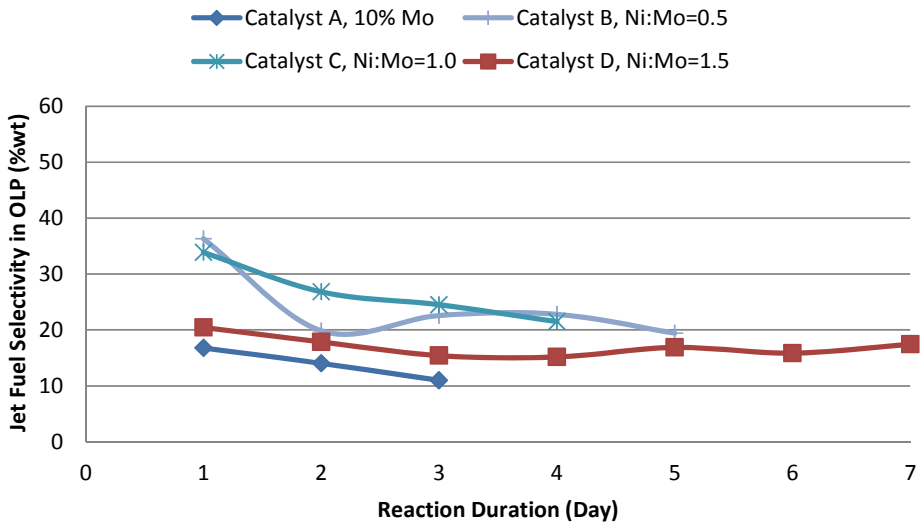

Figure 37. The effects of Ni/Mo ratio on jet fuel selectivity in OLP

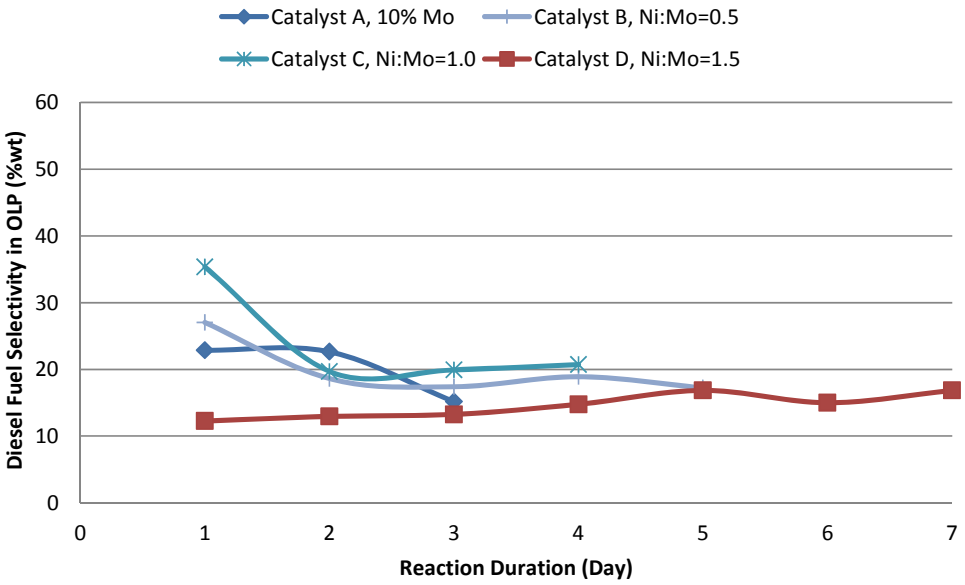

Figure 38. The effects of Ni/Mo ratio on diesel fuel selectivity in OLP

The NiMo/ZSM-5 is a bi-functional catalyst with both cracking and hydrogenation activities. The cracking function in the catalysts is provided by its support, i.e., ZMS-5, which contains highly acidic sites necessary for cracking[140]. The hydrogenation function can be attributed to Ni-Mo transition metals dispersed over the supporting surface. The hydrogenation reactions catalyzed by those metals follow the free-radical mechanism[141] and the atomic ratio of the metals had a strong influence on the activity and selectivity[142].

While maintaining a 10%wt metal loading, four NiMo/ZSM-5 carbide catalysts (Ni/Mo=0, 0.5, 1, 1.5) were prepared to study the effects of Ni/Mo molar ratio on the hydrocracking process. The experiments were conducted at 400 ^{o}C and 650 psi. Again, full conversion of triglycerides was obtained for all of the experiments.

The OLP yield and selectivity to the different cracking products are presented in Figure 35-38 for Ni-Mo/ZSM-5 carbide catalyst with different Ni/Mo atomic ratios. The reactions over the catalyst with only Mo metal loading experienced a very severe plugging problem after three days. Almost no gasoline, jet fuel and diesel range hydrocarbons were obtained in the final products. A large amount of higher hydrocarbons (> C23) was found in the products. According to synergistic mechanism of the Ni/Mo bimetallic catalysts, nickel plays a role in hydrogen activation, transferring protons and electrons to the molybdenum[143]. With a lack of Ni for hydrogen activation and transferring, polymerization might be the dominant reaction over the Mo/ZSM-5 carbide catalyst, resulting in the catalyst bed plugging when the Ni/Mo ratio was 0. It can be seen from Figure 37-38 that catalysts with Ni/Mo ratios from 0.5-1.5 showed similar selectivity to jet and diesel hydrocarbons. However, the selectivity to gasoline range hydrocarbons decreased with the increasing Ni/Mo ratio (Figure 36). This might due to the fact that with the increasing amount of Ni

content on the catalyst, the deoxygenated and cracked intermediates might be hydrogenated to more gaseous products instead of gasoline to diesel fuel range hydrocarbons, which could result in a decreasing amount of OLP as shown in Figure 35).

5.4. Conclusions

Non-sulfided bimetallic hydrocracking catalysts, Ni-Mo carbides and nitrides supported on ZSM-5 were prepared by a temperature-programmed reaction method. Three main hydrocracking operating parameters were studied in terms of their effects on organic liquid product yields and product selectivity. Complete conversion of soybean oil and up to 50%wt yield of hydrocarbon fuels were obtained from vegetable oil over the catalysts under a low reaction pressure (650 psi). Both of the carbide and nitride catalysts are active for methanation but the nitride catalyst showed a higher activity for methane production. Study on the effect of temperature revealed that the catalyst under a low reaction temperature (360 ^{o}C) is not resistant to water poisoning and large amount of carboxylic acid products were produced. Increasing the oil-catalyst contact time can enhance the hydrocarbon fuel contents in the organic liquid products. Hydrocracking products are affected by the Ni/Mo atomic ratio of catalyst. Higher amount of Ni content improves the hydrogenation activity of the catalyst.

In conclusion, Ni-Mo carbide supported on ZSM-5 showed high activity and selectivity for one-step conversion of vegetable oils into the gasoline to diesel range. This study provides a promising approach for preparing drop-in fuels from renewable resources under a lower pressure without sulfurization reagents involved in the process.

CHAPTER 6. HYDROTREATING OF SOYBEAN OIL OVER NIMO CARBIDE ON FIVE DIFFERENT SUPPORTS

6.1 Introduction

Due to the increasing price of fossil fuel, energy security reasons, environmental and economic issues, it is highly demanding to develop the techniques to produce biofuels from alternative and renewable sources to displace commercial petroleum products. It is well known that triglyceride based vegetable oils, animal fats, and recycled grease have the potential to be a suitable feedstock of renewable fuels under the right processing conditions.

Currently, the above mentioned renewable feedstocks can be converted into liquid hydrocarbon fuels by the methods of hydrotreating process similar to what is found in the oil and gas refining industry [3, 4]. Conventional γ-Al_2O_3 supported sulfided bimetallic catalysts (usually Mo- or W-based sulfides promoted with Ni or Co) as presently used for desulphurization of fossil diesel streams are used in the process under high energy consumption conditions, such as high temperature, high pressure, and large amount of hydrogen consumption[24]. The products obtained are essentially n-paraffins (n-C15 up to n-C18) solidifying at subzero temperatures. So, they are unsuitable for high quality diesel fuels, kerosene and gasoline compounds[26]. The process is costly and the yield of product can be low because of formation of coke, which causes its deactivation and pressure build-up in the reactor[25]. More importantly, the base metals in these hydrocracking catalysts need to be maintained in their sulfided form in order to be active at process conditions, and therefore a sulfurization co-feed needs to be added to the feedstock.

In order to resolve the above issues, a number of studies have been carried out to develop non-sulfided catalysts with high activity, good selectivity and long lifetime in a hydrotreating process[9-12,

[33, 34]. Among them, the nitrides and carbides of early transition metals have been identified as a new class of hydrotreating catalysts which are competitive with the conventional bimetallic sulfided catalysts. These catalysts exhibit high activity similar to the noble metals because the introduction of carbon or nitrogen into the lattice of the early transition metals results in an increase of the lattice parameter a_0 and leads to an increase in the d-electron density[27]. Han et al.[33] reported –ª °–#transition metal carbide catalyst, Mo_2C, supported on multi-walled carbon nanotubes showed 90% conversion and 91% hydrocarbon selectivity for one-step conversion of vegetable oils into branched diesel-like hydrocarbons.#Nitrides of molybdenum, tungsten and vanadium supported on γ-Al_2O_3 were also used for hydrodeoxygenation of oleic acid and canola oil[34]. The oxygen removal exceeded 90% over the supported molybdenum catalyst for a long reaction duration (450 hours) and the yield of middle distillate hydrocarbons (diesel fuel) ranged between 38 and 48 wt%. Moreover, bimetallic nitride and carbide catalysts were found to be much more active and stable than the mono-metallic ones[28] even though no application of them in the biomass hydrotreating process has been reported.

Though the nitrides and carbides of early transition metals have been studied in the above mentioned literatures as hydrotreating catalysts to convert vegetable oils to biofuels due to their unique structural and electronic properties, as it can be observed, up to now, no clear information exists on the effect of the support on the hydrotreating activity of the catalysts. However, the support plays the important role of the cracking function in the hydrotreating catalyst [144, 145]. It contributes to the cracking of the C-O or C-C bond and to the isomerization of the n-olefins formed, which after hydrogenation are transformed into isoparaffins[12, 76]. Thus, the aim of this work is to prepare bimetallic (NiMo) carbides catalysts supported on different supports and investigate the support effects on the catalyst hydrotreating activity.

In this study, the preparation of Al-SBA-15 with Si/Al=80 and hydrotreating catalysts based on this mesoporous material along with commercialized γ-Al_2O_3, ZSM-5, Zeolite β and USY zeolite are presented. Nickel and molybdenum are impregnated as active metals. The carbides of the catalysts were evaluated for hydrotreating of soybean oil in a bench-scale plugged flow reactor.

6.2 Experimental

6.2.1 Preparation of Al-SBA-15

Al-SBA-15 with Si/Al=80 was synthesized following the synthesis procedure of Wu et al.[146]. A typical synthesis procedure was as the following: 20 grams of commercialized SBA-15 powder (*ACS Materials, LLC*, Medford, MA) was dispersed in 150 mL hexane. Then 0.067g aluminum isopropoxide dispersed in a small amount of hexane was added with stirring. After 10 minutes, the solution was diluted by adding more hexane (150 mL) and the stirring was continued to another 24 h at room temperature. The mixture solution was filtered and the obtained solid products were washed thoroughly with hexane followed by overnight drying at 60^{o}C in the oven. Finally, the solid products were calcined at 773 K for 4 h to obtain Al-SBA-15 with a final Si/Al ratio of 80.

6.2.2 Catalyst Preparation

The oxide precursors were prepared through incipient wetness impregnation of Al-SBA-15, γ-Al_2O_3, ZSM-5, Zeolite β and USY zeolite using aqueous solutions with the appropriate salts. The γ-Al_2O_3 support was supplied by *US Research Nanomaterials, Inc.*, Houston, TX. All of the zeolite supports were purchased from *Zeolyst International*, Kansas City, KS. All supports materials are calcined at 350 ^{o}C before usage for the purpose of stable the crystal structure. For the impregnation, 10g of $Ni(NO_3)_2$ and 7.3g of $(NH_4)_6Mo_7O_{24}\cdot 4H_2O$ (*Sigma-Aldrich*, St. Louis, MO) were dissolved in a volume of water equal to the total pore volume of the catalyst support. This solution was then

immediately poured over 40g of catalyst support and agitated slightly to ensure that the entire pore volume of the catalyst was impregnated. Following this, the impregnated catalyst was placed in a 50°C oven for 12 hours, and then dried in a programmable high-temperature oven for 12 hours at 120^{o}C, followed by calcination at 400°C for 6 hours. The final step in the procedure is the carburization or nitriding of the metal oxide precursor using the temperature-programmed reduction (TPR)[131-133]. Firstly, 10 grams of the metal oxide precursor is loaded into a quartz reactor and placed in a temperature-controlled oven. Then the carburization is carried out using a flow of 250 cm^3 min^{-1} of 20 vol % CH_4/H_2 over the metal oxides at a heating rate of 10K min^{-1} to 250^{o}C and then at a 1.98 K min^{-1} to a final temperature of 730°C, which previous studies have shown to be suitable for carbide formation[134]. In the final stage, the temperature was maintained at 730 ^{o}C for half an hour to complete the reaction. The ammonia nitridation of oxides is carried out in a flow of 100 cm^3 min^{-1} of ammonia. In the first stage, the temperature was increased at 10 K min^{-1} to 250^{o}C. In the second stage, the temperature was raised to 700^{o}C and held for half an hour. Finally, the sample was cooled down to room temperature in argon and then passivated in flowing mixed gases (1% O_2/Ar) for 2 hours[28].

6.2.3 Catalyst Characterization

An X-ray Diffraction (XRD) analysis was carried out using a Rigaku RU2000 rotating anode powder diffractometer (Rigaku Americas Corporation, TX) at a scan rate of 4° /min.

A Brunauer-Emmett-Teller (BET) analysis was carried out to determine the surface area and pore size of the catalysts using a Micromeritics model ASAP 2010 surface area analyzer (Micromeritics Instrument Corporation, GA), with nitrogen (99.99% purity) as the analysis gas. The catalyst samples were heated to 150°C at a rate of 10 °C/min and then held for 2 hours under a nitrogen atmosphere, and the adsorption/desorption isotherms were acquired at 77.35 K using a 5 second

equilibrium time interval. The catalyst samples were degassed at 150°C for 6 hours prior to analysis to remove any adsorbed molecules from the pores and surfaces.

Transmission electron microscopy (TEM) of the samples was done on a JEOL-2010 FasTEM microscope operating at 100 kV. The calcined sample was dispersed in hexane, deposited on a Cu grid and dried. Aluminum content in Al-SBA-15 was estimated by EDAX.

6.2.4 Activity tests

Catalysts activity tests were carried out in a BTRS – Jr® tubular reactor (Autoclave Engineers, PA) ◦ıng soybean oil as a feedstock. The reactor is a fixed bed reactor with the dimension of 1.31 cm i.d. × 61 cm. Approximately 2 g of the catalyst was loaded in the reactor. Quartz beads with a size about 200 μm were used to dilute the catalyst bed at a 1:1 (v/v) ratio in order to improve the mass and heat transfer of the catalyst beds. Prior to the reaction, the catalyst was reduced in a hydrogen flow (50 mL/min) at 450^{o}C for two hours. The reactions were carried out at 400 ^{o}C and 650psi. After the temperature and pressure were stabilized, soybean oil was fed at 1 h^{-1} liquid hourly space velocity (LHSV) while maintaining hydrogen flow rate at 50 mL/min. The liquid and gaseous products were separated in the gas-liquid-separator after the reaction. An experiment was considered to be in a steady state when the liquid product yield and the selectivity for gasoline to diesel range hydrocarbons maintain relatively constant on a daily basis, usually after 4–5 days on stream. Gaseous products were analyzed by an online gas chromatograph (Perkin Elmer, Calculus 500) equipped with a built-in Arnel Model 2106 Analyzer and a thermal conductivity detector (TCD). Helium and nitrogen are used as carrier gases. Liquid samples were collected at intervals of 24 h. The organic liquid product (OLP) was separated from the aqueous phase using a syringe. Hydrocarbon fuels in the OLP, such as gasoline (C_5-C_{12}), jet fuel (C_8 - C_{16}) and diesel (C_{12} - C_{22}),

were analyzed quantitatively by a GC with a capillary glass column (100% dimethyl polysiloxane 60m×0.32×1.0μm, *Restek*, PA) and a flame ionization detector.

6.3 Results and discussion

6.3.1 Catalyst Characterization

Figure 39 exhibits the nitrogen adsorption-desorption isotherms of the five supported NiMoC catalysts. It can be seen the isotherm curve of NiMoC/Al-SBA-15 is type IV and the adsorption hysteresis loop is type A according to De Boer's theory, which means that NiMoC/Al-SBA-15 has a meso porous structure with uniform regular channel distribution. The specific adsorption capacity is as high as 450 m^2/g. NiMoC/γ-Al_2O_3 shows a type IV isotherm curve and the adsorption hysteresis loop is type E. It indicates that NiMoC/γ-Al_2O_3 catalyst has a meso-porous structure with irregular and un-uniform channels inside. And its specific adsorption capacity is also much lower than NiMoC/Al-SBA-15.

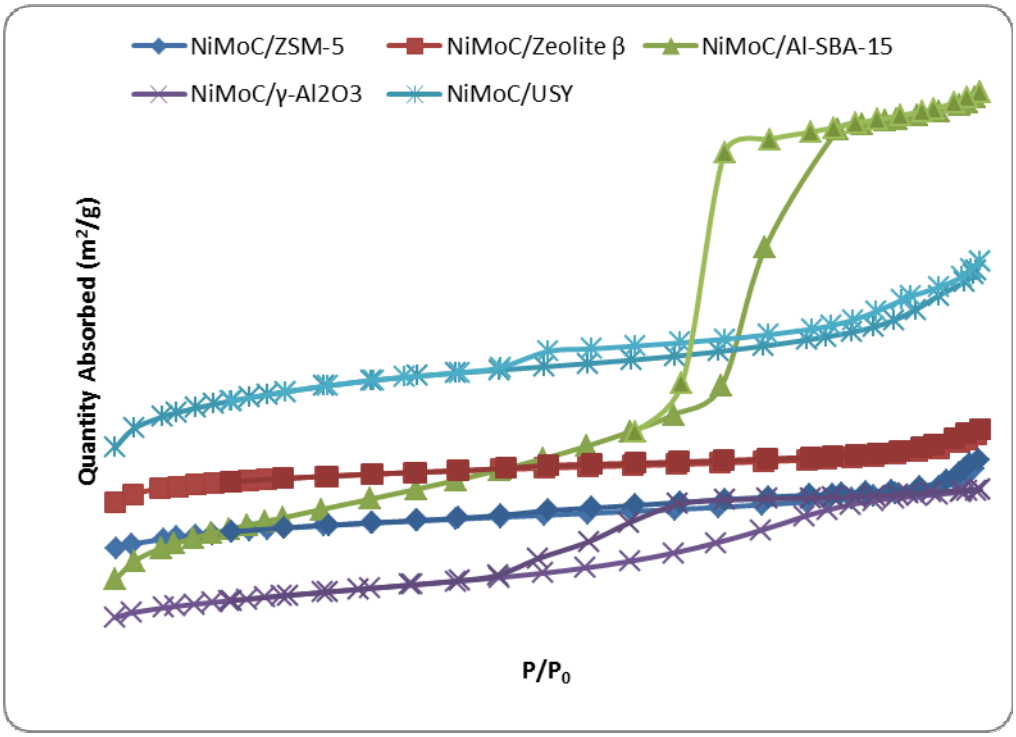

Figure 39. Nitrogen adsorption-desorption isotherms of the catalysts

Table 12. Textural properties of NiMoC catalysts using different supports

Catalyst	Surface Area (m^2 g^{-1})	Pore Volume (cm^{-3} g^{-1})
NiMoC/ZSM-5	446.8	0.13
NiMoC/Zeolite β	466.7	0.09
NiMoC/USY	475.6	0.25
NiMoC/γ-Al_2O_3	216.0	0.21
NiMoC/Al-SBA-15	711.5	0.71

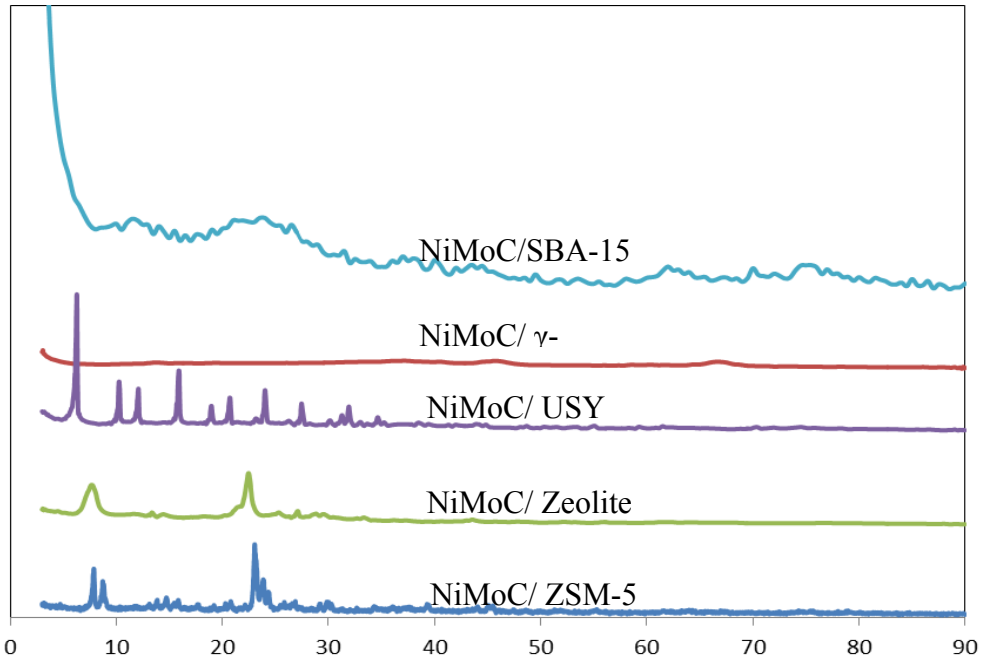

Figure 40. XRD patterns of the five supported NiMo carbide catalysts

The other three zeolites supported catalysts (NiMoC/ZSM-5, NiMoC/Zeolite β and NiMoC/USY) exhibited profiles of microporous structures (Type I isotherms) with relatively small external surface, which is characterized by an initial rapid increase in the amount adsorbed and a long nearly flat region at higher pressures [147]. The specific adsorption capacity follows this order:

NiMoC/USY > NiMoC/ZSM-5 and NiMoC/Zeolite β. In addition, Table 12 lists the textural properties of the catalysts. It can be observed that NiMoC/Al-SBA-15 has the highest surface area (711.5/ m^2 g^{-1}) compared to the other four catalysts.

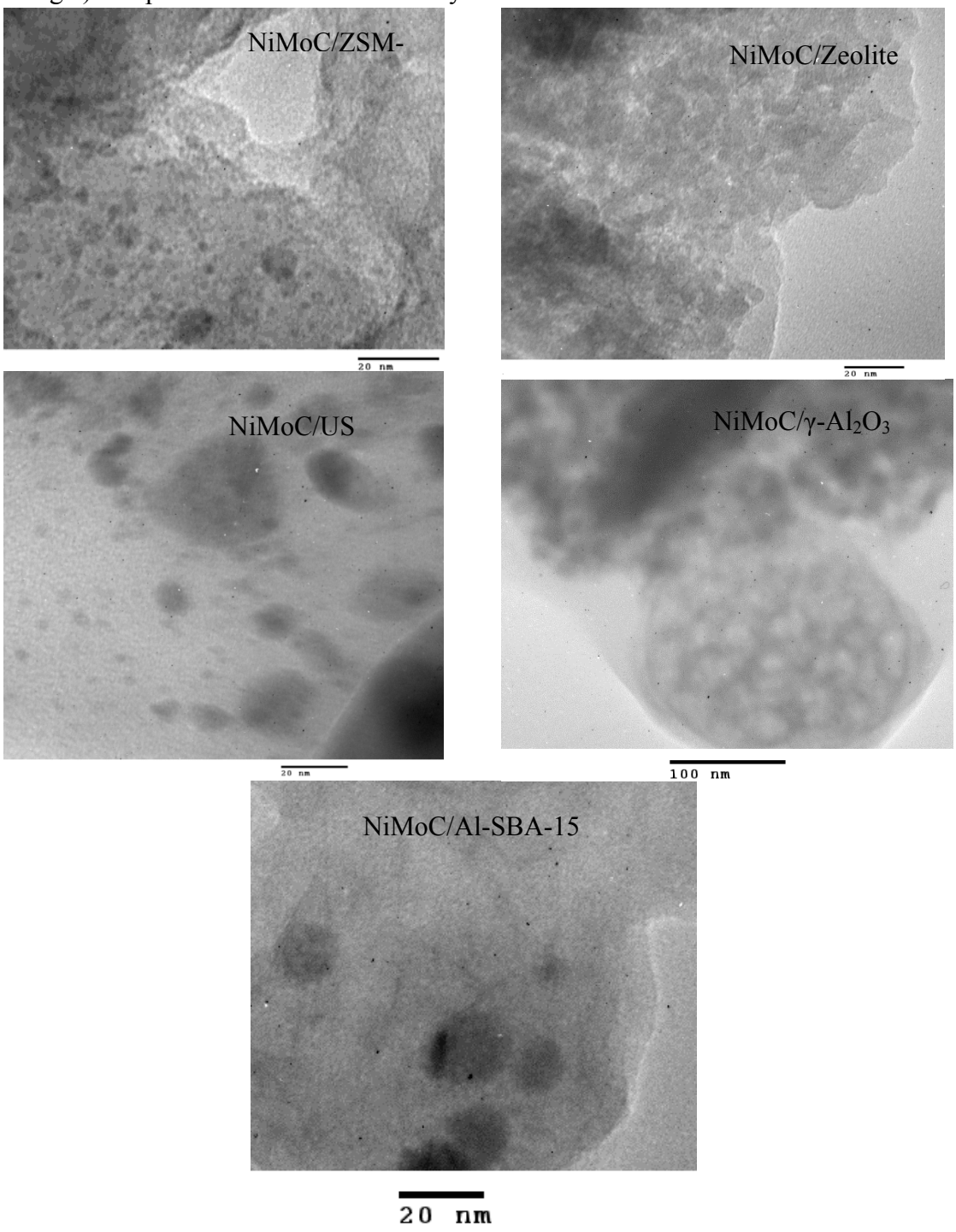

Figure 41. TEM images of the catalysts

Figure 40 illustrates the X-ray diffractions of the five supported carbide catalysts within the range of 3-90°. No characteristic peaks belong to Ni/Mo carbides or oxides can be observed for the supported carbide catalysts. For NiMoC/Al-SBA-15, only the diffuse peaks of noncrystalline silica have been observed. It indicates that the crystallite sizes of Ni/Mo carbides or oxides are below the lower limit for XRD detectability (5 nm), or an amorphous metal carbides or oxides are formed[148].

Figure 41 shows the transmission electron micrographs (TEM) of NiMoC/ZSM-5, NiMoC/Zeolite β, NiMoC/USY, NiMoC/γ-Al_2O_3 and NiMoC/Al-SBA-15. TEM images of catalysts confirmed their nanostructure. The black spots on the images denote the metallic particles (NiMo carbides and/or oxides) of on the catalysts. The metallic particles had irregular shapes on zeolite β and γ-Al_2O_3. The comparison of the five supports indicates that Al-SBA-15 support allows obtaining the smallest metallic particle size and the particles are well dispersed.

6.3.2 Hydrotreating activities of the catalysts

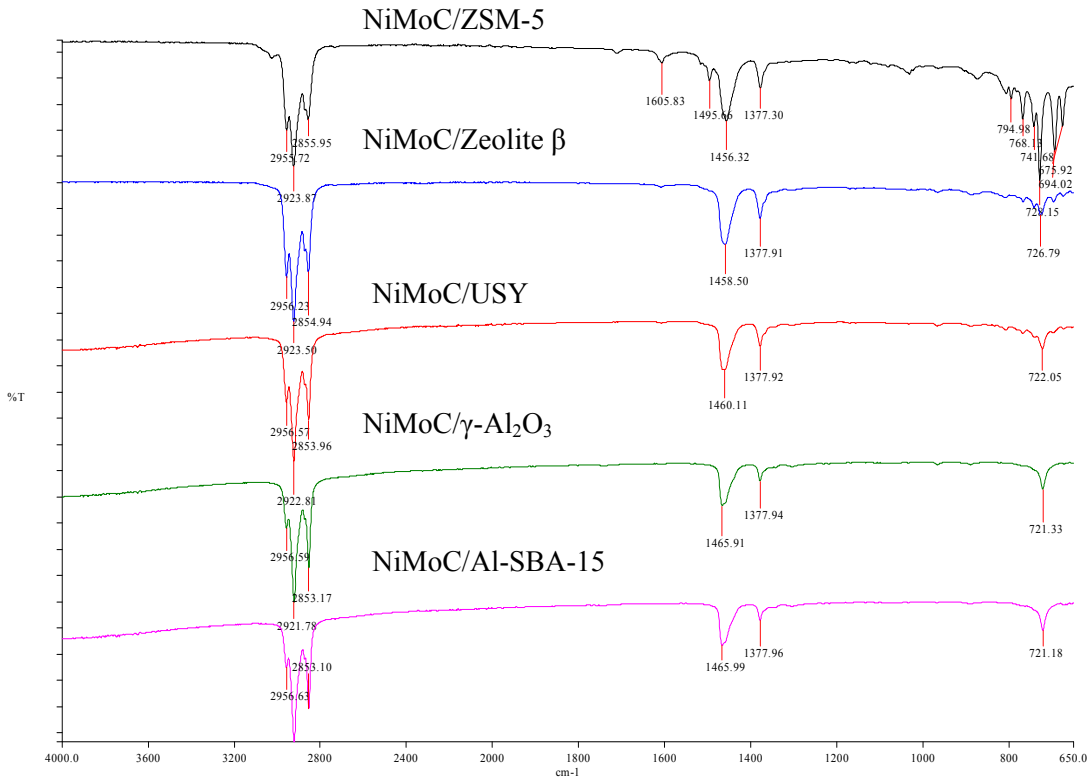

Figure 42. FTIR spectra of the OLPs over the five supported NiMoC catalysts

The effect of the catalyst supports was correlated with their hydrotreating catalytic activity in the 400°C reaction temperature range and 650psi pressure. The conversion of triglycerides was found to be 100% over the five catalysts by monitoring the concentration of triglycerides in the products.

It can be seen from Figure 42 that neither carboxyl nor ester group absorption could be found on the FTIR spectra of the OLPs from all of the catalysts. Therefore, both triglycerides and free fatty acids in the feedstock were converted. Basic composition of soybean oil hydrotreating products is similar for all catalysts used. The reaction yields an organic liquid product (OLP), together with gaseous products and water. Beside hydrocarbon fuels, the OLP may also contain other side products, such as partially converted triglycerides, oxygenates, monomers, dimers, tars, among others. The gaseous products are composed unreacted hydrogen, carbon monoxide, carbon dioxide and small hydrocarbon molecules (C1-C4).

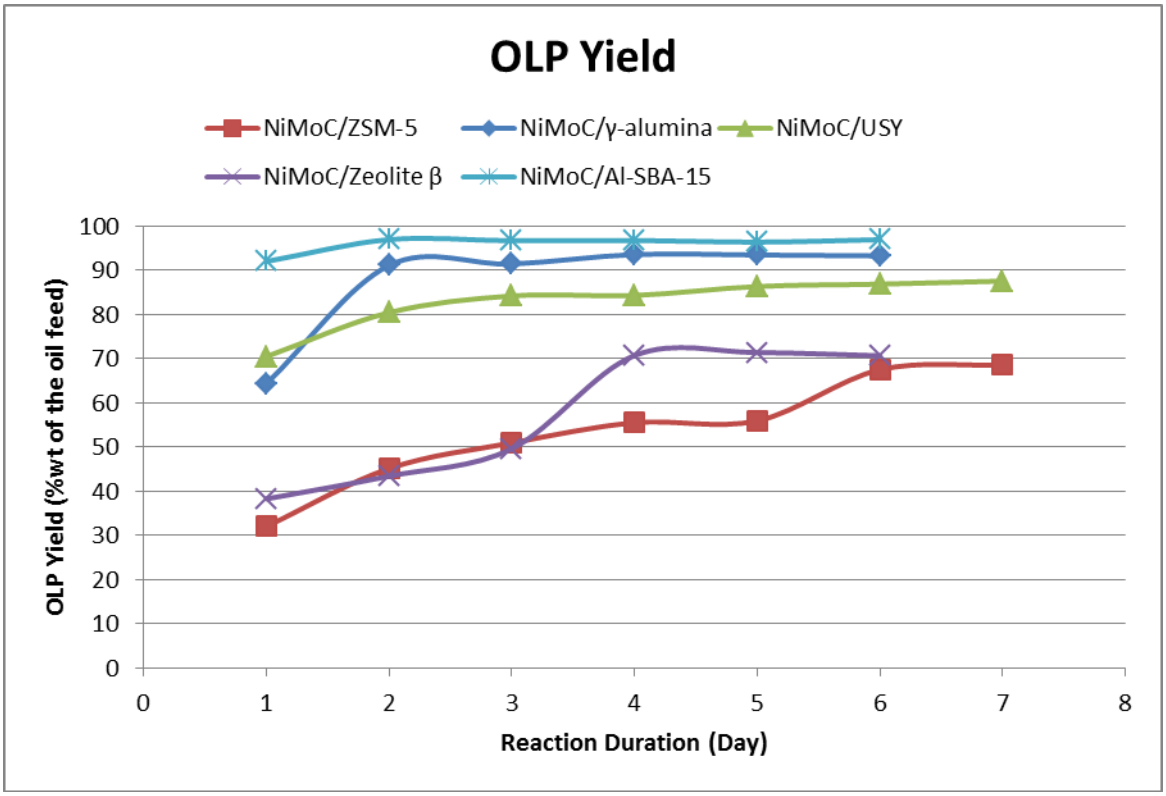

Figure 43. Organic liquid product (OLP) yield

The OLP yields and selectivities to gasoline kerosene/jet, and diesel hydrocarbons are given in Figure 43-46. It can be seen from Figure 43 that the OLP yields from NiMoC/Al-SBA-15 and NiMoC/γ-Al_2O_3 are superior to those from the zeolites supported catalysts, NiMoC/ZSM-5, NiMoC/Zeolite β and NiMoC/USY. It can be explained by the meso-structure property of Al-SBA-15 and γ-Al_2O_3, which can provide a larger diffusion space for the large size triglyceride molecules (around 5.3-7.4Å longitudinal section diameter and 30-45 Å chain length[76]) than the micro-porous supports. NiMoC/Al-SBA-15 shows the highest yield of OLP as it has the largest pore size. Figure 27 also shows that among the micro-porous materials OLP yield from NiMoC/USY is higher than those from NiMoC/ZSM-5, NiMoC/Zeolite β. It might be due to the higher specific adsorption capacity of NiMoC/USY than that of NiMoC/ZSM-5 or NiMoC/Zeolite β. A higher specific adsorption capacity could be a result of more active sites on the catalyst surface[149].

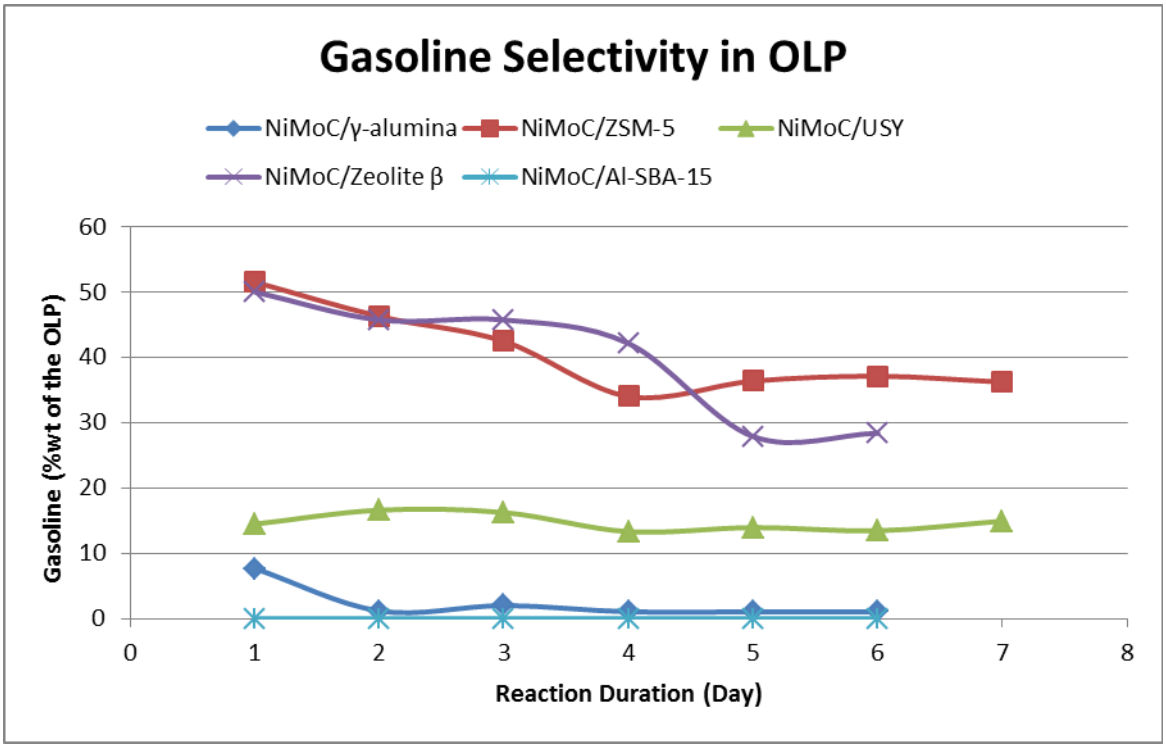

Figure 44. Gasoline selectivity in OLP

The results of hydrotreating activity indicate that a lower gas yield was obtained with mesoporous molecular sieve (SBA-15) and amorphous alumina (γ-Al_2O_3) based catalysts as compared with zeolites based catalysts. The liquid yield was very low (60-80%) in case of zeolite based catalysts as compared with γ-Al_2O_3 and SBA-15 supported catalysts (90% and 96% respectively). It was reported by *Leng et al.*[120] that lighter compounds such as gaseous hydrocarbons and gasoline range hydrocarbons are mainly produced from the secondary cracking during the catalytic cracking process of vegetable oils. Micro-porous catalysts provide smaller channel and longer diffusion trial for reactant molecules than meso-porous ones. Therefore, micro-porous supports, ZSM-5, Zeolite β, USY can provide more cracking sites for gasoline production reactions than Al-SBA-15 and γ-Al_2O_3. It can be seen from Figure 44 that 20-50% of gasoline range hydrocarbons in OLP were obtained over the zeolite supported catalysts, NiMoC/ZSM-5, NiMoC/USY and NiMoC/Zeolite β while almost no gasoline was produced over the other two non-zeolite supported catalysts, NiMoC/Al-SBA-15 and NiMoC/γ-Al_2O_3. In comporison of NiMoC/ZSM-5, NiMoC/USY and NiMoC/Zeolite β, it can be found that NiMoC/ZSM-5 and NiMoC/Zeolite β yield more gasoline range hydrocarbons than NiMoC/USY. The explanation can be found according to the pore volumes of the catalysts shown in Table 12. Pore volume of NiMoC/USY is the highest 0.25 cm^{-3}/g; while NiMoC/ZSM-5 and NiMoC/Zeolite β are only 0.13 and 0.09 cm^{-3}/g, respectively. The diffusion of the triglyceride molecule within the large pore volume catalyst is much easier and therefore the secondary cracking is limited. Thus, less gasoline products were obtained over the larger pore volume catalyst (NiMoC/USY) than those over the NiMoC/ZSM-5 and NiMoC/Zeolite β catalysts.

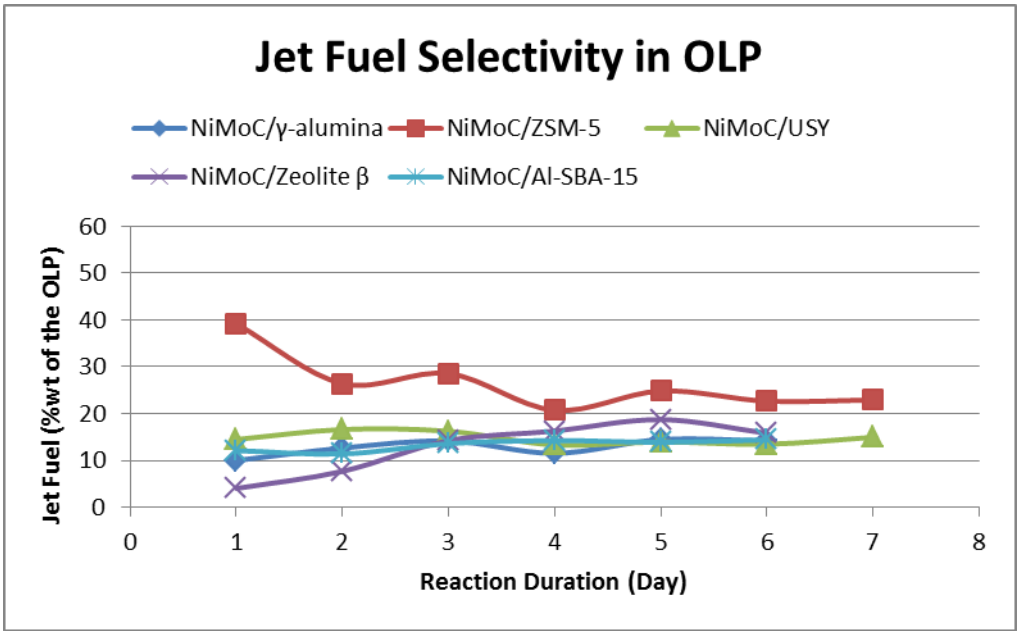

Figure 45. Jet fuel selectivity in OLP

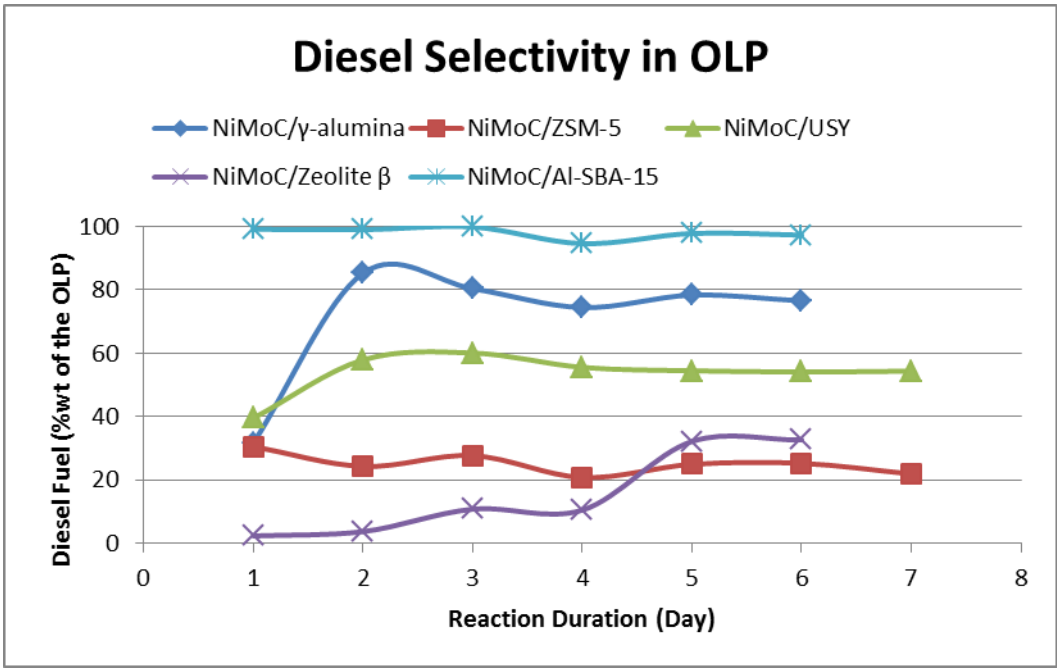

Figure 46. Diesel fuel selectivity in OLP

Diesel range hydrocarbons were mainly obtained as a result of the preferential removal of the oxygen from the triglyceride molecules by decarbonylation, decarboxylation and/or hydrodeoxygenation[120]. Therefore, porous structure of catalysts plays an important role in controlling the diesel selectivity. Smaller porous structure will cause more secondary cracking of heavy hydrocarbons and lead to a lower diesel selectivity. Larger porous structure of mesoporous supports as compared with zeolites makes it excellent candidates for applications where large organic molecules as triglycerides are accessible to the well dispersed active sites located inside the pores[150]. As shown in Figure 46, NiMoC/Al-SBA-15 and NiMoC/γ-Al_2O_3 have higher selectivities to diesel range hydrocarbons than NiMoC/ZSM-5, NiMoC/Zeolite β and NiMoC/USY. Furthermore, NiMoC/Al-SBA-15 is superior to NiMoC/γ-Al_2O_3 regarding selectivity to diesel range hydrocarbons (≈97%) under the condition tested. The organic liquid product is consisted predominantly of n-alkanes (C15-C18), only minor amounts of iso-alkanes and olefins have been found. This may be due to the different channel properties of these two catalysts as shown in Figure 3. NiMoC/Al-SBA-15 has a regular and uniform channel structure. Therefore, reactant diffusion inside the pores is easy and fluent. NiMoC/γ-Al_2O_3 has a meso-porous structure. However, its channel is non-uniform and irregular. Therefore, reactant diffusion inside the pores is not uniform. In contrast to the supports of amorphous alumina (γ-Al_2O_3) and microporous molecular sieves (zeolites), the mesoporous molecular sieve support (SBA-15) also have very high specific surface areas (Table 12) which allows very high dispersions and loadings of the supported active phase [151]. So, NiMoC/Al-SBA-15 has the highest activity and selectivity to diesel hydrocarbons than other four catalysts.

6.4 Conclusions

The hydrotreating of soybean oils on supported NiMo carbide catalysts makes possible the production of gasoline to diesel range liquid hydrocarbons. Because of specific pore structures, all of the zeolites-supported catalysts have a strong cracking activity by producing more gaseous and gasoline products. The meso-porous γ-Al_2O_3 and Al-SBA-15 supported catalysts led to a larger production of green diesel containing mostly C15-C18 hydrocarbons, which are mainly formed by decarboxylation/decarbonylation and/or hydrodeoxygenation reactions, respectively. The high surface area, large porosity and regular channel structure of the A-lSBA-15 supported catalyst led to high conversion (100%) and selectivity to green diesel (97%), in the hydrotreating of soybean oil at 400^{o}C, 650 psi, oil LSHV = 1, during 7 days of reaction. When compared with other reported hydrotreating catalysts, the NiMoC/Al-SBA-15 catalyst showed the highest hydrotreating activity and selectivity to diesel hydrocarbons. The results showed that the present NiMoC/Al-SBA-15 could be considered as a promising catalytic system for hydrotreating vegetable oil to green diesel.

CHAPTER 7. RESEARCH CONCLUSIONS AND RECOMMENDATIONS

7.1 Conclusions

The work in this dissertation shows that the developed catalysts exhibited excellent activity and selectivity for hydrotreating of renewable feedstock. NiMoC/Al-SBA-15 was found to be a promising catalytic system for hydrotreating vegetable oil to green diesel compared to other tested catalysts. The following conclusions can be obtained according to the three distinct experimental phases:

Jet fuel hydrocarbons production FROM Catalytic cracking over ZSM-5 and hydrocracking over Ru/ZSM-5 of soybean oil

- The yield of kerosene jet was as high as 21% during the catalytic cracking process over ZSM-5.

- The catalytic cracking process suffered from severely plugging due to large amount of coke and tar production.

- Jet fuel (16%) was obtained under a much lower pressure (650 psi) over a non-sulfided precious metal catalyst (Ru/ZSM-5 catalyst).

- Less tar and coke were formed during the hydrocracking process and stable continuous flow reaction was obtained by using the bifunctional Ru/ZSM-5 catalyst.

Hydrocarbon Fuels Production from Hydrocracking of Soybean Oil Using Transition Metal Carbides and Nitrides Supported on ZSM-5

— Complete conversion of soybean oil and up to 50%wt yield of hydrocarbon fuels were obtained from vegetable oil.

— Nitride catalyst showed a higher activity for the methanation reaction.

— Catalyst under a low reaction temperature (360^{o}C) is not resistant to the water poison and large amount of carboxylic acid products was produced.

— Increasing the oil-catalyst contact time by decreasing the oil flow rate can enhance the hydrocarbon fuel contents in the organic liquid products.

— Highest yield of biofuels was obtain over the catalyst with a small amount of Ni (Ni/Mo=0.5).

Hydrotreating of Soybean Oil over NiMo Carbide Supported on Five Different Supports

— 20-50% of gasoline range hydrocarbons in the OLP were obtained over the zeolite supported catalysts, NiMoC/ZSM-5, NiMoC/USY and NiMoC/Zeolite β.

— The meso-porous γ-Al_2O_3 and Al-SBA-15 supported catalysts led to a larger production of green diesel containing mostly C15-C18 hydrocarbons.

— NiMoC/Al-SBA-15 supported catalyst led to high conversion (100%) and selectivity to green diesel (97%), in the hydrotreating of soybean oil at 400^{o}C, 650 psi, oil LSHV = 1, during 7 days of reaction.

In conclusion, this study provides a promising approach for preparing drop-in fuels from renewable resources under milder reaction condition compared to the industrial process. The application of the technology eliminates the need to add a sulfur compound to a biomass-derived feedstock. This study fills the gaps in the literature by investigating the hydrotreating activities and selectivity of bimetallic (NiMo) carbides and nitrides catalysts.

7.2 Recommendations

Recommendations for the future study on the production of hydrocarbon fuels especially green diesel from renewable feedstocks using a supported NiMo carbide catalyst are as follows:

— Modify the catalyst formulation using the obtained Al-SBA-15 as the support material. The bimetallic combinations should be further varied to determine the one having high hydrogenation and oxygen removal activities with a longer catalyst life.

— Adopt the concept of combining the mesoporous supports and zeolites to achieve higher selectivity in the gasoline to jet range hydrocarbon fuels.

— Study the catalyst activity and selectivity by varying the renewable feedstocks, especially non-food based feedstocks, such as algae oil, waste cooking oil, yellow grease, brown grease, etc.

— A more detailed analysis of the product, such as oxygenate contents, olefin to paraffin ratio, coke and tar compositions. A thorough fuel property test including cetane number, cold flow property, viscosity, pour point and oxidative stability should be carried out with the green diesel products.

— Investigate the catalyst deactivation mechanism and find the way to regenerate the catalyst.

— Develop the thermal kinetic model and cost model so that the process can be evaluated on a cost basis.

REFERENCES

1. Dandik, L.; Aksoy, H. A.; Erdem-Senatalar, A., Catalytic conversion of used oil to hydrocarbon fuels in a fractionating pyrolysis reactor. *Energy & Fuels* **1998,** 12, (6), 1148-1152.
2. Knothe, G.; Van Gerpen, J.; Krahl, J., The biodiesel handbook. *AOCS press: Campaign, IL,* **2005**.
3. Huber, G. W.; Corma, A., Synergies between Bio- and Oil Refineries for the Production of Fuels from Biomass. *Angewandte Chemie International Edition* **2007,** 46, (38), 7184-7201.
4. Stumborg, M.; Wong, A.; Hogan, E., Hydroprocessed vegetable oils for diesel fuel improvement. *Bioresource Technology* **1996,** 56, (1), 13-18.
5. Rahmes, T., Status of Sustainable Biofuel Efforts for Aviation. *Boeing Management Company* **2004**.
6. Dolbear, G. E., Hydrocracking catalysts and processes. *Abstracts of Papers of the American Chemical Society* **1995,** 210, 9-PETR.
7. Morel, F.; Kressmann, S.; Harle, V.; Kasztelan, S. In *Processes and catalysts for hydrocracking of heavy oil and residues*, 1997; Froment, G. F.; Delmon, B.; Grange, P., Eds. 1997; pp 1-16.
8. Ward, J. W., Hydrocracking processes and catalysts. *Fuel Processing Technology* **1993,** 35, (1-2), 55-85.
9. Mäki-Arvela, P.; Kubickova, I.; Snåre, M.; Eränen, K.; Murzin, D. Y., Catalytic Deoxygenation of Fatty Acids and Their Derivatives. *Energy & Fuels* **2006,** 21, (1), 30-41.

10. Mäki-Arvela, P. i.; Rozmysłowicz, B.; Lestari, S.; Simakova, O.; Eränen, K.; Salmi, T.; Murzin, D. Y., Catalytic Deoxygenation of Tall Oil Fatty Acid over Palladium Supported on Mesoporous Carbon. *Energy & Fuels* **2011,** 25, (7), 2815-2825.
11. Murata, K.; Liu, Y.; Inaba, M.; Takahara, I., Production of Synthetic Diesel by Hydrotreatment of Jatropha Oils Using Pt−Re/H-ZSM-5 Catalyst. *Energy & Fuels* **2010,** 24, (4), 2404-2409.
12. Sotelo-Boyás, R.; Liu, Y.; Minowa, T., Renewable Diesel Production from the Hydrotreating of Rapeseed Oil with Pt/Zeolite and NiMo/Al_2O_3 Catalysts. *Industrial & Engineering Chemistry Research* **2010,** 50, (5), 2791-2799.
13. Huber, G. W.; O'Connor, P.; Corma, A., Processing biomass in conventional oil refineries: Production of high quality diesel by hydrotreating vegetable oils in heavy vacuum oil mixtures. *Applied Catalysis A: General* **2007,** 329, 120-129.
14. W.K. Craig, D. W. S., Production of hydrocarbons with a relativelyhigh cetane rating. *US Patent 4,992,605* **1991**.
15. Simácek, P.; Kubicka, D.; Sebor, G.; Pospísil, M., Hydroprocessed rapeseed oil as a source of hydrocarbon-based biodiesel. *Fuel* **2009,** 88, (3), 456-460.
16. da Rocha Filho, G. N.; Brodzki, D.; Djéga-Mariadassou, G., Formation of alkanes, alkylcycloalkanes and alkylbenzenes during the catalytic hydrocracking of vegetable oils. *Fuel* **1993,** 72, (4), 543-549.
17. Krár, M.; Kovács, S.; Kalló, D.; Hancsók, J., Fuel purpose hydrotreating of sunflower oil on CoMo/Al2O3 catalyst. *Bioresource Technology* **2010,** 101, (23), 9287-9293.
18. Pérot, G., Hydrotreating catalysts containing zeolites and related materials--mechanistic aspects related to deep desulfurization. *Catalysis Today* **2003,** 86, (1-4), 111-128.

19. Zuo, D.; Li, D.; Nie, H.; Shi, Y.; Lacroix, M.; Vrinat, M., Acid-base properties of NiW/Al2O3 sulfided catalysts: relationship with hydrogenation, isomerization and hydrodesulfurization reactions. *Journal of Molecular Catalysis A: Chemical* **2004,** 211, (1-2), 179-189.

20. H. Topsøe, B. S. C., F.E. Massoth, Hydrotreating Catalysis-Science and Technology. *Springer, Berlin,* **1996**.

21. Kaufmann, T. G.; Kaldor, A.; Stuntz, G. F.; Kerby, M. C.; Ansell, L. L., Catalysis science and technology for cleaner transportation fuels. *Catalysis Today* **2000,** 62, (1), 77-90.

22. I.E, M., Zeolite catalysis in hydroprocessing technology. *Catalysis Today* **1987,** 1, (4), 385-413.

23. Choudhary, N.; Saraf, D. N., Hydrocracking: A Review. *Product R&D* **1975,** 14, (2), 74-83.

24. Egeberg, G. R.; Michaelsen, H. N.; Skyum, L., Novel hydrotreating technology for production of green diesel *presented at ERTC* **2009**.

25. Egeberg, R. G.; Knudsen, K., Industrial-scale production of renewable diesel. *Published in PTQ Q3* **2011**.

26. Koivusalmi, E.; Piilola, R.; Aalto, P., Process for producing branched hydrocarbons *United States Patent Publication 0302001* **2008**.

27. Furimsky, E., Metal carbides and nitrides as potential catalysts for hydroprocessing. *Applied Catalysis A: General* **2003,** 240, (1-2), 1-28.

28. Zhang, W.; Zhang, Y.; Zhao, L.; Wei, W., Catalytic Activities of NiMo Carbide Supported on SiO2 for the Hydrodeoxygenation of Ethyl Benzoate, Acetone, and Acetaldehyde. *Energy & Fuels* **2010,** 24, (3), 2052-2059.

29. Diaz, B.; Sawhill, S. J.; Bale, D. H.; Main, R.; Phillips, D. C.; Korlann, S.; Self, R.; Bussell, M. E., Hydrodesulfurization over supported monometallic, bimetallic and promoted carbide and nitride catalysts. *Catalysis Today* **2003,** 86, (1-4), 191-209.

30. Ramanathan, S.; Oyama, S. T., New Catalysts for Hydroprocessing: Transition Metal Carbides and Nitrides. *The Journal of Physical Chemistry* **1995,** 99, (44), 16365-16372.

31. Santillán-Vallejo, L. A.; Melo-Banda, J. A.; Reyes de la Torre, A. I.; Sandoval-Robles, G.; Domínguez, J. M.; Montesinos-Castellanos, A.; de los Reyes-Heredia, J. A., Supported (NiMo,CoMo)-carbide, -nitride phases: Effect of atomic ratios and phosphorus concentration on the HDS of thiophene and dibenzothiophene. *Catalysis Today* **2005,** 109, (1-4), 33-41.

32. Ramanathan, S.; Oyama, S. T., New catalysts for hydroprocessing: Transition metal carbides and nitrides. *Journal of Physical Chemistry* **1995,** 99, (44), 16365-16372.

33. Han, J.; Duan, J.; Chen, P.; Lou, H.; Zheng, X.; Hong, H., Nanostructured molybdenum carbides supported on carbon nanotubes as efficient catalysts for one-step hydrodeoxygenation and isomerization of vegetable oils. *Green Chemistry* **2011,** 13, (9), 2561-2568.

34. Monnier, J.; Sulimma, H.; Dalai, A.; Caravaggio, G., Hydrodeoxygenation of oleic acid and canola oil over alumina-supported metal nitrides. *Applied Catalysis A: General* **2010,** 382, (2), 176-180.

35. Dunn, R. O., Alternative jet fuels from vegetable-oils. *Transactions of the Asae* **2001,** 44, (6), 1751-1757.

36. Sustainable Oils Inc. *http://www.susoils.com/* **2009**.

37. Freerks, R.; Muzzell, P. A. In *Production and characterization of synthetic jet fuel produced from Fischer-Tropsch hydrocarbons*, 2004; 2004; pp 50-PETR.

38. Muzzell, P. A.; Freerks, R.; Baltrus, J. P.; Link, D. D. In *Composition of syntroleum S-5 and conformance to JP-5 specification*, 2004; 2004; pp 51-PETR.

39. de Klerk, A. In *Environmentally friendly refining: Fischer-Tropsch versus crude oil*, 2007; 2007; pp 560-565.

40. (IATA), I. A. T. A., IATA 2008 Report on Alternative Fuels. **2008**.

41. Kunkes, E. L.; Simonetti, D. A.; West, R. M.; Serrano-Ruiz, J. C.; Gartner, C. A.; Dumesic, J. A., Catalytic conversion of biomass to monofunctional hydrocarbons and targeted liquid-fuel classes. *Science* **2008,** 322, (5900), 417-421.

42. Daniel M. Ginosar, L. M. P., David N. Thompson, Conversion of crop seed oil to jet fuel and associated methods. *U. S. Patent Publication No. 0,071,872* **2009**.

43. Wayne A. Seames, T. A., Method for cold stable biojet fuel *U.S. Patent Publication No. 0,092,436* **2008**.

44. Morgan, W. D., Production of Fuels with Superior Low Temperature Properties from Tall Oil or Fractionated Fatty Acids. *United States Patent Publication No. 0049739* **2009**.

45. Ramin Abhari, L. T., Peter Havlik, Nathan Jannasch, Process for Co-Producing Jet Fuel and LPG from Renewable Sources *U. S. Patent Publication No. 0,244,962* **2008**.

46. Syntroleum, Bio-Synfining™. *http://www.syntroleum.com/proj_rba_bio-synfining.aspx#* **2009**.

47. Marckley, K. S., Fatty Acids, 2nd ed. *New York: Interscience* **1960**.

48. Srivastava, A.; Prasad, R., Triglycerides-based diesel fuels. *Renewable & Sustainable Energy Reviews* **2000,** 4, (2), 111-133.

49. CE Goering, A. S., MJ Daugherty, EH Pryde, AJ Heakin, Fuel properties of eleven vegetable oils. *Trans. ASAE* **1982**, 1472.

50. *http://www.indexmundi.com/agriculture/?country=us&commodity=soybean-oilseed&graph=production.*

51. Achten, W. M. J.; Mathijs, E.; Verchot, L.; Singh, V. P.; Aerts, R.; Muys, B., Jatropha biodiesel fueling sustainability? *Biofuels Bioproducts & Biorefining-Biofpr* **2007,** 1, (4), 283-291.

52. de Oliveira, J. S.; Leite, P. M.; de Souza, L. B.; Mello, V. M.; Silva, E. C.; Rubim, J. C.; Meneghetti, S. M. P.; Suarez, P. A. Z., Characteristics and composition of Jatropha gossypiifolia and Jatropha curcas L. oils and application for biodiesel production. *Biomass & Bioenergy* **2009,** 33, (3), 449-453.

53. Achten, W. M. J.; Verchot, L.; Franken, Y. J.; Mathijs, E.; Singh, V. P.; Aerts, R.; Muys, B., Jatropha bio-diesel production and use. *Biomass & Bioenergy* **2008,** 32, (12), 1063-1084.

54. Spolaore, P.; Joannis-Cassan, C.; Duran, E.; Isambert, A., Commercial applications of microalgae. *Journal of Bioscience and Bioengineering* **2006,** 101, (2), 87-96.

55. Donald E. Trimbur, C.-s. I., Harrison F. Dillon, Anthony G. Day, Scott Franklin, Anna Coragliotti, Renewable Diesel and Jet Fuel from Microbial Sources. *United States Patent Publication 0047721* **2009**.

56. http://www.oilgae.com/. **2009**.

57. Alternative Fuels. *http://www.iata.org/pressroom/facts_figures/fact_sheets/alt_fuels.htm* **2009**.

58. Ratledge, C., Fatty acid biosynthesis in microorganisms being used for Single Cell Oil production. *Biochimie* **2004,** 86, (11), 807-815.

59. Morgan, W. D., Production of Fuels with Superior Low Temperature Properties from Tall Oil or Fractionated Fatty Acids. *United States Patent Publication 0049739* **2009**.

60. Jianhua Yao, E. L. S. I., Joseph B. Cross, James B. Kimble, Hsu-hui Hsing, Marvin M. Johnson, Dhananjay B. Ghonasgi, Process for converting triglycerides to hydrocarbons *United States Patent Publication 0175795* **2007**.

61. Li Wang, H. G., HYDROCRACKING CATALYST TECHNOLOGY. *AIChE Spring National Meeting* **2004**.

62. Idem, R. O.; Katikaneni, S. P. R.; Bakhshi, N. N., Catalytic conversion of canola oil to fuels and chemicals: Roles of catalyst acidity, basicity and shape selectivity on product distribution. *Fuel Processing Technology* **1997,** 51, (1-2), 101-125.

63. Katikaneni, S. P. R.; Adjaye, J. D.; Bakhshi, N. N., Catalytic conversion of canola oil to fuels and chemicals over various cracking catalysts. *Canadian Journal of Chemical Engineering* **1995,** 73, (4), 484-497.

64. Twaiq, F. A.; Zabidi, N. A. M.; Bhatia, S., Catalytic conversion of palm oil to hydrocarbons: Performance of various zeolite catalysts. *Industrial & Engineering Chemistry Research* **1999,** 38, (9), 3230-3237.

65. Rollmann, L. D.; Valyocsik, E. W.; Shannon, R. D., Zeolite Molecular Sieves. In *Inorganic Syntheses*, Smith, L. H., Jr., Ed. 2007; pp 61-68.

66. Breck, D. W., **Crystalline zeolite Y**. *United States Patent 3130007* **1964**.

67. Aalto P, P. O., Kiiski U., Manufacture of middle distillate from vegetable oils. *Finnish patent FI 100,248* **1997**.

68. Maxwell, I. E., Zeolite catalysis in hydroprocessing technology. *Catalysis Today* **1987,** 1, (4), 385-413.

69. Stephen J. Miller, Production of Biofuels and Biolubricants From a Common Feedstock *United States Patent Publication 0084026* **2009**.

70. Sulimma, H., Production of a Diesel Fuel Cetane Enhancer from Canola Oil Using Supported Metallic Carbide and Nitride Catalysts. *Thesis, Department of Chemical Engineering, University of Saskatchewan* **2008**.

71. McCall, M. J.; Anumakonda, A.; Bhattacharyya, A.; Kocal, J., Feed-Flexible Processing of Oil-Rich Crops to Jet Fuel. *AIChE Meeting, Chicago, IL* ***September 23*****, 2008**.

72. Prasad, Y. S.; Bakhshi, N. N., EFFECT OF PRETREATMENT OF HZSM-5 CATALYST ON ITS PERFORMANCE IN CANOLA OIL UPGRADING. *Applied Catalysis* **1985,** 18, (1), 71-85.

73. Gusmao J, B. D., Djega-Mariadassou G, Frety R, Completely conversion into hydrocarbons using Ni,Mo / ɣ-Al_2O_3 in the presence of H_2. *Catalysis Today* **1989,** 5.

74. Donnis, B.; Egeberg, R. G.; Blom, P.; Knudsen, K. G., Hydroprocessing of Bio-Oils and Oxygenates to Hydrocarbons. Understanding the Reaction Routes. *Topics in Catalysis* **2009,** 52, (3), 229-240.

75. Maesen, T. L. M.; Calero, S.; Schenk, M.; Smit, B., Alkane hydrocracking: shape selectivity or kinetics? *Journal of Catalysis* **2004,** 221, (1), 241-251.

76. *Nasikin, M.*; *Susanto, B. H.*; *Hirsaman, M. A.*; *Wijanarko, A.*, Biogasoline from Palm Oil by Simultaneous Cracking and Hydrogenation Reaction over NiMo/zeolite Catalyst. *World Applied Sciences Journal* **2009,** 5 (Special Issue for Environment).

77. Smejkal, Q.; Smejkalova, L.; Kubicka, D., Thermodynamic balance in reaction system of total vegetable oil hydrogenation. *Chemical Engineering Journal* **2009,** 146, (1), 155-160.

78. Charusiri, W.; Vitidsant, T., Kinetic study of used vegetable oil to liquid fuels over sulfated zirconia. *Energy & Fuels* **2005,** 19, (5), 1783-1789.

79. Romero, M. S.; Seldes, A. M., Steroids from aquatic organisms .10. Minor sterols from the marine bivalve aulacomya-ater. *Anales De La Asociacion Quimica Argentina* **1985,** 73, (2), 215-220.

80. Gao, Z. H.; Crowley, W. R.; Shukla, A. J.; Johnson, J. R.; Reger, J. F., Controlled-release of contraceptive steroids from biodegradable and injectable gel formulations - in-vivo evaluation. *Pharmaceutical Research* **1995,** 12, (6), 864-868.

81. Perevozchikov, A. P., Sterols and their transport in animal development. *Russian Journal of Developmental Biology* **2008,** 39, (3), 131-150.

82. Bondioli, P.; Cortesi, N.; Mariani, C., Identification and quantification of steryl glucosides in biodiesel. *European Journal of Lipid Science and Technology* **2008,** 110, (2), 120-126.

83. Van Hoed, V.; Zyaykina, N.; De Greyt, W.; Maes, J.; Verhe, R.; Demeestere, K., Identification and occurrence of steryl glucosides in palm and soy biodiesel. *Journal of the American Oil Chemists Society* **2008,** 85, (8), 701-709.

84. Moreau, R. A.; Scott, K. M.; Haas, M. J., The identification and quantification of steryl glucosides in precipitates from commercial biodiesel. *Journal of the American Oil Chemists Society* **2008,** 85, (8), 761-770.

85. Lee I, P. L., Poppe GB, Powers E, Haines T, The role of sterol glucosides on filter plugging. *Biodiesel Mag* **2007,** 4, 105-112.

86. Ruppel, T.; Hall, G., Free and total glycerin in B100 biodiesel by gas chromatography. *Lc Gc Europe* **2007**, 45-45.

87. Neff, W. E.; Jackson, M. A.; List, G. R.; King, J. W., Qualitative and quantitative determination of methyl esters, free fatty acids, mono-, di-, and triacylglycerols via HPLC

coupled with a flame ionization detector. *Journal of Liquid Chromatography & Related Technologies* **1997,** 20, (7), 1079-1090.

88. Trathnigg, B.; Mittelbach, M., Analysis of Triglyceride Methanolysis Mixtures Using Isocratic HPLC With Density Detection. *Journal of Liquid Chromatography* **1990,** 13, (1), 95-105.

89. Foglia, T. A.; Jones, K. C., Quantitation of neutral lipid mixtures using high performance liquid chromatography with light scattering detection. *Journal of Liquid Chromatography & Related Technologies* **1997,** 20, (12), 1829-1838.

90. Holcapek, M.; Jandera, P.; Fischer, J.; Prokes, B., Analytical monitoring of the production of biodiesel by high-performance liquid chromatography with various detection methods. *Journal of Chromatography A* **1999,** 858, (1), 13-31.

91. Di Nicola, G.; Pacetti, M.; Polonara, F.; Santori, G.; Stryjek, R., Development and optimization of a method for analyzing biodiesel mixtures with non-aqueous reversed phase liquid chromatography. *Journal of Chromatography A* **2008,** 1190, (1-2), 120-126.

92. Fu, Y. J.; Zu, Y. G.; Wang, L. L.; Zhang, N. J.; Liu, W.; Li, S. M.; Zhang, S., Determination of fatty acid methyl esters in biodiesel produced from yellow horn oil by LC. *Chromatographia* **2008,** 67, (1-2), 9-14.

93. Gaita, R., A reversed phase HPLC method using evaporative light scattering detection (ELSD) for monitoring the reaction and quality of biodiesel fuels. *Lc Gc North America* **2006**, 51-51.

94. Hajek, M.; Skopal, F.; Machek, J., Determination of free glycerol in biodiesel. *European Journal of Lipid Science and Technology* **2006,** 108, (8), 666-669.

95. Hayes, L.; Lowry, R.; Tinsley, I., Cholesterol interference in analysis of fatty acid methyl esters. *Lipids* **1971,** 6, (1), 65-66.

96. Ringwald SC, F. C., Biodiesel characterisation in the QC environment. *In: Proceedings of the 98th AOCS meeting, Que´bec City, 13–16 May* **2007,** 13-16, 15 (section analytical/industrial oil products).

97. Oliveira, L.; Freire, C. S. R.; Silvestre, A. J. D.; Cordeiro, N.; Torres, I. C.; Evtuguin, D., Steryl glucosides from banana plant Musa acuminata Colla var cavendish. *Industrial Crops and Products* **2005,** 22, (3), 187-192.

98. Wipf, P.; Werner, S.; Twining, L. A.; Kendall, C., HPLC determinations of enantiomeric ratios. *Chirality* **2007,** 19, (1), 5-9.

99. ASTM, Standard specification for biodiesel fuel blend stock (B100) for middle distillate fuels. **2007,** Designated D6751-07b.

100. Gerpen, J. H. V.; Hammond, E. G.; Yu, L.; Monyem, A., Determining the influence of contaminants on biodiesel properties. *Society of Automotive Engineers Technical Paper Series,* **1997,** Paper no. 971685, SAE, Warrendale.

101. ASTM, Standard test method for acid number of petroleum products by potentiometric titration. *Designated D 664-07* **2007**.

102. Knothe, G., Analyzing biodiesel: Standards and other methods. *Journal of the American Oil Chemists Society* **2006,** 83, (10), 823-833.

103. Fuhr, B.; Banjac, B.; Blackmore, T.; Rahimi, P., Applicability of total acid number analysis to heavy oils and bitumens. *Energy & Fuels* **2007,** 21, (3), 1322-1324.

104. Hamblin, P.; Rapenne-Jacob, I.; Reyes-Gavilan, J.; Rohrbach, P., Standard test methods for TAN assessement and modifications thereof. *Tribology & Lubrication Technology* **2004,** 60, (11), 40-46.

105. Mahajan, S.; Konar, S. K.; Boocock, D. G. B., Determining the acid number of biodiesel. *Journal of the American Oil Chemists Society* **2006,** 83, (6), 567-570.

106. Komers, K.; Skopal, F.; Stloukal, R., Determination of the neutralization number for biodiesel fuel production. *Fett-Lipid* **1997,** 99, (2), 52-54.

107. Dong, J.; van de Voort, F. R.; Ismail, A. A.; Akochi-Koble, E.; Pinchuk, D., Rapid determination of the carboxylic acid contribution to the total acid number of lubricants by Fourier transform infrared spectroscopy((c)). *Lubrication Engineering* **2000,** 56, (6), 12-20.

108. Kauffman, R. E., Rapid, portable voltammetric techniques for performing antioxidant, total acid number (TAN) and total base number (TBN) measurements. *Lubrication Engineering* **1998,** 54, (1), 39-46.

109. Jyonosono, K.; Imato, T.; Imazumi, N.; Nakanishi, M.; Yagi, J., Spectrophotometric flow-injection analysis of the total base number in lubricants by using acid-base buffers. *Analytica Chimica Acta* **2001,** 438, (1-2), 83-92.

110. Watanabe, T.; Jyonosono, K.; Soh, N.; Imato, T.; Imazumi, N.; Nakanishi, M.; Yagi, J., Spectrophotometric flow-injection analysis of the total base number and the total acid number in lubricants containing both acid and base compounds. *Bunseki Kagaku* **2003,** 52, (1), 41-50.

111. Wang, S. S., Engine oil condition sensor: method for establishing correlation with total acid number. *Sensors and Actuators B-Chemical* **2002,** 86, (2-3), 122-126.

112. Graboski, M. S.; McCormick, R. L., Combustion of fat and vegetable oil derived fuels in diesel engines. *Progress in Energy and Combustion Science* **1998,** 24, (2), 125-164.

113. ASTM, Standard Test Method for Engler Specific Viscosity of Tar Products. *Designated D1665-98* **2000**.

114. MIL-DTL-83133E, Turbine fuels, aviation, kerosene types, NATO F-34 (JP-8), NATO F-35, AND JP-8+100. **1999**.

115. Bezergianni, S.; Kalogianni, A.; Vasalos, I. A., Hydrocracking of vacuum gas oil-vegetable oil mixtures for biofuels production. *Bioresource Technology* **2009,** 100, (12), 3036-3042.

116. Bezergianni, S.; Voutetakis, S.; Kalogianni, A., Catalytic Hydrocracking of Fresh and Used Cooking Oil. *Industrial & Engineering Chemistry Research* **2009,** 48, (18), 8402-8406.

117. Taufiqurrahmi, N.; Bhatia, S., Catalytic cracking of edible and non-edible oils for the production of biofuels. *Energy & Environmental Science* **2011,** 4, (4), 1087-1112.

118. Tamunaidu, P.; Bhatia, S., Catalytic cracking of palm oil for the production of biofuels: Optimization studies. *Bioresource Technology* **2007,** 98, (18), 3593-3601.

119. Ooi, Y. S.; Zakaria, R.; Mohamed, A. R.; Bhatia, S., Catalytic cracking of used palm oil and palm oil fatty acids mixture for the production of liquid fuel: Kinetic modeling. *Energy & Fuels* **2004,** 18, (5), 1555-1561.

120. Leng, T. Y.; Mohamed, A. R.; Bhatla, S., Catalytic conversion of palm oil to fuels and chemicals. *Canadian Journal of Chemical Engineering* **1999,** 77, (1), 156-162.

121. Twaiq, F. A. A.; Mohamad, A. R.; Bhatia, S., Performance of composite catalysts in palm oil cracking for the production of liquid fuels and chemicals. *Fuel Processing Technology* **2004,** 85, (11), 1283-1300.

122. Bhatia, S., Zeolite Catalysts: Principles and Applications. *CRC Press: Boca Raton, FL* **1990**.

123. Katikaneni, S. P. R.; Adjaye, J. D.; Bakhshi, N. N., Conversion of canola oil to various hydrocarbons over Pt/HZSM-5 bifunctional catalyst. *Canadian Journal of Chemical Engineering* **1997,** 75, (2), 391-401.

124. Katikaneni, S. P. R.; Adjaye, J. D.; Bakhshi, N. N., Studies on The Catalytic Conversion of Canola Oil to Hydrocarbons - Influence of Hybrid Catalysts and Steam. *Energy & Fuels* **1995,** 9, (4), 599-609.

125. Prasad, Y. S.; Bakhshi, N. N.; Mathews, J. F.; Eager, R. L., Catalytic Conversion of Canola Oil to Fuels and Chemical Feedstocks .1. Effect of Process Conditions on The Performance of HZSM-5 Catalyst. *Canadian Journal of Chemical Engineering* **1986,** 64, (2), 278-284.

126. Gaita, R., A Reversed Phase HPLC Method Using Evaporative Light Scattering Detection (ELSD) for Monitoring the Reaction and Quality of Biodiesel Fuels. *LC GC North America* **2006**.

127. Zoccolillo, L.; Alessandrelli, M.; Felli, M., Simultaneous determination of benzene and total aromatic fraction of gasoline by HPLC-DAD. *Chromatographia* **2001,** 54, (9-10), 659-663.

128. Ong, Y. K.; Bhatia, S., The current status and perspectives of biofuel production via catalytic cracking of edible and non-edible oils. *Energy* **2010,** 35, (1), 111-119.

129. Chang, C. D.; Silvestri, A. J., The conversion of methanol and other O-compounds to hydrocarbons over zeolite catalysts. *Journal of Catalysis* **1977,** 47, (2), 249-259.

130. HPinnovations, Process incorporates renewables as part of refining operations. *Hydrocarbon Processing* **2006,** 85, (11), 33.

131. Iglesia, E.; Ribeiro, F. H.; Boudart, M.; Baumgartner, J. E., Synthesis, Characterization, and Catalytic Properties of Clean and Oxygen-Modified Tungsten Carbides. *Catalysis Today* **1992,** 15, (2), 307-337.

132. Lee, J. S.; Oyama, S. T.; Boudart, M., Molybdenum Carbide Catalysts .1. Synthesis of Unsupported Powders. *Journal of Catalysis* **1987,** 106, (1), 125-133.

133. Lee, J. S.; Boudart, M., In situ carburization of metallic molybdenum during catalytic reactions of carbon-containing gases. *Catalysis Letters* **1993,** 20, (1), 97-106.

134. Claridge, J. B.; York, A. P. E.; Brungs, A. J.; Green, M. L. H., Study of the temperature-programmed reaction synthesis of early transition metal carbide and nitride catalyst materials from oxide precursors. *Chemistry of Materials* **2000,** 12, (1), 132-142.

135. Chatterjee, S.; Greene, H. L., Effects of catalyst composition on dual site zeolite catalysts used in chlorinated hydrocarbon oxidation. *Applied Catalysis A: General* **1993,** 98, (2), 139-158.

136. Pines, H.; Haag, W. O., Alumina: Catalyst and Support. I. Alumina, its Intrinsic Acidity and Catalytic Activity1. *Journal of the American Chemical Society* **1960,** 82, (10), 2471-2483.

137. Eilers, J.; Posthuma, S. A., Process for preparation of hydrocarbon fuels. *EP 0, 583,836, A1* **Feb 23, 1994, assigned to Shell Int. Res. Co.**

138. Abazajian, A.; Tomlinson, H. L.; Havlik, P. Z.; Clingan, M. D., Integrated Fischer-Tropsch process with improved alcohol processing capability. . *EP 1,449,906 A1* **Aug 25, 2004, assigned to Syntroleum Corporation.**

139. O'Connor, C. T.; Langford, S. T.; Fletcher, J. C. Q., The effect of oxygenates on the propene oligomerization activity of ZSM-5. *Proceedings of the 9th International Zeolite Conference, Montreal, Canada,* **1992**, 467-474.

140. Doronin, V.; Sorokina, T., Chemical design of cracking catalysts. *Russian Journal of General Chemistry* **2007,** 77, (12), 2224-2231.

141. Molenda, J.; Rutkowski, A., Hydroprocessing in Petroleum Refinery Industry *WNT, Warszawa* **1980**, 61-71.

142. Isabel Vazquez, M.; Escardino, A.; Corma, A., Activity and selectivity of nickel-molybdenum/HY ultrastable zeolites for hydroisomerization and hydrocracking of alkanes. *Industrial & Engineering Chemistry Research* **1987,** 26, (8), 1495-1500.

143. Pratt, K. C.; Sanders, J. V.; Tamp, N., The role of nickel in the activity of unsupported Ni---Mo hydrodesulfurization catalysts. *Journal of Catalysis* **1980,** 66, (1), 82-92.

144. Scherzer, J.; Gruia, A. J., Hydrocracking Science and Technology. *1st Edition. CRC Press. ISBN 0-8247-9760-4.* **1996**.

145. Ancheyta, J.; Speight, J. G., Hydroprocessing of Heavy Oils and Residua. *1st Edition. CRC Press. ISBN 0-8493-7419-7* **2007**.

146. Wu, S.; Huang, J.; Wu, T.; Song, K.; Wang, H.; Xing, L.; Xu, H.; Xu, L.; Guan, J.; Kan, Q., Synthesis, Characterization, and Catalytic Performance of Mesoporous Al-SBA-15 for Tert-butylation of Phenol. *Chinese Journal of Catalysis* **2006,** 27, (1), 9-14.

147. Sing, K. S. W.; Everett, D. H.; Haul, R. A. W.; Moscou, L.; Pierotti, R. A.; Rouquerol, J.; Siemieniewska, T., Reporting physisorption data for gas/solid systems with special reference to the determination of surface area and porosity (Recommendations 1984). *Pure and Applied Chemistry* 57, (4), 603-619.

148. Panpranot, J.; Kaewkun, S.; Praserthdam, P.; Goodwin, J. G., Effect of Cobalt Precursors on the Dispersion of Cobalt on MCM-41. *Catalysis Letters* **2003,** 91, (1), 95-102.

149. Ma, X.; Kim, J. H.; Song, C., Effect of Methyl Groups at 4- and 6-Positions on Adsorption of Dibenzothiophenes over CoMo and NiMo Sulfide Catalysts. *Fuel Chemistry Division Preprints* **2003,** 48, (1), 135-137.

150. Kubička, D.; Šimáček, P.; Žilková, N., Transformation of Vegetable Oils into Hydrocarbons over Mesoporous-Alumina-Supported CoMo Catalysts. *Topics in Catalysis* **2009,** 52, (1), 161-168.

151. Corma, A., From microporous to mesoporous molecular sieve materials and their use in catalysis. *Chemical Reviews* **1997,** 97, (6), 2373-2419.

ABSTRACT

BIOFUELS PRODUCTION FROM HYDROTREATING OF VEGETABLE OIL USING SUPPORTED NOBLE METALS, AND TRANSITION METAL CARBIDE AND NITRIDE

by

HUALI WANG

May 2012

Advisors: Dr. K. Y. Simon Ng and Dr. Steven O. Salley

Major: Chemical Engineering

Degree: Doctor of Philosophy

The focus of this research is to prepare non-sulfided hydrotreating catalysts, supported noble metal and transition metal carbide/ nitride, and evaluate their hydrocracking activities and selectivities by using soybean oil as the feedstock. For comparison study, catalytic cracking of soybean oil over a commercialized ZSM-5 was investigated. However, steady state could not be reached because significant amounts of tar and coke were generated during the reaction though a high yield (21%) of jet fuel was obtained from the process. Compared to the catalytic cracking process, less tar and coke were formed during the hydrocracking process and stable continuous flow reaction was obtained by using the bifunctional Ru/ZSM-5 catalyst. 16% yield of jet fuel, which is comparable to yields over commercialized sulfided NiMo catalysts while at a much lower pressure of 650 psi was produced. A 20 - 29% diesel yield was also obtained during the process. But coke was the issue with this noble metal catalyst.

In the following stage, novel bi-functional catalysts, NiMo carbide or nitride supported on ZSM-5, zeolite β, USY, γ-alumina oxide, and Al-SBA-15 were prepared by the temperature-programmed reaction method and the effects of process parameters on catalytic hydrocracking of soybean oil were investigated. 100% conversion of soybean oil was attained under the 650 psi and

360-450 ^{o}C reaction conditions. Among them, three zeolite supported carbide catalysts showed high selectivity to green gasoline (about 15-40%) due to the high cracking activities. γ-alumina and Al-SBA-15 supported catalysts mainly produced green diesel fuels. Especially Al-SBA-15 supported NiMo carbide catalyst gave the highest yield of organic liquid product (96%) and highest selectivity (97%) to hydrocarbons in the boiling range of the diesel fraction. The study of carbide and nitride catalysts provides a promising approach for preparing drop-in fuels from renewable resources under a lower pressure without sulfurization reagents involved in the process. NiMoC/Al-SBA-15 showed the greatest potential for producing green diesel from renewable feedstock.

AUTOBIOGRAPHICAL STATEMENT

HUALI WANG

huali@wayne.edu

EDUCATION:

- PhD in Chemical Engineering , Wayne State University, Detroit, USA, 2012
- Master of Science in Chemical Engineering, Wayne State University, Detroit, USA, 2010
- Master of Science in Chemical Engineering, Northwest University, Xi'an, China, 2005

RECENT PUBLICATIONS:

1. H.L. Wang, S. Yan, M. Kim, S. O. Salley, and K. Y. S. Ng, "Hydrotreating of Soybean Oil over NiMo Carbide Supported on Different Supports", patent pending

2. H.L. Wang, S. Yan, S. O. Salley, and K.Y.S. Ng, "Hydrotreating of Soybean Oil over NiMo Carbide Catalyst on Five Different Supports", Applied Catalysis A: General, xxx (2012) xxx–xxx, Submitted

3. H.L. Wang, S. Yan, S. O. Salley, and K. Y. S. Ng, "Hydrocarbon Fuels Production from Hydroprocessing of Soybean Oil Using Supported Transition Metal Carbides and Nitrides", Industrial & Engineering Chemistry Research, xxx (2012) xxx–xxx, Accepted

4. H.L. Wang, S. Yan, S. O. Salley, and K. Y. S. Ng, "Biojet Production from Catalytic Cracking and Hydrocracking of Soybean Oil", Current Catalysis, xxx (2012) xxx–xxx, Accepted

5. S. Yan, C. DiMaggio, H.L. Wang, S. Mohan, M. Kim, L. K. Yang, S. O. Salley, and K. Y. S. Ng, "Catalytic Conversion of Triglycerides to Liquid Biofuels through Transesterification, Cracking, and Hydrotreatment Processes", Current Catalysis, 1(2012):41-51

6. M. Kim, C. DiMaggio, S. Yan, H.L. Wang, S. O. Salley, and K. Y. S. Ng, "Performance of Heterogeneous ZrO_2 Supported Metal Oxide Catalysts for Brown Grease Esterification and Sulfur Removal", Bioresource Technology, 102(3):2380-6. (2010).

7. H.L. Wang, H.Y. Tang, S. O. Salley, and K. Y. S. Ng, "Analysis of Sterol Glycosides in Biodiesel and Biodiesel Precipitates", Journal of the American Oil Chemists Society, 87 (2):215-221,. (2009)

8. H.L. Wang, H.Y. Tang, J. Wilson, S.O. Salley, and K. Y. S. Ng. "Total Acid Number Determination of Biodiesel and Biodiesel Blends," Journal of the American Oil Chemists Society, 85 (11):1083-1086. (2008).